ISSA - SCUOLA
TERNAZIONALE
SUPERIORE
TUDI AVANZATI
TRIESTE
Strada Costiera 11

ISAS - INTERNATIONAL SCHOOL
FOR ADVANCED STUDIES

PROPERTIES OF SPIRAL GALAXIES: A STUDY OF THE VIRGO CLUSTER

Thesis submitted for the degree of

"Magister Philosophiae"

Astrophysics Sector

Candidate:

Mauro D'Onofrio

Supervisors:

Prof. Massimo Capaccioli

Academic Year 1988/89

TRIESTE

PROPERTIES OF SPIRAL GALAXIES: A STUDY OF THE VIRGO CLUSTER

Thesis submitted for the degree of
"Magister Philosophiæ"

Astrophysics Sector

Candidate:

Mauro D'Onofrio

Supervisors:

Prof. Massimo Capaccioli

October 1989

To Cristiana

Contents

Chapter 1

Introduction

It seems today well established that spiral galaxies exist in a variety of shapes and that the different morphologies among them are related to continuous variations in a number of basic physical parameters, such as the bulge–to–disk ratio, the mass–to–luminosity ratio, the HI content, the maximum rotation velocity, the velocity dispersion, and so on (Tremaine, 1988). Much of these variations result from the various forms of the past history of star formation (*e.g.*, Searle, Sargent and Bagnuolo, 1973) and from the available amount of neutral hydrogen gas (*e.g.*, Sandage, Freeman and Stokes, 1970). Moreover, there are increasing evidences that the local environment and the dark matter content play an important role in the evolution of spiral galaxies (Kormendy, 1989).

Attempts have been made in these years to look for possible statistical correlations among the structural parameters of spiral galaxies. In particular it has been analyzed the behaviour of the structural parameters as a function of the morphological types (de Vaucouleurs, 1977; Kent, 1985; Kodaira *et al.* 1986). Such investigations have led to the conviction that the properties of spiral galaxies should be explainable from a limited number of fundamental physical parameters: " The fact that there are so many different classification systems for galaxies (Sandage, 1975) demonstrates that we are still searching for the fundamental properties of these objects " (Whitmore, 1984).

The aim of this thesis is to review some properties of the spiral galaxies, mainly connected with the photometric studies. The discussion consist of two parts.

The first is focused on two aspects: the analysis of the most important structural parameters and their interrelations, and the study of the mass–to–luminosity ratio related to the dark matter content.

The second part presents a description of the Virgo cluster as a whole and of its spiral members, with a particular attention to the evolutionary effects attributed to the intergalactic medium of the cluster, in the HI and CO content.

The reason of this division, reside in the fact that the purpose of my Ph.D. thesis is the photometric analysis of several spiral galaxies in the Virgo cluster.

This study has been conceived in order to exploit the advantages of a new photometric technique, that couples large scale plate materials with CCD images of the center of the galaxies, and has been succesfully applied by Capaccioli *et al.* (1987, 1988a) and by Caon *et al.* (1989) to some elliptical galaxies. Its goal is to provide better measurements of the photometric structural parameters of the spiral galaxies. These data might contribute to our knowledge of the characteristics of the structural parameters and of their link with the Hubble type. Furthermore, they could be of fundamental importance for understanding the role of the cluster environment on the evolution of the spiral galaxies.

The work is subdivided as follows:

Chapter 2 presents a discussion of the most famous morphological classification systems, from Hubble and his contemporaries up to the present–days. The principal characteristics of spirals are described; in particular, the properties of the bulge and disk component and the color of the disks, are treated with more details.

Chapter 3 is devoted to the question of the bulge–to–disk ratio and of the central surface brightness. I discuss some of the basic statistical correlations involving these parameters.

Chapter 4 concerns the mass–to–luminosity ratio and the observational evidences of the presence of dark matter in spiral galaxies. In the first part I describe some results of the surface photometry (in particular for edge–on systems), while in the second part the analysis is concentrated on the characteristics of the rotation curves.

Chapter 5 and 6 are reserved to the discussion of the Virgo cluster. In the former I review the morphology, the dynamics and the luminosity function of the cluster members, while in the further I discuss the properties of the Virgo spiral galaxies related to the HI and CO content.

The last chapter is an introduction to the photometric work. It is a technical description of the surface photometry and of the most important detectors. It contains also some comments about the advantages of the new photometric technique, cited before.

References

Capaccioli, M., Held, E., and Nieto, J.L.: 1987, *Astron. J.*, **94**, 1519.

Capaccioli, M., Piotto, G., and Rampazzo, R.: 1988a, *Astron. J.*, **96**, 497.

Caon, N., Capaccioli, M., and Rampazzo, R.: 1989, *Astrophys. J. Supp.*, submitted.

Kent, S.M.: 1985, *Astrophys. J. Supp.*, **59**, 115.

Kodaira, K., Watanabe, M., and Okamura, S.: 1986, *Astrophys. J. Supp.*, **62**, 703.

Kormendy, J.: 1989, Proceedings of First Yellow Mountain Summer School on Physics and Astrophysics, *Origin, Structure and Evolution of Galaxies*, ed. Fang Li Zhi (Singapore: World Scientific Publishing Co.), in press.

Sandage, A.: 1975, in *Star and Stellar System IX: Galaxy and the Universe*, eds. A. Sandage, M. Sandage, and J. Kristian, (Chigago: Chigago University Press), p.1.

Sandage, A., Freeman, K.C., and Stokes, N.R.: 1970, *Astrophys. J.*, **160**, 831.

Searle, L., Sargent, W.L.W., and Bagnuolo, W.G.: 1973, *Astrophys. J.*, **179**, 427.

Tremaine, S.: 1988, in *Structure and Dynamics of Elliptical Galaxies*, IAU Symp. No.127, eds.

Vaucouleurs, G. de: 1977, in *The Evolution of Galaxies and Stellar Populations*, eds. B.M. Tinsley, and R.B. Larson.

Whitmore, B.C.: 1984, *Astrophys. J.*, **278**, 61.

Chapter 2

Basic properties of spiral galaxies

2.1 Morphology

Spiral galaxies are spectacular objects. Many astronomers tried to classify them in different ways, depending on which of their characteristics they were impressed. The most peculiar of these characteristics is the large variety of forms and shapes of the spiral arms, and so, several classification schemes have been based on their appearances. The classification of the galaxies have also been based on other structural parameters, such as the concentration of the luminosity in the center and the stellar content. Table 2.1 shows a comparison in the classification of some galaxies by different authors.

Simple descriptions of the galaxies have been provided by Wolf (1908) and Vorontson–Velyaminov *et al.* (1962, 1963, 1964, 1968). These descriptions do not constitute a classification system, in which the objects are set into classes according to some continuously varying parameter. The Wolf's system was the first to use a linear sequence which proceeds from amorphous forms with no spiral patterns (indicated with the letter from d to k), to fully developed spirals (from r to w). Among the studies that used the Wolf's classification, we remember the Reinmuth's (1926) study of the Herschel galaxies, the Lundmark's (1927) summary of galaxian research to 1926, the Holmbergh's (1937) work on double galaxies, the Reiz's (1941) study of the surface distribution of galaxies, and the Danver's (1942) work on the forms of spiral arms. Lundmark (1926,1927) proposed a classification based on a major division of galaxies into three groups (amorphous ellipticals, true spirals, and Magellanic Cloud–type irregulars), further dividing the groups according to the concentration of light toward the center. Shapley (1928) also proposed a classification based on concentration, but included the nonintrinsic properties of apparent magnitude and apparent flattening in his notation.

The Hubble's classical tuning fork diagram is one of the most famous classification schemes, used, with few modifications, also today. Fig.2.1 shows its

Name NGC	Hubble	Holmberg	de Vaucouleurs	van den Bergh	Morgan
			Thin Multiple-Armed Spirals (Plate II)		
5273	$S0_2$/Sa(s)	—	SA(s)0^{0}	E 1(p?)	gKD2
1302	Sa	—	(R)SB(r)0/a	S(B)a	kBl
2811	Sa	—	SB(rs)a	Sb^{+} II-III	—
3898	Sa	—	SA(s)ab	Sb^{-} II	kD5-KS5
2841	Sb	Sb^{-}	SA(r:)b	Sb^{-} I	kS5
488	Sb	Sb^{-}	SA(r)b	Sb^{-} I	kS2
			Plate III		
5055	Sb	Sb^{+}	SA(rs)bc	Sb^{+} II	gS4
628	Sc	Sc^{-}	SA(s)c	Sc I	fgSl
5457	Sc	Sc^{-}	SAB(rs)cd	Sc I	fSl
3810	Sc	Sc^{-}	SA(rs)c	Sc I	fS3
6643	Sc	Sc^{-}	SA(rs)c	Sc I-II	—
5204	Sc/Irr	Sc^{+}	SA(s)m	Ir^{+} IV	fI-fS4
			Massive-Armed Spirals Plate IV		
4293	Sa	—	RSB(s)0/a	Pec	fg:S6
4569	Sb	Sb^{+}	SAB(rs)ab	Sb^{+}n	fS4p
3623	Sa	Sa	SAB(rs)a	Sbn II:	gS5
6814	Sb	—	SAB(rs)bc	Sb^{+} I	—
5248	Sc	Sc^{-}	SAB(rs)bc	Sc I	fS4
5194	Sc	Sc^{-}	SA(s)bcp	Sc(t) I	fSl
157	Sc	Sc^{-}	SA(rs)bc	Sc(*) I	afS3
598	Sc	Sc^{+}	SA(s)cd	Sc II-III	fS3
			Ordinary-Barred Transitions Plate V		
4579	Sb/SBb	Sb^{-}	SAB(rs)b	Sbn	gkS3-gKB
3504	SBb(s)/Sb	—	SAB(s)ab	Sb(t?)	fg Bl?
6951	SBb(s)Sb	Sb^{+}	SAB(rs)bc	Sbp I-II	f:Slp-f:BpN
5236	Sc/SBb	—	SAB(s)c	—	fgSl
4088	SBc/Sc	Sc^{-}	SAB(s)bc	Sc* I-II	a:B:4
925	Sc/SBc	Sc^{+}	SAB(s)d	S(B)c II-III	afB
			Barred Spirals r and s Types Plate VI		
7743	SBa(s)	—	(R?)SB(s)0^{+}	Sa?	gkBl
3185	SBa(s)	Sa	(R)SB(r)a	S(B)b^{+} III	fB
1300	SBb(s)	Sb^{+}	SB(rs)bc	SBb I	fB2
7741	SBc(s)	Sc^{+}	SB(s)cd	SBc II	afB
4643	$SB0_3$/SBa(r)	—	SB(rs)0/a	SBa	kB
1398	SBb(r)	—	(R')SB(r)ab	S(B)b^{-} I	kB2
2523	SBb(r)	—	SB(r)bc	SBb^{-} I	fgB
1073	SBc(sr)	Sc^{+}	SB(rs)c	S(B)c II	afBl
			Magellanic Cloud and Irregular Types Plate VII		
4395	Sc/Irr	Sc^{+}	Sa(s:)m	S^{+} IV-V	aSl
SMC	Irr	—	IB(s)mp	III-IV	—
LMC	Irr	—	SB(s)m	Ir IV-V	—
Hol II	Irr	Ir I	Im	Ir IV-V	—
2366	Irr	Ir I	dIB(s)m	Ir IV-V	aL?
IC 2574	Irr	Ir I	SAB(s)m	Ir IV-V	—

Table 2.1: Classification of the galaxies by different authors (from Sandage, 1977).

famous structure, with the ellipticals, S0s, and the two families of spiral galaxies, ordinary (A) and barred (B), with the three types (a,b,c), forming a physically significant sequence. As explained in detail in the "Hubble Atlas of Galaxies" (Sandage, 1961), the Hubble class for spiral galaxies is assigned on the basis of the following criteria:

- the winding of the spiral arms,
- the degree of resolution into stars and HII regions,
- the relative size of the bulge with respect to the disk.

The third item is likely to be related to the angular momentum distribution of the original protogalaxy, and to the time of earliest star formation relative to the collapse time. The other two are probably related to the present rate of conversion of gas in stars in a rotating galaxy.

For most galaxies these independent criteria are in good agreement with each other, but in some cases a conflict arise, and then priority is set to the arm characteristics.

If one tries to quantify each characteristic by itself, however, one finds a relatively large intrinsic scatter within each Hubble type. For example, as shown by Kennicutt (1981), the mean pitch angle (the angle between the tangent to the arm and the circle $r = constant$) increases from $6° \pm 3°$ for Sa's to $18° \pm 5°$ for Sc's.

Already Hubble noted the large spread in total luminosity of spiral galaxies. The brightest spirals have an absolute magnitude in the blue spectral region of $M_B \sim -23$, and the faintest have $M_B \sim -17$.

The first true spirals are called Sa. They show tightly wound spiral patterns, and they may or may not have tight spiral arms of luminous matter. The arms are invariably smooth, with no resolution into stars. Galaxies of type Sb have definite and pronounced spiral arms which, at the beginning are tightly wound (Sab), and at the end become more massive and more open (Sbc). Regular spiral dust lanes are a prominent feature of the Sb type. The spiral structure dominates Sc galaxies. The arms are the most conspicuous part of the form. They are usually branched, highly resolved into stars, and open or unwound. Spiral dust lanes are highly important feature of the spiral pattern. The brightest Sa's are intrinsically brighter than the brightest Sc's, and generally have also a higher surface brightness.

The nuclear regions of Sa galaxies can be either large or small. There is not a unique connection between the relative size of the nuclear region and the arm pattern, but there does appear to be a strong correlation between the tightness of the spiral pattern and the lack of resolution of the arms into stars and HII regions. The Sb spirals can be separated into two major divisions: galaxies in the first division have relatively large amorphous nuclear regions (there are either two predominant arms or a multiple arm system); galaxies in the second division of Sb are characterized by small nuclear regions with the typical Sb intermediate spiral pattern. Sc galaxies have very small amorphous central regions, and there

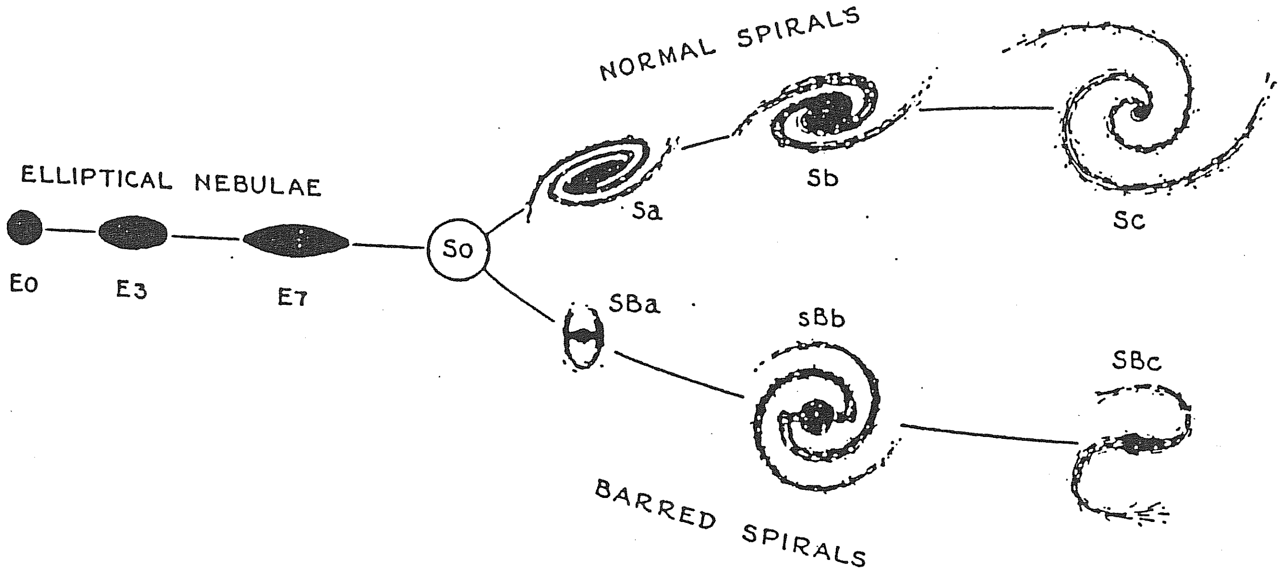

Figure 2.1: The original tuning fork diagram as published by Hubble in 1936 in his *Realm of the Nebulae.*

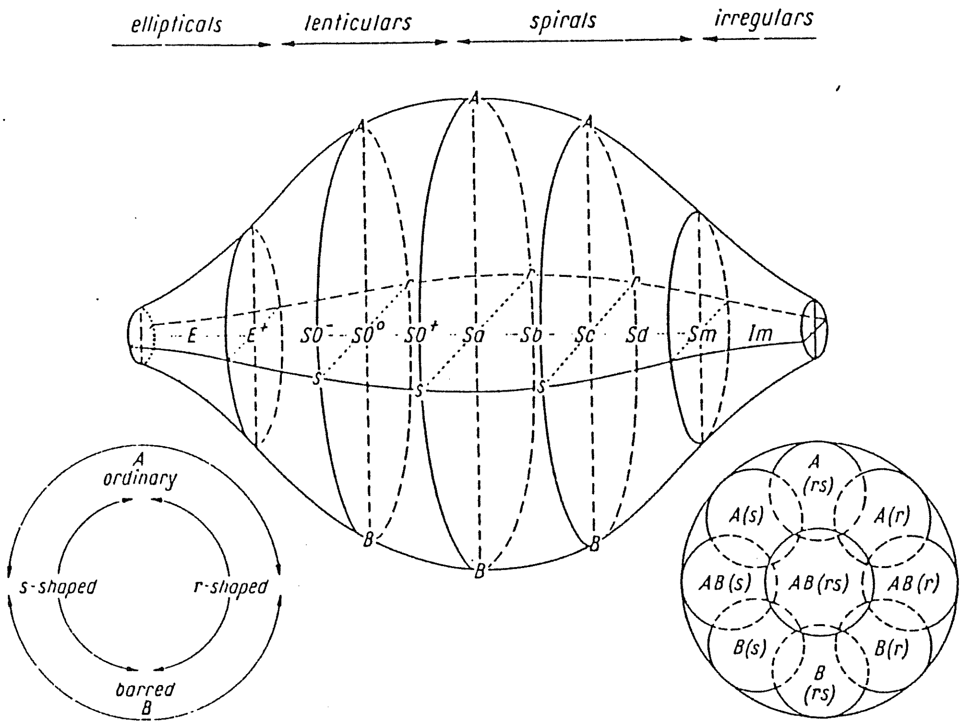

Figure 2.2: The classification scheme of de Vaucouleurs (from de Vaucouleurs, 1959a.

is a great variation of structural form along the section from early Sc to late Sc, based on the appearence of the spiral pattern.

The SB class includes the 15% of the brighter galaxies. The members do not differ systematically from normal spirals either in luminosity, dimension, spectral characteristics, and distribution over the sky. In several respects, such as the unwinding of the arms and their progressive resolution, the sequence resembles that of normal spirals and, was subdivided into the three sections SBa, SBb, and SBc, plus an SB0 class which represents a transitional stage between the ellipticals and the true barred spirals.

Features common to the entire family are a nucleus, a lens of lower intensity concentric with the nucleus, the bar which usually terminates on the periphery of the lens, and occasionally an outer envelope and/or an external ring. The arms can either begin tangent to an internal ring, or can spring from the ends of the bar; this division is not prominent in SBa types, but is a dominant feature of SBb and SBc galaxies.

One of the most important extension of this scheme was made by de Vaucouleurs (1959a), who introduced the 'r' and 's' varieties, for indicating 'ring' and 's–shapes' structures. Fig.2.2 illustrate the revision. The division into gross types is made along the axis of the figure from left (E) to right (Sm), the division into the ordinary and the barred family is by position on the surface.

Since galaxies originally classified Sc by Hubble cover a large interval along the sequence, ranging from regular well–developed arms to nearly chaotic structures, de Vaucouleurs introduced an extension of the Sc and SBc families, with the subdivision in cd, d, dm, m, and Im types. He also proposed to recognize the characteristics of the spiral arms explicitly by adding the symbols m (for massive) and f (for filamentary) after the type designation.

Another classification of disk galaxies, based on the degree of development of the spiral arms, has been proposed by van den Bergh (1960). Galaxies with long, thin, well developed arms of relatively high surface brightness can be distinguished from those with undeveloped stubby arm patches. This criterium seems to be, in general, well correlated with the luminosity of the galaxies, but here also the replacement of qualitative impressions by quantitative data shows that an intrinsic scatter is present (Sandage and Tamman, 1981). Measurements of arm lengths (Kennicutt, 1982) show only a weak dependence on luminosity.

The distinction between grand design spirals, where the spiral structure is dominated by a few, usually two, major arms, and flocculent spirals, having only armlike filaments, is the basis of the classification scheme of Elmegreen and Elmegreen (1982). Again the main variable is the degree of coherence in the spiral pattern. From a large sample of galaxies, they drew the following conclusion on the frequency of occurrence of grand design spirals: Only 30% of the isolated SA galaxies show a grand design, as opposed to 70% of SA's in binaries and groups. Barred spirals and intermediate types (SB and SAB) show a grand design in almost all cases, except for the very messy barred irregulars.

Today, it is possible to outlined the spiral arms by means of several tracers. On broad band photographs of grand design spirals one usually sees the luminous arms made up by HII regions and OB associations, and dark lanes of absorbing material displaced very often towards the concave side. Hα or UV photographs can also be used, and modern 21 cm line studies are now sensitive enough and have sufficiently high angular resolution to show the spiral structure in the neutral gas, while recent work on the CO lines in several nearby spirals has demonstrated a close correspondence of the molecular gas with arms.

Even if classification schemes has mainly been based on the appearence of the spiral structure, there exist tentative classification systems based on different important features of spiral galaxies. One of these, is for example, the classification based on the difference in stellar content between the spiral arms and the spheroidal component. Such difference was very well known after Baade's study in 1944, and is apparent from the change of integrated colors along the classification sequence as the relative importance of the bulge component with respect to the disk, in going from S0 to Sm systems, decreases. Morgan and Mayall (1957) noted that the composite spectral class correlates well with the degree of dominance of the spheroidal component alone, *i.e.*, with the concentration of the luminosity toward the center. Morgan (1958,1959) developed his spectral type–

concentration correlation into a classification system whose color–class notation explicitly isolates the spectral type that is expected on the basis of the correlations. This system contains information on the state of stellar evolution in the central region of galaxies.

Although the bulge, the disk and the peculiar spiral pattern are the most evident characteristics of a spiral galaxy, there exist others important structures that are seen on a photograph of a spiral galaxy, and that only recently have had the attention they merit. These are: bars, rings, lenses and dust lanes.

For example, the differences between bars in various Hubble types are very distinct: in early type spirals they are smooth, with no dust patches or lanes and no sign of resolution into lumps or knots. In many cases one finds that the luminosity of the bar does not decrease monotonically along its major axis, but rather that the bar can be described as consisting of a central part and two smooth luminous regions of varied size, called ansae, diametrically opposed from the center and equidistan from it. Only in the later types is the bar clearly resolved in luminous knots or stars. Athanassoula and Martinet (1980) found a correlation between bulge size and bar length, both measured with respect to the disk size. The mean ratio of bar length to bulge diameter is 2.6 ± 0.7.

Rings frequently occur in both ordinary and barred spirals, inner ring being more frequent than outer ones. About 20% of SA's and 30% of SB's are of the (r)–variety (de Vaucouleurs, 1963), and there is a large fraction of the (rs)–variety as well. Statistics of the frequency of rings with Hubble type show a preponderance of rings among S0's and early type spirals, and their virtual absence in late type systems (de Vaucouleurs, 1975). Inner rings in barred spirals surround the bar and more or less touch its extremities, while outer rings have a mean radius of order 2.2 times that of the bar major axis on inner ring size. The ratio of inner ring to disk size was found to vary regularly with Hubble type and it has been used as a distance indicators (de Vaucouleurs and Buta, 1980). Two extreme types of outer rings can be distinguished: broad stellar and truely closed outer rings, which have a very smooth light distribution and red colors, and gaseous (near) rings consisting of two or more narrow spiral arms very tightly wound. Kormendy (1979) found that outer rings lie preferentially perpendicular to the bar, if present.

A lens can be defined as a shelf in the luminosity distribution of a disk galaxies occurring in between the bulge and the disk, with a shallow brightness gradient and a steep outer edge. At present there is still a great deal of confusion about the nature of lenses. According to Kormendy (1980), one would distinguish between those located in early type galaxies (S0 to Sa), which would be called lenses, and those located in later types (Sb to Sm), which would be called ovals. Lenses are predominantly present in types SB0 to SBab among the barred galaxies.

Dust lanes are often present in galaxies of type SBb or later along the bar. They can be found in two shapes: straight or curved. Dust is not only found in the bar, of course, but also in the spiral arms and in the inner and outer rings.

In some grand design spiral, like M51, the primary dust lanes are continuous and located at the inside edge of the luminous spiral arms. However, for the majority of galaxies the situation is more complicated and the dust and HII regions do not form a nice spatial sequence.

2.2 Bulge and Disk components

Surface photometry shows that spiral and S0 galaxies have two main components: a spheroidal and an exponential disk component. In general, the light profile of the inner spheroidal component follows fairly well the $r^{1/4}$ law tipical of elliptical galaxies, whereas the outer disk has an exponential distribution: $I(r) = I_0 e^{-\alpha R}$.

The old traditional picture of bulge components in spiral and S0 galaxies is that they are elliptical galaxies living in the middle of a disk. This view is based on the similarity of many basic properties of bulges and ellipticals, including morphology (Sandage, 1961; Sandage, Freeman, and Stokes, 1970), stellar content (Faber, 1977), and the shape of the brightness profile (de Vaucouleurs, 1959b). Both components also have the same relationship $L \propto \sigma_0^n$, $n \sim 4$, between luminosity and central velocity dispersion (Faber and Jackson, 1976; Sargent *et al.* 1977). However, significant differences has recently been found between bulges and ellipticals, both in the photometric structure (Kormendy, 1980; Boroson and Kormendy, 1982; Capaccioli, 1987), and in their dynamical properties.

Radially, disks are supported almost entirely by rotation, and their flattening is determined by the balance between rotation and the perpendicular velocity dispersion. It seemed natural in early models of ellipticals (Prendergast and Tomer, 1970; Wilson, 1975) to assume that they also had shapes determined by rotation. But, starting from the pioneering work of Bertola and Capaccioli (1975), and Illingworth (1977), many authors have demonstrated that elliptical galaxies are flattened mainly by the anisotropic velocity dispersion, while bulges of disk galaxies appear to be rotationally supported (Schechter and Gunn, 1979; Whitmore, Kirshner, and Schechter, 1979; Whitmore and Kirshner, 1981; Kormendy and Illingworth, 1982; Illingworth and Schechter, 1982; Dressler and Sandage, 1983; Whitmore, Rubin, and Ford, 1984).

Thus, we now see a striking dichotomy in the properties of ellipticals and disks. In ellipticals the initial random motion has been preserved, while in disks the dissipation during galaxy formation was strong enough to convert nearly all of the kinetic energy into ordered motion. It is therefore natural, in this contest, to ask whether bulges are objects with intermediate properties.

Preliminary data already suggested that bulges rotate faster than ellipticals.

The central region of M31 has long been known to rotate rapidly (Babcock, 1939; Rubin *et al.* 1973; Pellet, 1976; Peterson, 1978a; Richstone and Schectman, 1980). Also Bertola and Capaccioli (1977) found that the bulge of the edge–on S0 NGC 128 rotates at $\sim$ 150 km s^{-1}even 8$''$.0 up from the disk. This is comparable to the disk rotation rate. NGC 128 is an extreme example of a galaxy with box–shaped bulge; one might expect rapid rotation in such objects (Freeman, 1975). Further, a particularly striking example is NGC 3115, whose bulge rotates almost as rapidly as predicted by oblate spheroid models in which the flattening is due to rotation (Rubin *et al.* 1982; Illingworth and Schechter, 1982).

The bulges of barred galaxies show further differences from ellipticals: many are triaxial, like bars (Kormendy and Koo, 1982), and these rotate even more rapidly than SA bulges (Kormendy, 1982a). The bulges of many barred galaxies seem to be surprisingly disklike in their photometric and kinematic properties and in their tendency to show recent star formation.

However, since bulges of disk galaxies share several common properties with ellipticals, it is quite natural to ask the following question: are bulges of disk galaxies also triaxial? There are two tentative ways of detecting triaxial bulges. The first one is based on the photometry of the galaxy and consist of revealing a misalignement of the major axes of the disk and of the bulge, which would be not present if the structure were axisymmetric. Already more than 30 years ago this phenomenon has been pointed out by Lindblad (1956) for the Andromeda galaxy and successively investigated by Stark (1977). Several cases of twisting in non–barred S0 and spiral galaxies have been found by Bertola, Vietri and Zeilinger (1988). The second manifestation of triaxiality in bulges is the presence of non circular motions in the gaseous disk induced by the non–axisymmetric potential, as indicated by Gerhard and Vietri (1986,1987). Evidence of non–circular motions were noticed by Rubin and Graham (1987) in the Sa galaxy NGC 4845.

Relatively recent data also support the facts that some small but significant differences do exist between bulges and elliptical galaxies. The first of these is the shape of the minor axis luminosity profile. Whereas ellipticals are well approximated by a de Vaucouleurs $r^{1/4}$ law (*e.g.*, de Vaucouleurs and Capaccioli, 1979), except possibly for the core regions, to the limits of available photometry, deviations from the $r^{1/4}$ law are not unknown on the minor axes of galactic bulges (Kormendy and Bruzual, 1978; Jensen and Thuan, 1981; Capaccioli, 1987,1989).

There is also an increasing body of evidence suggesting that there are differences between the shapes of elliptical galaxies and the bulge of disk galaxies. No elliptical galaxy is known which shows a clear box or peanut shaped morphology of their isophotes.

As far as the disk is concerned, we can say that the disk contribute a large part of the total light and of the angular momentum. For example, in M31, which has a fairly prominent spheroidal component, more than 75 % of the blue light (de Vaucouleurs, 1958) and probably more than 95 % of the total angular momentum (Takase, 1967) come from this exponential disk.

Freeman (1970) has made a pioneering investigation on this subject. He found that:

1) The light profile modelling the disk distribution is usually exponential, $I(r) = I(0)e^{-\alpha r}$, in agreement with results of de Vaucouleurs (1959);

2) Sometimes the exponential cuts off toward smaller radii before the spheroid becomes dominant;

3) The scale length is $2 \lesssim \alpha^{-1} \lesssim 10$ kpc in S0–Sbc galaxies, but only $2 \lesssim \alpha^{-1} \lesssim 5$ kpc in Sc–Im galaxies;

4) Most surprisingly, the corrected central disk brightness is constant at $B(0)_c = 21.65 \pm 0.30$ mag arcsec^{-2}for 28 of 36 galaxies.

According to Eggen, Lynden–Bell, and Sandage (1962), the galactic disk formed from matter which had remained gaseous during the rapid–collapse phase. This matter lost its random kinetic energy through inelastic encounters of gas clouds and, conserving its angular momentum, settled to a disk, approximately in centrifugal equilibrium. Because the disk is so flat, and because it is difficult to dissipate the energy of the random stellar motions perpendicular to the galactic plane, it seems very likely that the settling to the disk was virtually complete before the main burst of star formation in the disk began.

However, the exponential disk is not only a property of the old disk population. For example, in M33 (de Vaucouleurs, 1959b), which is an almost pure exponential disk, the ultraviolet luminosity distribution is exponential with the same gradient α as in the blue and in the visual. Since the young Population I presumably contributes significantly to the U band, this means that the young population is also exponentially distributed.

Looking at the disk of our Galaxy we have learned that the disk includes stars covering a wide range of ages, abundances, and kinematical properties. The chemical and kinematical properties of nearby disk stars are correlated with their age, in the sense that the oldest stars have the lowest [Fe/H] values, the largest velocity dispersion, and therefore the largest scale heights.

The old disk is supported by its velocity dispersion in the z direction, and mainly by its rotation in the radial direction. Near the Sun, its velocity dispersion components are about (40,25,20) km s^{-1}respectively (Hartkopf and Yoss, 1982), while the circular velocity is about 220 km s^{-1}. This means that the old disk near the Sun is relatively cold. The value of the disk stability parameter Q (Toomre, 1964) is about 1.3. Since disks are locally unstable to bar modes if $Q > 1$, a mechanism should be present that suppress this instability. For example, the Galaxy may contain a significant fraction of spherically distributed matter in its inner regions (Efstathiou *et al.* 1982; Ostriker and Peebles, 1973). The inner bulge component and the dark corona may contribute to the stability of the disk. Further, the disk may be hotter in the inner parts (Kalnajs, 1972). However, surface photometry of edge–on galaxies suggest that the inner parts of their disks may not be so cold. Observations show that the vertical scale height and the ratio σ_R/σ_z are approximately constant with radius (van der Kruit and Searle, 1982). Lewis (1986) has measured radial velocities for about 600 K giants in the Baade's window, where the reddening is known and quite low. These stars show that the velocity dispersion in the R direction (σ_R), for the old disk, varies smoothly over the interval $2 < R < 18$ kpc, and follows closely the form $\sigma_R(R) = 106exp[-R/2h_R]$, where $h_R = 4.4$ kpc, that is what we would expect for a disk with the properties discussed above.

In the disk, the rotation of the gas and stellar components are similar. The studies of the disk gas component have mainly been performed through aperture synthesis observations in the 21 cm line. HI velocity fields are now available for several tens of spiral galaxies. From the data, astronomers arrived to the following conclusions:

(i) Many spiral galaxies have large scale deviations from axial symmetry. Four categories of distinctive signatures can be recognized in the velocity field: a) spiral arm motions, b) bars and oval distorsions, c) warps, and d) asymmetries.

(ii) Rotation curves are fairly flat out to large radii. The HI extent of a galaxy is not very predictable: in some cases large HI envelope are found, while in other cases the HI is confined to the optical image.

(iii) From HI data alone it is difficult to find a dynamical basis for Hubble types. This is partly due to the lack of angular resolution in the central parts of galaxies and partly because HI has not been detected in the central parts of some early type galaxies with large bulges.

Finally, the use of millimiter wave CO emission as a tracer of molecular hydrogen in the Galaxy (Scoville and Solomon, 1975) showed that, unlike HI, most of the H_2 is concentrated in the inner part of the Galaxy in a "ring" between 4–8 kpc and in the inner 1 kpc. Subsequent surveys (Gordon and Burton, 1976; Cohen and Thaddeus, 1977; Solomon *et al.* 1979) confirmed this picture. The Giant Molecular Clouds are confined to a layer with a half thickness of 60 pc only, and constitute an important component of the galactic disk because their masses range from 10^5 to 3×10^6 $M_\odot$. They affect the dynamics of the disk by contributing significantly to the surface density and through their individual gravitational interactions with stars.

2.3 Color of spiral galaxies

The integrated UBV properties of galaxies and, more specifically, their distribution in the $(U - B, B - V)$ diagram have been the subject of a vast number of investigations. The main problem, of course, lies in trying to explaine the large range of observed integrated colors of galaxies over the entire Hubble sequence.

A field of astronomy that is mainly concerned with this kind of problems is the study of the photometric evolution of galaxies. Numerical and analytical methods (reviewed by Tinsley, 1975), attempt to give an answer to two basic questions concerning the stellar content of galaxies:

1) what is the present distribution of stars, according to mass, age and metallicity?

2) how did this present day distribution arise or what is the history of star formation and chemical enrichement?

The principal tools for finding answers to these questions are the distributions of light and colors.

The models used for synthesizing the stellar systems, must take into account many processes which are active in producing the final observed distribution; to name a few:

- the rate of star formation of new stars;
- the mass distribution of the newly formed stars;
- the evolution of the stars;
- the chemical enrichement of the interstellar gas by novae and supernovae ;
- non–stellar contributions to the light (dust, non–thermal sources);
- the dynamics of the galaxy as a whole.

Clearly, many of these processes are interdependent, and one has to make a number of simplifying assumptions to calculate a model. Searle, Sargent and Bagnuolo (1973) proposed a model which was particularly successful in reproducing the observed colors of galaxies. Their model was later modified by Huchra (1977) and Larson and Tinsley (1978). We can summarize the results of these works, in the following general statements:

1) normal galaxies form a well defined empirical sequence in the $(U-B, B-V)$ plane;

2) model galaxies can be constructed such that they closely follow the empirical relation in the $(U-B, B-V)$-diagram under the assumptions that:

a) all galaxies are 10^{10} years old,

b) the star formation rate (SFR) can be represented by a declining function of time and the sequence runs from the single–burst for ellipticals to roughly constant SFR for the latest types,

c) the galaxies deviating from the sequence are often interacting and can be understood as the result of one or more periods of enhanced star formation in the more recent past.

Observations tell us that the most significant feature of the radial color distributions, is the relative constancy of the color index and the lack of any systematic trends of this quantity. Schweizer (1976), Talbot *et al.* (1979) and Wevers (1984) found similar results, and they contradict the finding of de Vaucouleurs (1961) that spiral galaxies become bluer at large radii.

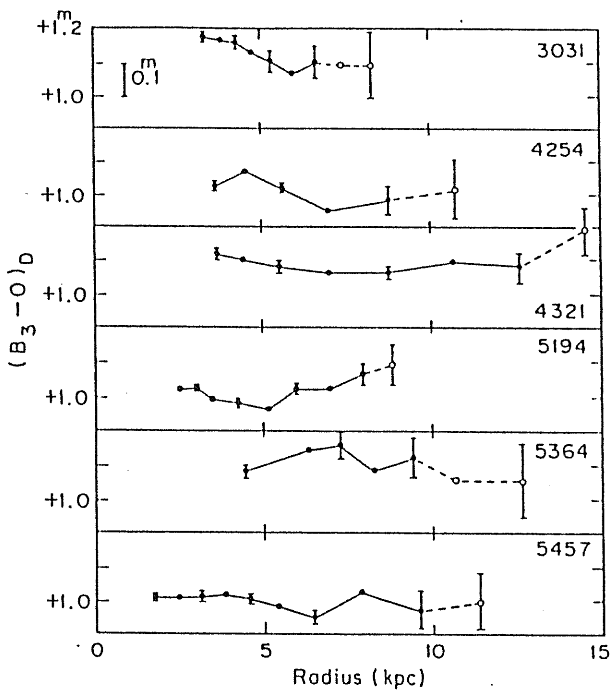

Figure 2.3: The color index $(B_3 - O)_D$ of the disk as a function of radius. The error bars show the sky subtraction error. (from Schweizer, 1976).

In spiral galaxies, the light is dominated by the disk component. Thus, in integrating the amount of light in rings in the plane of the galaxy, one effectively obtains the light distribution of the old, underlying disk of the galaxy onto which a relatively minor contribution from small active regions in the arms is superimposed. Hence, at all radii, the light comes from a mixture of stars of all types of different ages. This should be clearly distinguished from the light distribution of elliptical galaxies and of bulges of spirals, where the stars are thought to be all equally old. Hence, any radial color changes in elliptical galaxies and in bulges of disk galaxies are the direct result of abundance gradients, whereas color gradients in disk galaxies predominantly reflect differences in photometric evolution.

The disk colors are very uniform, with radial gradients mostly below the detection limit (± 0.010 mag kpc^{-1} in B_V), and lie in the narrow range of colors between old galactic clusters ($(B-V) \sim +0.7$) and giant elliptical galaxies ($(B-V) \sim +0.9$). Fig.2.3 show the tipical color distributions of spiral galaxies. The photometric band is different by the standard UBV system and has been devised by Schweizer (1976) to discriminate between young and old stars. Straightforward conversion to the Johnson system are in Schweizer (1974).

The arms are significantly bluer than the disks and have a highly composite spectrum, as judged from the color indices. The ratio of arm intensity to disk intensity increases with radius, which explains the well known outward bluing of spiral galaxies. There are also indications that the ratio of total arm intensity to total disk intensity, which is a coarse measure of the strength of star formation, correlates with the compression strength index of the gas introduced by van der Kruit (1973a).

From the constancy of the $(J - F)$ color index and the absence of clear gradients in $(U' - J)$, Wevers (1984) inferred that the time dependence of the star formation rate is not a strong function of radius. Since a significant change in the slope of the initial mass function (IMF) with radius would involve an observable color gradient, the IMF is, to the first approximation, also independent of radius. Stronger evidence for a constant IMF with radius is supplied by two types of observations: one pertaining to both surface photometry and HI observations of edge–on galaxies, the other to HI observations of face–on galaxies. For example, since from HI observations of the face–on galaxies NGC 3938, NGC 628 and NGC 1058 (Van der Kruit and Shostak, 1982, 1983; Shostak and Van der Kruit, 1983), the velocity dispersion (in the z direction) turns out to be roughly constant over the whole disk (to within 30%), it is reasonable to assume a constant M/L ratio throughout the old disk of a spiral galaxy.

Since the light of spiral galaxies come mainly from three sources: the old stars of the disk, the young Population I stars of the spiral arms, and the Population II stars of the bulge and the halo, to study the distribution of the old disk population and of the young arm population, it is necessary an *operational definition* of the "disk" and the "arms".

The "*disk*" is the axisymmetrical part of the light distribution which one obtains (1) by selecting, on each azimuthal profile, the two deepest minima separated by more than 90° in azimuth, and (2) by drawing a level line at the mean surface brightness of these two points (see Fig.2.4). In selecting the minima, dips produced by dust lanes must be carefully avoided.

The "*arms*" are correspondingly defined as the average amount of light above the axisymmetrical disk. One obtains this amount by subtracting the SB of the disk from the mean SB of each profile. However, if the distribution of the old disk population is not axisymmetrical, the above definition assign some of the light from this old disk to the arms.

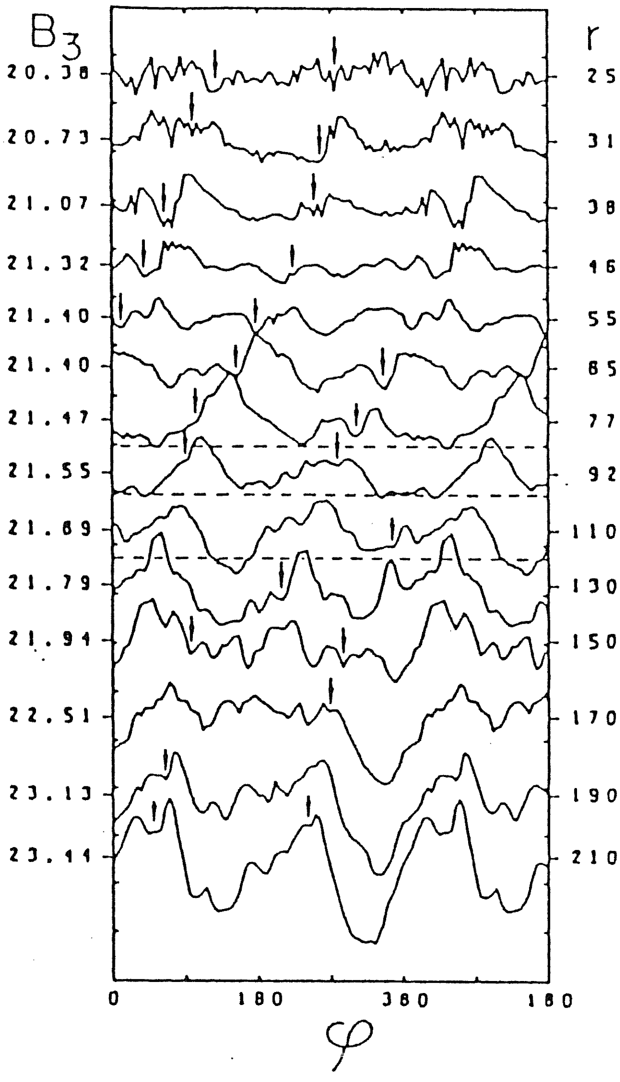

Figure 2.4: Azimuthal surface–brightness profile of NGC 5194. The dashed line below three profiles indicate the levels chosen for the axisymmetrical disk. Arrows pointing downward indicate the locations of strong dust lanes (from Schweizer, 1976).

References

Athanassoula, E., and Martinet, L.: 1980, *Astron. Astrophys.*, **87**, L10.
Babcock, H.W.: 1939, *Lick Obs. Bull.*, **19**, 41.
Bergh, S. van den: 1960, *Astrophys. J.*, **131**, 215 and 558.
Bertola, F., and Capaccioli, M.: 1975, *Astrophys. J.*, **200**, 439.
Bertola, F., and Capaccioli, M.: 1977, *Astrophys. J.*, **211**, 697.
Bertola, F., Vietri, M., and Zeilinger, W.W.: 1988, *The Messanger*, **52**, 24.
Boroson, T., and Kormendy, J.: 1982,
Capaccioli, M.: 1987, in IAU Symp. No. 127, *Structure and Dynamics of Elliptical Galaxies*, (Princeton), ed. T.P. de Zeew, Reidel:Dordrecht, p.47.
Capaccioli, M.: 1989,
Cohen, R.S., and Thaddeus, P.: 1977, *Astrophys. J. Letters*, **217**, 155.
Danver, C.G.: 1942, *Lund Obs. Ann.*, Vol. 10.
de Vaucouleurs, G.: 1958, *Astrophys. J.*, **128**, 465.
de Vaucouleurs, G.: 1959, *Hand. der Physik*, **53**, 311.
de Vaucouleurs, G.: 1959a, *Hand. der Physik*, **53**, 275.
de Vaucouleurs, G.: 1961, *Astrophys. J. Supp.*, **5**, 233.
de Vaucouleurs, G.: 1963, *Astrophys. J. Supp.*, **8**, 31.
de Vaucouleurs, G.: 1975, *Astrophys. J. Supp.*, **29**, 193.
de Vaucouleurs, G., and Buta, R.: 1980, *Astron. J.*, **85**, 637.
Dressler, A., and Sandage, A.: 1983, *Astrophys. J.*, **265**, 664.
Efstathiou, G., Lake, G., and Negroponte, J.: 1982, *Mont. Not. R. astr. Soc.*, **199**, 1069.
Eggen, O.J., Lynden–Bell, D., and Sandage, A.: 1962, *Astrophys. J.*, **136**, 748.
Elmegreen, D.M., and Elmegreen, B.G.: 1982, *Mont. Not. R. astr. Soc.*, **201**, 1021.
Faber, S.M.: 1977, in *The Evolution of Galaxies and Stellar Population*, eds. B.M. Tinsley and R.B. Larson (New Haven: Yale University Observatory), p.157.
Faber, S.M., and Jackson, R.E.: 1976, *Astrophys. J.*, **204**, 668.
Freeman, K.C.: 1979, *Astrophys. J.*, **160**, 811.
Freeman, K.C.: 1975, in *Star and Stellar Systems IX: Galaxies and the Universe*, eds. A. Sandage, M. Sandage, and J. Kristian (Chicago: University of Chicago Press), p.409.
Gerhard, O.E., and Vietri, M.: 1986, *Mont. Not. R. astr. Soc.*, **223**, 377.
Gerhard, O.E., and Vietri, M.: 1987, in *Strucure and Evolution of Elliptical Galaxies*, IAU Symp. No.127, ed. P.T. de Zeeuw (Reidel:Dordrecht), p.399.
Gordon, M.A., and Burton, W.B.: 1976, *Astrophys. J.*, **208**, 346.
Hartkopf, W.I., and Yoss, K.M.: 1982, *Astron. J.*, **87**, 1679.
Holmberg, E.: 1937, *Lund Obs. Ann.*, Vol. 6.
Huchra, J.P.: 1977, *Astrophys. J.*, **217**, 928.

Illingworth, G.: 1977, *Astrophys. J. Letters*, **218**, L43.
Illingworth, G., and Schechter, P.L.: 1982, *Astrophys. J.*, 256, 481.
Jensen, E.B., and Thuan, T.X.: 1982, *Astrophys. J. Supp.*, **50**, 421.
Kalnajs, A.: 1972, *Astrophys. J.*, **133**, 413.
Kennicutt, R.C.: 1981, *Astron. J.*, **86**, 1847.
Kennicutt, R.C.: 1982, *Astron. J.*, **87**, 255.
Kormendy, J.: 1979, *Astrophys. J.*, **227**, 714.
Kormendy, J.: 1980, in *ESO Workshop on Two Dimensional Photometry*, eds. P. Crane and K. Kjär (Geneva: ESO), p.191.
Kormendy, J.: 1982a, *Astrophys. J.*, **257**, 75.
Kormendy, J., and Bruzual, A.G.: 1978, *Astrophys. J. Letters*, **223**, L63.
Kormendy, J., and Illingworth, G.: 1982, *Astrophys. J.*, **256**, 460.
Kormendy, J., and Koo, D.: 1982,
Kruit, P.C., van der: 1973a, *Astron. Astrophys.*, **29**, 263.
Kruit, P.C., and Searle, L.: 1982, *Astron. Astrophys.*, **110**, 61.
Kruit, P.C. van der, and Shostak, G.S.: 1982, *Astron. Astrophys.*, **105**, 351.
Kruit, P.C. van der, and Shostak, G.S.: 1983, in *Internal Kinematics and Dynamics of Galaxies*, IAU Symp. No.100, ed. E. Athanassoula (Reidel: Dordrecht), p.69.
Larson, R.B., and Tinsley, B.M.: 1978, *Astrophys. J.*, **219**, 46.
Lewis, J.R.: 1986, *Ph.D. Thesis*, Aust. Natl. Univ., Canberra.
Lindblad, B.: 1956, *Stockholm Obs. Ann.*, **19**, No.2.
Lundmark, K.: 1926, *Ark. Math. Astr. Phys.*, Ser. B, Vol. 19, No. 8.
Lundmark, K.: 1927, *Medd. Astr. Obs. Uppsala*, No. 30.
Morgan, W.W.: 1958, *Publ. Astron. Soc. of Pacific*, **70**, 364.
Morgan, W.W.: 1959, *Publ. Astron. Soc. of Pacific*, **71**, 394.
Morgan, W.W., and Mayall, N.U.: 1957, *Publ. Astron. Soc. of Pacific*, **69**, 291.
Ostriker, J.P., and Peebles, P.J.E.: 1973, *Astrophys. J.*, **186**, 467.
Pellet, A.: 1976, *Astron. Astrophys.*, **50**, 421.
Peterson, C.J.: 1978a, *Astrophys. J.*, **221**, 80.
Prendergast, K.H., and Tomer, E.: 1970, *Astron. J.*, **75**, 674.
Reinmuth, K.: 1926, *Veroff. Sternw. Heidelbergh*, Vol.9.
Reiz, A.: 1941, *Lund Obs. Ann.*, Vol. 9.
Richstone, D.O., and Schectman, S.A.: 1980, *Astrophys. J.*, **235**, 30.
Rubin, V.C., and Graham J.A.: 1987, *Astrophys. J.*, **316**, L67.
Rubin, V.C., Ford, W.K., and Kumar, C.K.: 1973, *Astrophys. J.*, **181**, 61.
Rubin, V.C., Ford, W.K., and Thonnard, N.: 1982, *Astrophys. J.*, **261**, 439.
Sandage, A.: 1961, *The Hubble Atlas of Galaxies*, Carnegie Institute of Washington.
Sandage, A.: 1975, in *Star and Stellar System IX: Galaxies and the Universe*, eds. A. Sandage, M. Sandage, and J. Kristian, (Chigago: University of Chigago Press), p.1.
Sandage, A., Freeman, K.C., and Stokes, N.R.: 1970, *Astrophys. J.*, **160**, 831.

Sandage, A., and Tamman, G.: 1981, *The Revised Shapley–Ames Catalogue*, (Washington: Carnegie Institute of Washington).
Sargent, W.L.W., Schechter, P.L., Boksemberg, A., and Shortridge, K.: 1977, *Astrophys. J.*, **212**, 326.
Schechter, P.L., and Gunn, J.E.: 1979, *Astrophys. J.*, **229**, 472.
Schweizer, F.: 1976, *Astrophys. J. Supp.*, **31**, 313.
Scoville, N.Z., and Solomon, P.M.: 1975, *Astrophys. J.*, **199**, L105.
Searle, L., Sargent, W.L.W., and Bagnuolo, W.G.: 1973, *Astrophys. J.*, **179**, 427.
Shapley, H.: 1928, *Harv. Bull.*, **849**.
Shostak, G.S., and Kruit, P.C. van der: 1983, *Astron. Astrophys.*,
Solomon, P.M., Sanders, D.B., and Scoville, N.Z.: 1979, IAU Symp. No.84, ed. B. Burton, p.35.
Stark, A.A.: 1977, *Astrophys. J.*, **213**, 368.
Talbot, R.J., Jensen, E.B., and Dufour, R.J.: 1979, *Astrophys. J.*, **229**, 91.
Takase, B.: 1967, *Pub. Astr. Soc. Japan*, **19**, 409.
Tinsley, B.M.: 1975, *Mem. Soc. Astron. It.*, **46**, 3.
Toomre, A.: 1964, *Astrophys. J.*, **139**, 1217.
Vorontsov–Velyaminov, B.A., Krasnogorskaia, A., and Arkipova, V.P.: 1962, *Morphological Catalog of Galaxies*, (Moscow), Vol.1.
Vorontsov–Velyaminov, B.A., Krasnogorskaia, A., and Arkipova, V.P.: 1963, *Morphological Catalog of Galaxies*, (Moscow), Vol.2.
Vorontsov–Velyaminov, B.A., Krasnogorskaia, A., and Arkipova, V.P.: 1964, *Morphological Catalog of Galaxies*, (Moscow), Vol.3.
Vorontsov–Velyaminov, B.A., Krasnogorskaia, A., and Arkipova, V.P.: 1968, *Morphological Catalog of Galaxies*, (Moscow), Vol.4.
Wevers, B.M.H.R.: 1984, *Ph.D. dissertation*, Groningen.
Wilson, C.P.: 1975, *Astron. J.*, **80**, 175.
Wolf, M.: 1908, *Pub. Ap. Inst. König. Heidelbergh*, Vol.3, No. 5.

Chapter 3

Bulge–to–Disk luminosity ratio and central surface brightness

3.1 Bulge–to–disk ratio

It is now a well accepted fact in the astronomical community that the two most fundamental components of spiral galaxies are a spheroidal or ellipsoidal distribution of stars (bulge) and a flat distribution of stars (disk).

Models for the formation of galaxies make an attempt to explain this observation. There is, for example, a class of models in which spheroids form during the initial collapse of a protogalaxy, with disks forming in a later phase from the infall of high–angular momentum gas (Faber, 1982; Gunn, 1982). In this hypotesis, the ratio of the spheroid luminosity to total luminosity measures the efficiency of the first burst of star formation. A second class of models would have spheroids formed from mergers of disks, with the process of spheroid formation continuing into the present (Toomre and Toomre, 1972; Toomre, 1977; Tremaine, 1981; White, 1982). In this hypotesis the ratio of spheroid to total luminosity measures the gas fraction locked into stars at the time when the last merger occurred.

The relative importance of the two components appears to vary smoothly along the Hubble sequence (de Vaucouleurs, de Vaucouleurs and Corwin, 1976 (RC2); Simien and de Vaucouleurs, 1983; Okamura, Kodaira and Watanabe, 1984). This relative importance is usually expressed by the bulge–to–disk luminosity ratio.

The observed ratio of spheroid luminosity to disk luminosity, measured in different environments and for galaxies of different absolute magnitude, provides fundamental data for constraining competing models of galaxy formation and evolution. At present, neither the "angular momentum drives morphology" model nor the "mergers drive morphology" model have been able to point quantitative predictions about the relative proportions of bulge and disk, and also do not make quantitative predictions about the variation of the bulge–to–disk ratio with Hubble type.

For having a good measure of this ratio, de Vaucouleurs (1958) first recognized the necessity of decomposing the observed light profiles into spheroid and disk components. He measured the B/D ratio of M31.

After him, van Houten (1961) and Kormendy (1977b) pointed out that the the necessity of the decomposition procedure reside in the fact that spheroids contribute significant light in the regions dominated by the disk. The decomposition method approximate the bulge and the disk components with a de Vaucouleurs' $r^{1/4}$ law and an exponential disk respectively:

$$\mu_{bulge} = \mu_e + 8.325[(r/r_e)^{1/4} - 1] \tag{3.1}$$

$$\mu_{disk} = \mu_0 + 1.082(r/h) \tag{3.2}$$

In this equations, μ is the surface brightness in $mag\ arcsec^{-2}$ at a radius r, μ_e and μ_0 are characteristic surface brightness, r_e is the effective radius containing one–half the total light of the bulge component, and h is the exponential scale length of the disk. These laws are strictly empirical fitting functions, and other laws (*e.g.*, a King model for the bulge) might provide equally good fits to a galaxy profile but with different bulge/disk parameters. Some galaxies cannot be fitted by these simple functions, as, *e.g.*, Freeman's (1970) type II disks, or galaxies with strong bars.

Two ways are used for the decomposition:

1. Iterative fitting.— It begins by making a least squares fit of an exponential in the disk range. This is extrapolated into the range of the spheroid, and subtracted from the observations to get a first estimate of the underlying spheroid. Fitted to this, is a de Vaucouleurs law which is then extrapolated into the disk range and subtracted from the observations to get the underlying disk. In 8 to 10 iterations both underlying profiles are determined. Nevertheless, there are problems with the unicity of the solutions (Kormendy, 1977b).

2. Standard nonlinear least-squares.—It solves for the parameters μ_e, μ_0, r_e and h, as introduced above, with the disk and the spheroid fitted simultaneously. The disadvantage is that the parameters are strongly coupled, and the relative contribution of spheroid and disk can be varied considerably without very much affecting the quality of the fit (Kormendy, 1977b).

Fig.3.1 shows an example of decomposition. The apparent spheroid and the disk profiles become fainter when the contamination by the other component is removed. The spheroid becomes steeper, reducing r_e slightly and making μ_e brighter. In contrast, the disk becomes much shallower, fainter and less exponential. As a result, α^{-1} is very large (essentially indeterminate), and $B(0)_c$ is formally much fainter.

Most interesting is the behaviour in the transition region. We can see that the underlying disk profile has a brightness cutoff as it enters the dominant part

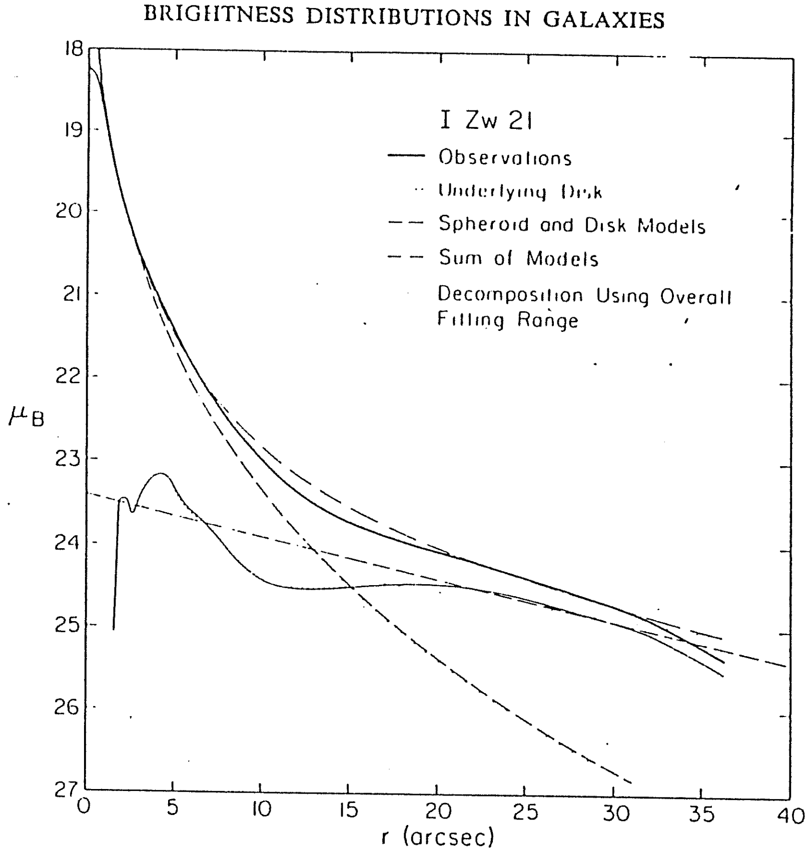

Figure 3.1: Decomposition of I Zw 21, using the iterative fitting algorithm (from Kormendy, 1977b).

of the spheroid. Burstein (1979) argued from his disk–to–bulge decomposition of S0 galaxies that the luminosity profiles of these galaxies can be adequately fitted with at most only a change in slope of the disk as it enters the bulge. Further information on inner cutoffs has been obtained by van Houten (1961) by comparing the major axis to the minor axis in galaxies which are nearly edge–on. He assumed that both the major and minor axis profiles near the centre were due to the bulge alone. With this assumption he got an axial ratio for the bulge and a disk profile along the major axis that cuts off near the centre. However, if the projected disk luminosity is comparable to the bulge in the centre, then the central axial ratio is due to both bulge and disk, and with his assumption van Houten made the disk–light contribution to disappear in the centre by definition.

An alternative method of profile decomposition which does not depend on the use of a priori fitting laws, has been developed by Kent (1986). It is assumed that both the bulge and disk have luminosity profiles that, in projection, have elliptical isophotes of constant flattening. This would be true if the bulge were an oblate spheroid and the disk were axisymmetric and thin. Then the galaxy major and minor axis profiles are each the sum of the two individual luminosity profiles of the bulge and disk but with different radial scale factors. If the apparent flattening of the bulge and disk are different, then the major and minor axis profiles can be decomposed uniquely to recover the individual profiles. Several factors influence the reliability of this decomposition. The bulge flattening is not always well determined because the bulge does not always dominate even in the centre. Seeing can distort the inner profile. Nonaxisymmetric structure in the disk and a change in flattening with radius in the bulge will also cause systematic errors.

Recently, Simien and de Vaucouleurs (1986) reviewed this subject. Mean values of spheroid and disk parameters are collected in Table 3.1. The symbol (I) is referred to the spheroidal component, and (II) to the disk. Δm_I is the magnitude difference between the spheroidal component and the total luminosity of the galaxy, while the other symbols have their classical meaning.

From photometric decompositions of 98 galaxies into bulge and disk components, they found the following results:
1) The mean fractional luminosity of the spheroidal component is a monotonically decreasing function of the Hubble type T, from early type lenticulars to late type spirals ($-3 \leq T \leq 7$). These data give no support to the suggestion that lenticulars form a gas poor sequence of disk systems parallel to the gas rich spiral sequence.
2) There is a suggestion that at a given Hubble stage barred spirals may have somewhat brighter and smaller bulges than ordinary spirals, and that spirals with stronger bulges tend to be redder than average.
3) The variations along the Hubble sequence of the mean absolute magnitudes, effective radii, and effective specific intensities of the spheroidal and disk compo-

MEAN VALUES OF SPHEROID AND DISK PARAMETERS

MEAN VALUES	T											
	−5	−3	−2	−1	0	1	2	3	4	5	6	7
$\langle \Delta m_1 \rangle$	0.00	0.57	0.60	0.63	0.74	1.13	1.22	1.62	1.85	2.52	3.43	4.06
m.e.	...	0.13	0.08	0.12	0.07	0.41	0.15	0.15	0.22	0.22	0.26	0.48
n	...	11	13	7	5	5	20	17	18	9	10	5
$\langle M_T(\mathrm{I}) \rangle$	−19.4	−18.59	−18.75	−19.09	−19.61	−18.68	−18.75	−18.53	−18.09	−16.65	−15.96	−13.88
m.e.	...	0.38	0.22	0.25	0.33	1.00	0.25	0.14	0.27	0.28	0.32	0.49
n	...	11	13	7	5	5	20	17	18	9	10	5
$\langle M_T(\mathrm{II}) \rangle$	...	−18.24	−18.66	−18.85	−19.37	−18.48	−19.51	−19.74	−19.64	−19.21	−19.37	−17.92
m.e.	...	0.26	0.27	0.35	0.30	0.35	0.16	0.20	0.15	0.29	0.44	0.19
n	...	11	13	7	5	5	20	17	18	9	10	5
$\langle M_T(\mathrm{I}+\mathrm{II}) \rangle$	−19.4	−19.34	−19.50	−19.81	−20.28	−19.55	−20.04	−20.10	−19.98	−19.33	−19.44	−17.95
m.e.	...	0.29	0.23	0.25	0.28	0.71	0.16	0.17	0.13	0.28	0.43	0.20
n	...	11	13	7	5	5	20	17	18	9	10	5
$\langle \mu_e(\mathrm{I}) \rangle$	22.4	20.18	21.00	20.28	20.50	23.05	21.50	21.49	21.65	21.64	22.20	22.20
m.e.	0.1	0.43	0.35	0.98	1.08	0.52	0.56	0.46	0.58	1.30	0.72	0.90
n	...	10	11	3	2	4	9	9	10	6	9	5
$\langle \mu_e(\mathrm{II}) \rangle$	...	23.64	23.43	23.04	24.08	24.36	23.53	23.62	23.38	22.59	23.57	23.98
m.e.	...	0.35	0.29	0.50	0.51	0.30	0.29	0.18	0.20	0.43	0.37	0.35
n	...	9	10	3	4	4	8	9	11	6	9	5
$\langle r_e(\mathrm{I}) \rangle$	1.20	0.92	1.23	1.01	1.24	3.13	1.43	1.42	1.33	1.40	0.82	0.25
m.e.	0.15	0.29	0.23	0.53	0.84	1.42	0.23	0.31	0.46	0.85	0.27	0.10
n	...	10	11	3	2	4	9	9	10	6	9	5
$\langle \log r_e(\mathrm{I}) \rangle$	0.08	−0.18	0.01	−0.11	−0.04	0.29	0.10	0.08	−0.08	−0.29	−0.29	−0.75
m.e.	0.11	0.12	0.09	0.21	0.36	0.26	0.08	0.09	0.14	0.31	0.16	0.17
n	...	10	11	3	2	4	9	9	10	6	9	5
$\langle r_e(\mathrm{II}) \rangle$	...	4.20	4.50	3.92	7.74	4.93	5.78	7.39	1.70	3.89	5.43	2.21
m.e.	...	0.81	0.77	0.25	1.72	0.65	0.96	0.95	0.54	0.77	0.60	0.32
n	...	9	10	3	4	4	8	9	11	6	9	5
$\langle \log r_e(\mathrm{II}) \rangle$	...	0.55	0.59	0.59	0.85	0.68	0.73	0.84	0.75	0.55	0.71	0.33
m.e.	...	0.10	0.08	0.03	0.11	0.06	0.06	0.05	0.04	0.08	0.06	0.07
n	...	9	10	3	4	4	8	9	11	6	9	5

Table 3.1: Mean values of spheroid and disk parameters (from Simien and de Vaucouleurs, 1986).

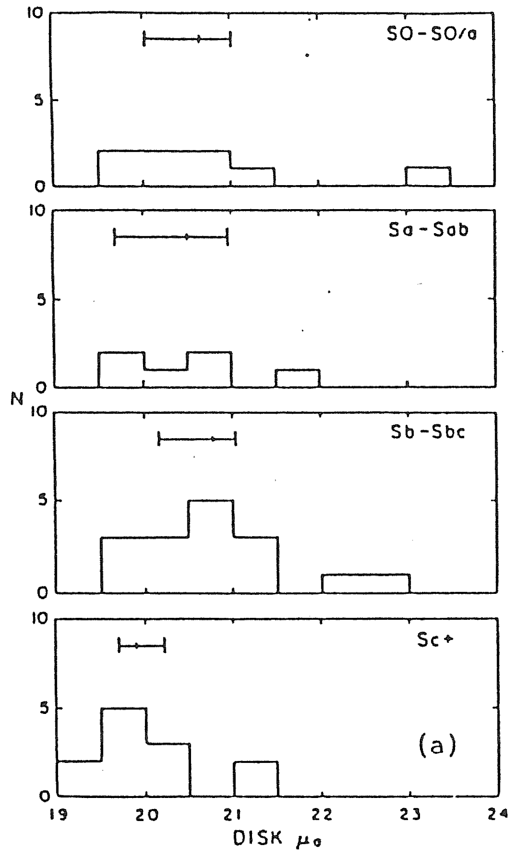

Figure 3.2: Distribution of μ_0 as a function of morphological type (from Kent, 1985).

nents, show that, on average, the spheroids of lenticular galaxies are systematically smaller and denser, but fainter in total luminosity than elliptical galaxies. *4)* The large range of absolute magnitudes, effective radii, and specific intensities of both spheroid and disk components at each stage do not support the view that the Hubble sequence is uniquely determined by the absolute magnitude of the spheroidal component.

Considerable efforts were made recently in deriving structural properties of spheroids and disks from detailed surface photometry using photographic plates (*e.g.*, Kormendy 1977a,b,c; King 1978; Burstein 1979a,b,c; Tsikoudi 1980; Boroson 1981; Hamabe 1982; Watanabe 1983; Boroson, Strom, and Strom 1983) or CCD and other electronic devices (*e.g.*, Thomsen and Frandsen 1983; Kent 1984, 1985; Lauer 1985; Kormendy 1985).

Only a few collections of homogeneous surface photometry data exist for a large samples of galaxies which are relevant to a statistical study of galaxy structure. One of the most important is that of Kent (1985), who made CCD photometry of 105 field spirals of all morphological types. He explored the correlations among the structural parameters and the Hubble type.

Looking at the disk parameters he found that the distribution of μ_0 does not depend noticeably on type, with the possible exception of type Sc and later,

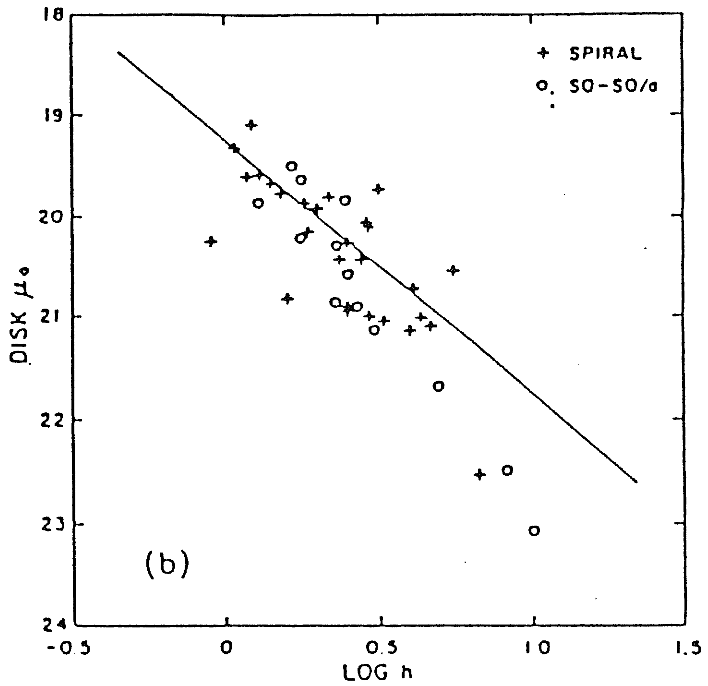

Figure 3.3: Correlation between μ_0 and h (from Kent, 1985).

but color effects may be present. The median value $\mu_0 = 20.5$ corresponds to a blue central surface brightness $\mu_0(B) \sim 21.3$, which is in close agreement with previous determinations. Fig.3.2 present the distribution of disk μ_0 sorted by morphological type. There is also a striking correlation between μ_0 and h, but this is virtually the line of constant luminosity, and the scatter of the diagram would be reduced if fainter disks are added to his sample. Fig.3.3 plots the disk parameters μ_0 against h.

It should be noted that the disks of S0 galaxies occupy the same region in the diagrams as those of spirals.

A set of similar plots shows the correlations found for the bulge parameters. Fig.3.4 plots the distribution in bulge surface brightness μ_e for different morphological types. Elliptical galaxies are also included in the plot. Unlike the disk component, the bulge surface brightness μ_e does show a dependence on type, declining by ~ 2 mag in going from S0 to Sc. The scatter in the ellipticals is much smaller than for the bulges, although part of this scatter is likely due to decomposition errors. Fig.3.5 show the relation between μ_e and r_e. There is a loose correlation between the two parameters, albeit with large scatter.

A statistical study of the correlations among structural parameters has been also provided by Kodaira, Watanabe, and Okamura (1986). Luminosity distributions of 167 galaxies in the Virgo cluster and the Ursa Major clouds are

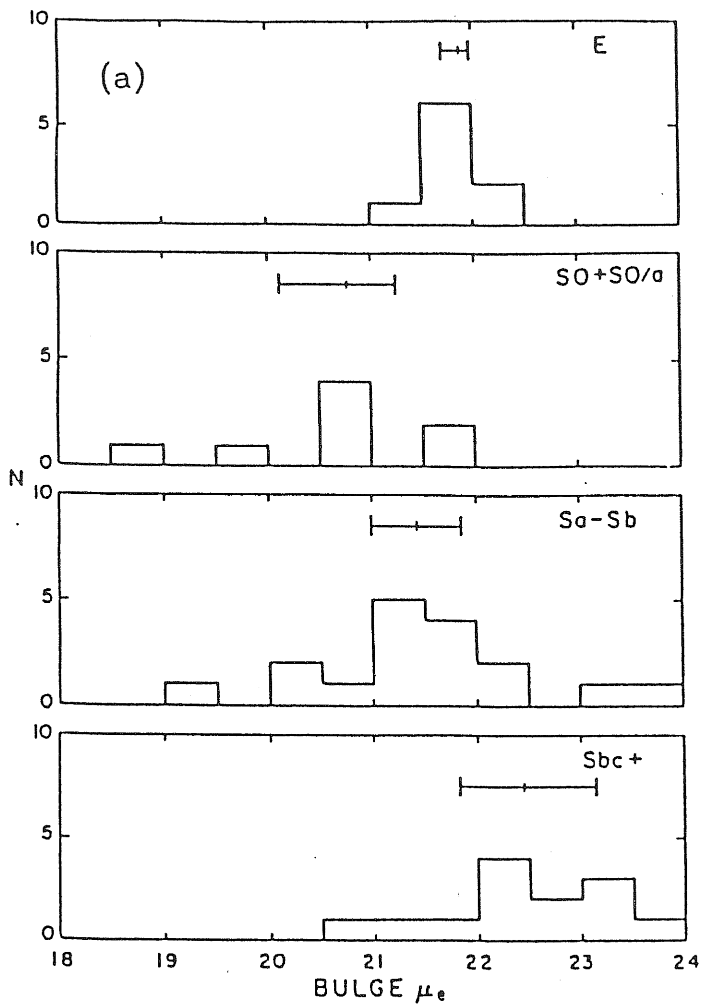

Figure 3.4: Distribution of μ_e as a function of morphological type (from Kent, 1985).

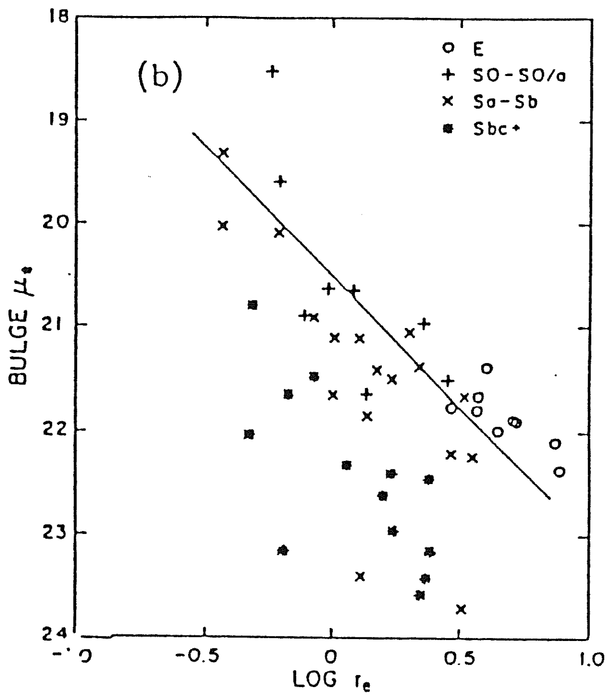

Figure 3.5: Correlation between μ_e and r_e. The line of constant luminosity is drawn (from Kent, 1985).

decomposed into spheroid and disk components.

Since the goodness of the fit to the observed radial luminosity profile is used as the only criterion to identify the best models ($r^{1/4}$, exponential, King or Hubble laws), the authors preferred to introduce a less subjective technique, in which reproducibility of global surface–photometric parameters such as luminosity and size, are taken as criteria to identify the best model. More precisely, they define a three–dimensional space of global surface–photometric parameters, diameter, mean surface brightness and mean concentration index. The distance in this space between a model and an observed galaxy is defined by:

$$d^2 = [\Delta log(D_{26}/\sigma_D)]^2 + (\Delta SB/\sigma_{SB})^2 + [\Delta X1(P)/\sigma_x]^2 \qquad (3.3)$$

where Δ means the difference of parameter values between the model and the galaxy and σ stands for the standard deviation of respective parameters in the sample of galaxy under consideration.

From their work we can extract the following results:
1) The majority (137 out of 167) of sample galaxies can be well approximated by two–component models with spheroid–to–disk luminosity ratios in the range of 0.1–10;

2) All the 21 elliptical galaxies in the sample are approximated by two–component models better then by one–component spheroid models.
3) Spheroids of disk galaxies are, on average, less luminous and have both fainter brightness–scale parameter, μ_e, and larger length–scale parameter, r_e, even at the same absolute magnitude, than those of elliptical galaxies. Spheroid parameters of disk galaxies cover a very wide range (10 mag in μ_e and 1.9 dex in r_e). This large scatter indicates that spheroid of disk galaxies cannot be regarded as a nearly one–parameter family. Spheroids of S0 galaxies appear to have structural parameters intermediate between those of elliptical and spiral galaxies.
4) Disk parameters of the majority of the sample galaxies are confined within a narrow range (4 mag in μ_0 and 0.7 dex in h), in contrast to the very wide range of spheroids. This may suggest that disks, at least those of very bright galaxies, can be formed through a process which is not affected very much by spheroid properties.
5) Hubble type does not show a tight correlation with either the spheroid magnitude, the disk magnitude, or the spheroid–to–disk luminosity ratio, contrary to the results of Simien and de Vaucouleurs (1986).

Fig.3.6 shows the correlation between the spheroid parameters, $\mu_{0,s}$ (equivalent to μ_e), and $\log(r_{0,s})$ (equivalent to r_e). The dashed diagonal line is that of constant total absolute magnitude, while the solid line is the Kormendy (1977c) relation between the brightness–scale and the length–scale parameters for elliptical and spheroid dominated S0 galaxies.

From this figure we can extract at least three points which may have important implications for the theory of galaxy formation. First, there is a systematic difference between the spheroids of elliptical galaxies and those of disk galaxies. Second, there exist very faint and large spheroids (with $\log(r_{0,s}) \gtrsim 0.5$ and $\mu_{0,s} \gtrsim 24$) in disk galaxies, and third, spheroids of later type spirals tend to have both fainter $\mu_{0,s}$ and larger $r_{0,s}$ than those of earlier type spiral galaxies.

Fig.3.7 is the analogous of Fig.3.6 for disk parameters. The most striking feature of the figure is the compactness of the distribution. With only a few exception the disk parameters fall in a restricted range, although this may partly caused by selection effects. Disk of early type galaxies exhibit a slightly different distribution from those of spiral galaxies: the distribution extend toward looser (larger $r_{0,d}$ and fainter $\mu_{0,d}$) and toward more compact (smaller $r_{0,d}$ and brighter $\mu_{0,d}$) direction.

It is not clear whether there is any systematic difference in the parameters between the field sample of Kent (1985) and the cluster sample of Kodaira, Watanabe and Okamura (1986).

It is well known that for half of the disk galaxies, decompositions of the galaxy light profile into bulge and disk components are not possible. This problem manifests itself in two ways. First, disks are seldom represented by a single exponential law over their entire range. Significant structure is introduced by

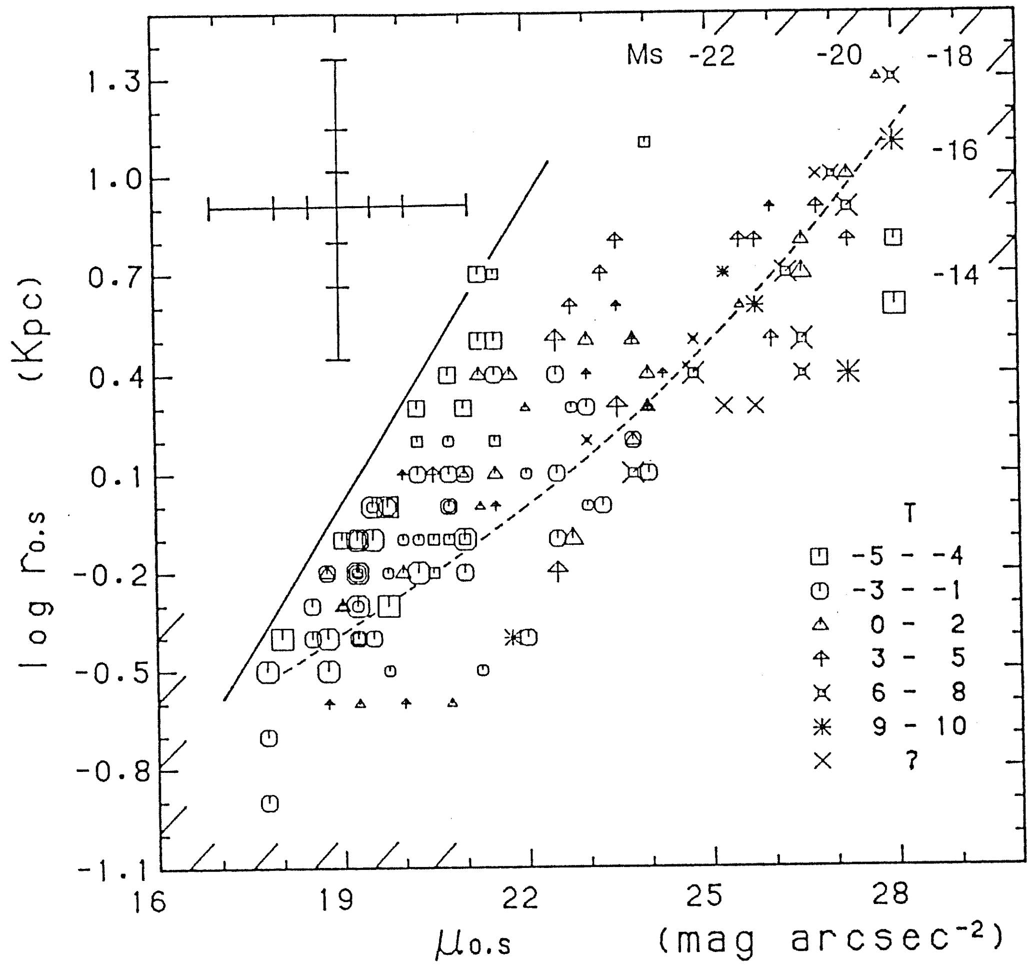

Figure 3.6: Correlation between length–scale parameter and brightness–scale parameter for spheroids. Galaxies are sorted into seven bins according to morphological type and plotted with different symbols (RC2). The size of the symbols varies with weight. Estimated errors for the three weight classes are indicated by the error bars at the left–hand corner (from Kodaira *et al.* 1986.

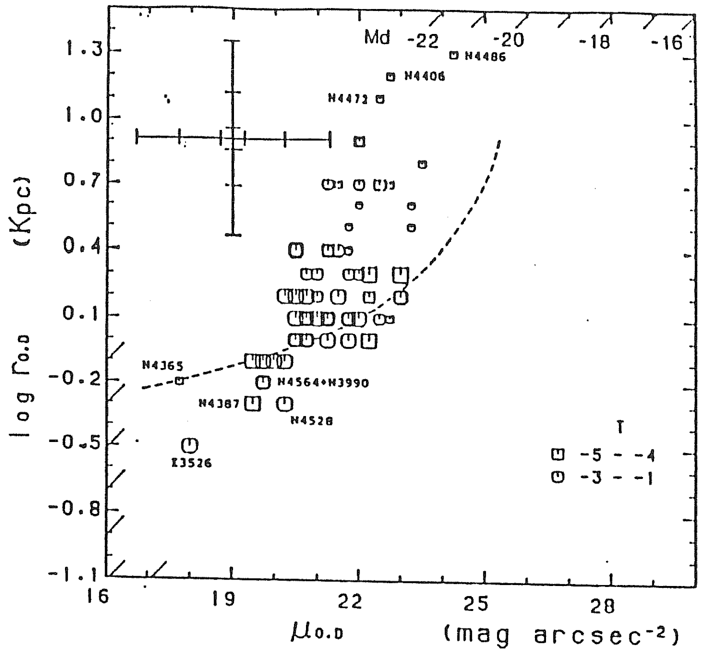

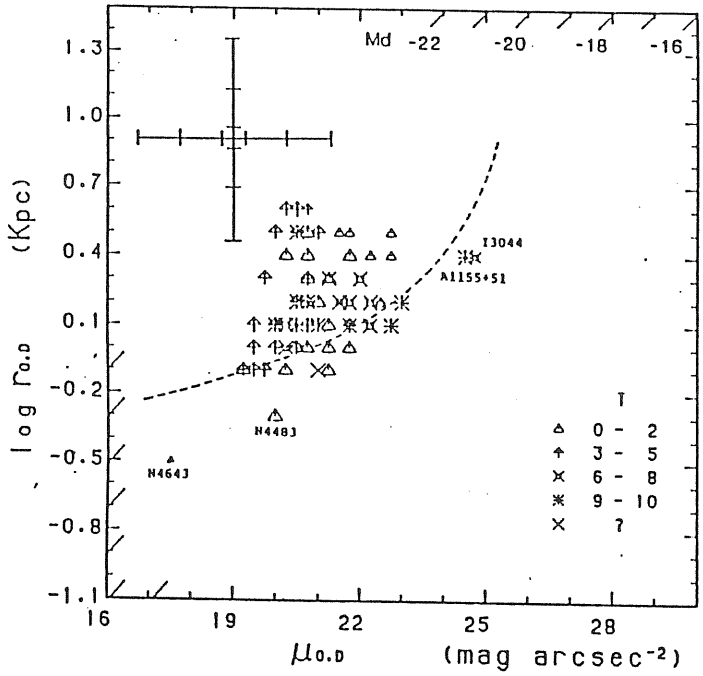

Figure 3.7: Correlation between length–scale parameter and brightness–scale parameter for disk of spirals and for those of elliptical and S0 galaxies. The size of the symbols varies with weight. Estimated errors for the three weight classes are indicated by the error bars at the left–hand corner (from Kodaira *et al.* 1986).

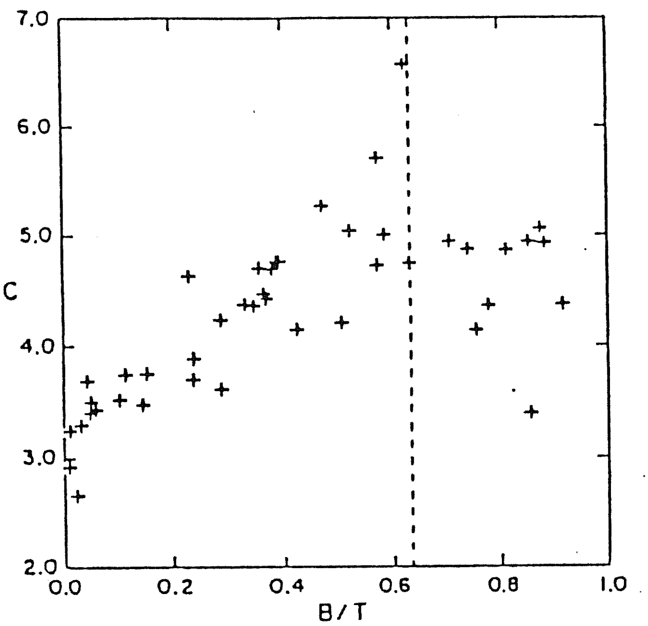

Figure 3.8: Correlation between concentration parameter c and B/T (from Kent, 1985).

spiral arms, lenses, and rings. Disks also can have global shapes that fall off less steeply or more steeply than exponential. Second, the bulges fall off more steeply than an $r^{1/4}$ law in regions where the disk dominates. For this reason, people tried to characterize the light distribution in a galaxy by some parameters which do not depend on the details of the light profile. One of these, is the concentration index (that we have already encountered above), defined to be the ratio of two radii, each of which contains some fixed fraction of the total galaxy luminosity. Formally, the concentration of a galaxy can be defined to be

$$c = 5log[r(0.8)/r(0.2)] \tag{3.4}$$

where $r(0.2)$ and $r(0.8)$ are the radii which contain 20% and 80% of the total luminosity respectively. There is indeed a good correlation between c and B/T (Fig.3.8). A similar dependence is found between c and morphological type, but this is expected since B/T also correlate with morphological type. Good correlations exist among c and $\overline{\mu_e}$ or $\overline{\mu_{24}}$ as well (which represent the mean surface brightness inside r_e and the $\mu_r = 24$ isophote).

It has been demonstrated that the four quantities c, B/T, $\overline{\mu_e}$ and morphological type are all strongly correlated with one another. A Principal Components Analysis (PCA) reveals that there is indeed only one significant correlation among the four variables. The strongest is between c and B/T (90%), and indeed all parameters correlate best with c.

Whitmore (1984) compiled a large number of observational parameters for the sample of spiral galaxies of Rubin *et al.* (1980, 1982) and performed also PCA. He demonstrated that roughly 85% of the observational variance in the most important observational properties can be explained by two dimensions, which he tentatively identified as the "scale" (a combination of the absolute blue luminosity and the absolute radius at the 25th B $mag\ arcsec^{-2}$ isophote) and the "form" (a combination of the $(B - H)$ color and the bulge–to–total light ratio).

At the basis of PCA is the fact that of n different observational properties, it could be that only m are really fundamental to completely describe the system. Therefore, the goal of PCA is to determine what m is. A detailed description of PCA can be found in several statistical texts as well as in the astronomical literature (Broshe, 1973; Faber, 1973).

Just to outline the method, its merits and defects, we can say the following: First of all, the various parameters are normalized to unit variance, by subtracting the mean and dividing by the standard deviation of the observed variance, so that each parameter will have equal weight. The correlation matrix is then computed and the eigenvectors ($e1$, $e2$, ...) and eigenvalues ($\lambda 1$, $\lambda 2$, ...) of this matrix are determined. The first eigenvector ($e1$) searches for the direction that maximizes the variance, or analogously, minimizes the distance from a line fit to the data points in this n–dimensional space. The remaining variance is then maximized for the second eigenvector ($e2$), and so on, until all the variance is explained. The resulting eigenvectors are independent, and the corresponding eigenvalues describe how much of the total variance belongs to each eigenvector.

Figure 3.9 shows the projections of the variable chosen to describe the system on the plane defined by the first two eigenvectors ($e1$ and $e2$). Such figure provide an excellent way to visualize the correlations and fulfill the goal of representing all the correlations simultaneously. The length of the vector shows how much of the variance in the parameter is explained by the first two dimensions. Variables with vectors that are nearly parallel have large correlation coefficient, while variable with vectors that are nearly perpendicular have very small correlation coefficient.

Because of noise in the data and non–linearity in the relations, the most important part in the PCA is therefore the determinations of where the significant dimension ends, and the noise begins. This, of course, requires a partially subjective judgment. Also the choice of the galaxies may tend to produce artificial correlations or mask real correlations.

Other studies (not using PCA) have suggested that spiral galaxies comprise a family with one dimension (Tully, Mould, and Aaronson, 1982; Ostriker, 1982), two dimensions (Balkowski, 1973; Shostak, 1978; Roberts, 1978; Rubin *et al.* , 1982), or more (Bothun, 1982).

These studies contribute significantly to alleviate the confusions in the theo-

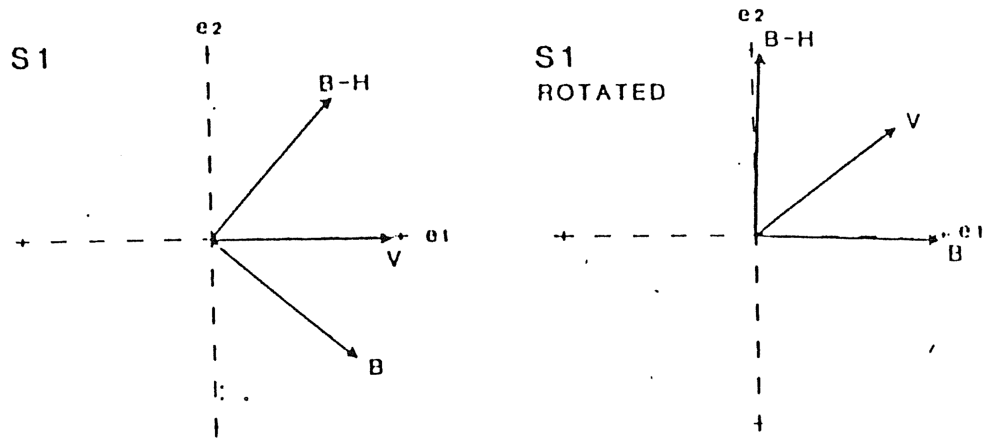

Figure 3.9: The correlation vector diagram (from Whitmore, 1984).

ries of the galactic dynamics and of the galaxy formation, because they suggest that the correlations between the observational properties must be explained simultaneously rather than one at a time.

3.2 The central surface brightness

In recent years there has been considerable debate on the question of whether or not the great majority of galactic disks have a face-on central surface brightness of the same value within a small range. After Freeman (1970) work, Disney (1976) examined this question in a clever, quantitative way and came up with the remarkable suggestion that it (and its equivalent in elliptical galaxies: Fish's (1964) law) were a result of the same observational selection effect. He argued that for galaxies to be selected against the sky background as suitable candidates for surface photometry, their central surface brightnesses had to fall within a limited range. Fainter central surface brightnesses generally result in smaller angular diameters and such galaxies are difficult to see against the sky background.

Brighter central surface brightnesses occur in system with small luminosity scalelengths and such galaxies appear starlike. An interesting conclusion concerning this problem is reported by Allen and Shu (1979). They also agree that there could have been a selection against faint central surface brightnesses, but they do conclude that there appears no bias against high surface brightnesses.

Phillipps and Disney (1983) argued that the presence of a bulge or spheroid could cause such effect: non–allowance for the bulge light at moderate and large radii results in values for the central surface brightness that are too high in fainter disks, which then decreases the scatter. On the other hand, they explain the constancy of central surface brightness from the hypothesis that at the levels of the outer isophotes the spheroid light dominates. They show that at about 25 B $mag\ arcsec^{-2}$ the logarithmic slope of actually observed spheroids has a value quite similar to that of an exponential disk with a central surface brightness of Freeman's value.

The radial distribution of surface brightness in galactic disks has been studied by van der Kruit (1987) for a sample of 51 galaxies, complete to a selection criterion of angular diameter larger than 2.′0 at the 26.5 J $mag\ arcsec^{-2}$ isophote over 450 square degrees of sky. He arrived to the following conclusions:

1) The observed face–on central surface brightness distribution has a narrow peak with a mean value and standard deviation of $\mu_0 = 21.8 \pm 0.6$ J $mag\ arcsec^{-2}$. Selecting only morphological types Sc or earlier the result is $\mu_0 = 21.5 \pm 0.4$ J $mag\ arcsec^{-2}$, which reproduces the Freeman's (1970) original value of 21.65, once the J magnitude is transformed to the B system.

2) Sample selection and bias as suggested by Disney (1976) cannot have produced this narrow peak. Allowance can be made for the known sample selection effects by weighing the contribution of each galaxy by the volume sampled. The frequency distribution of the central surface brightness has a peak with mean and standard deviation $\mu_0 = 22.7 \pm 0.9$ J $mag\ arcsec^{-2}$. The frequency distribution of scalelengths h declines sharply with about 1 dex every 2 kpc (using $H = 75$ $Km\ s^{-1} Mpc^{-1}$).

3) Comparison with the Virgo cluster sample of Watanabe (1983) confirms these results.

Fig.3.10 shows the distribution of $\mu_{0,app}$ and μ_0 (inclination corrected). The dashed lines show separate distributions of "non–dwarfs" (Hubble type Sc or earlier) and "dwarfs" (Hubble type Scd or later), where the dwarfs are the fainter histogram. There are some qualitative arguments that suggest that selection cannot have been a major agent in bringing the narrow distribution about. The peak in the top panel has a value of 21.3 J $mag\ arcsec^{-2}$ which is near to the sky brightness value of the plates. Selection would have given a fainter peak. Furthermore there are no systems with $\mu_{0,app}$ fainter than 23 J $mag\ arcsec^{-2}$, while diameters have been measured by eye at 26.5 J $mag\ arcsec^{-2}$ level. Again disks with $\mu_0 \sim 24$ or so are impossible to miss unless their diameters are too small.

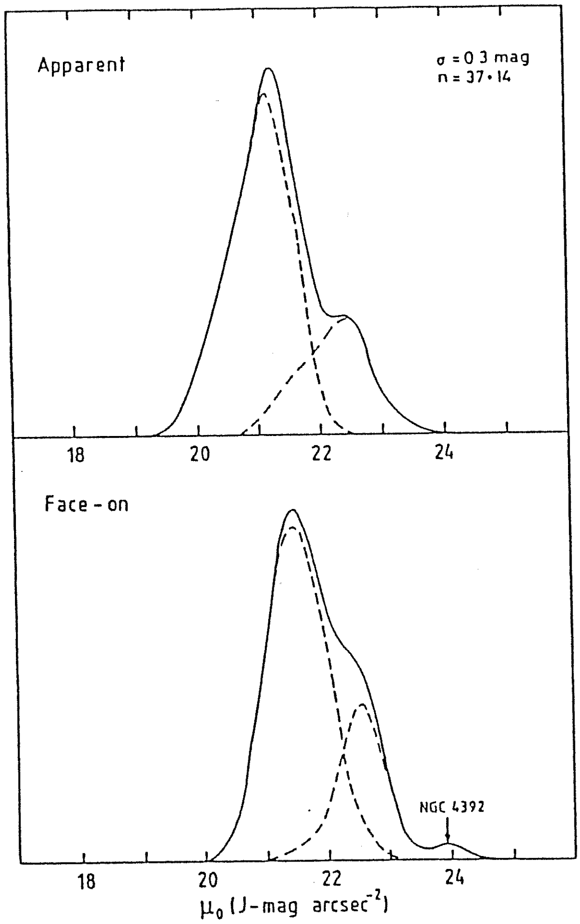

Figure 3.10: The generalized histograms of the central surface brightness (from van der Kruit, 1987).

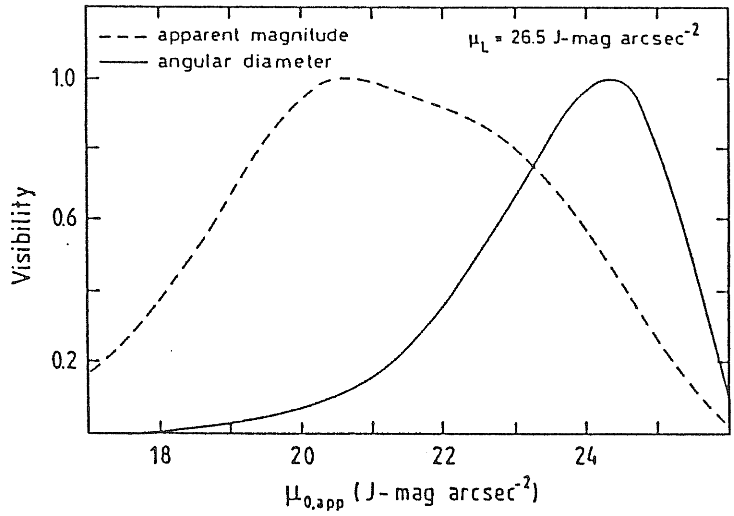

Figure 3.11: The visibility of the galaxies as defined by Disney and Phillipps (1983), (from van der Kruit, 1987).

Disney and Phillipps (1983) have developed the necessary mathematics to correct a sample, with known selection criteria, for selection effects. They define a visibility which is proportional to the maximum volume in which a galaxy of known characteristics may lie and still be included. For a face–on exponential disk they find that this volume has a radius in pc

$$d = \frac{0.4ln10}{\sqrt{(2\pi)}} \frac{\mu_L - \mu_0}{\Theta} dex 0.2(\mu_0 - M + 5) \tag{3.5}$$

where Θ is the minimum angular radius in arcsec which the galaxy should have at surface brightness μ_L to be included, and M the integrated magnitude corresponding to $L = 2\pi\lambda_0 h^2$ (λ_0 is the equivalent of μ_0 but expressed in $L_\odot pc^{-2}$). The visibility was calculated for the sample using $\mu_L = 26.5$ J $mag\ arcsec^{-2}$ and normalized to unity at the peak as shown in Fig.3.11. The peak occurs at 24.3 J $mag\ arcsec^{-2}$, a full three magnitudes fainter then the mean value of $\mu_{0,app}$ in the sample.

The sample was corrected for its selection criteria by giving each galaxy a weight inversely proportional to its visibility. The effects of correction for sample selection has been to make the means somewhat brighter and the standard deviations somewhat smaller.

In order to convert the observed distribution into ones that are corrected for sampling effects it is more useful to perform a distance–dependent analysis weighing each galaxy according to the volume it is sampling. At the basis of this is the fact that we can see a galaxy with a larger (linear) scalelength over a much larger volume than one with a smaller scalelength but with the same central surface brightness. Using the inverse of the volumes as weights rather than the inverse of the visibilities he found the "volume corrected" distribution of Fig.3.12. The top panel contains only those galaxies that have measured radial velocities. The main peak is provided by the dwarfs since the small volume they are sampling.

It is necessary to stress the difference between Fig.3.10 and Fig.3.12. The first shows the expected distribution when galaxies have been selected without bias towards μ_0 but over volumes of space that depend upon their integrated magnitude M (magnitude–limited sample). The second shows the same but now "volume–limited" and without qualifications on correlation between μ_0 and h.

A question of much interest is to what extent these fainter galaxies contribute to the cosmic luminosity density in the universe. Giving a weight to each galaxy proportional to the disk integrated luminosity van der Kruit (1987) found that morphological types S0 through Sc provide 76% of the luminosity density of disk populations. Conversely, only 28% is contributed by disks with $\mu_0 \gtrsim 22.0$ J $mag\ arcsec^{-2}$. It can be seen that galaxies with scalelengths longer than 3 kpc contribute only 22% to the cosmic luminosity density of disk population. About 23% comes from dwarfs and 55% comes from non–dwarfs ($\mu_0 \lesssim 22$ J $mag\ arcsec^{-2}$) with $h < 3$ kpc.

The Virgo cluster galaxies, being all nearly at the same distance, seem to be a good comparison sample for testing these properties. Luminosity profiles (in the V–band) are presented by Watanabe (1983). Van der Kruit (1987) used 116 of these galaxies for which the luminosity profile can be fitted by an exponential disk. In the comparison it must be taken into account the difference between the "generalized" profiles used by Watanabe and the "azimuthally averaged" profiles given by van der Kruit. First are derived by collapsing all the two dimensional information onto the major axis followed by rectification solving an integral equation. This treats galaxies in a uniform way but does have a number of disadvantages. For example it does not take into account the actual inclination of the galaxy and, moreover, the profiles contain strong signatures of features such as spiral arms and bars where these cross the major axis. The advantage of the method of azimuthally averaged profiles is that such structures are smoothed out. A further point is that the generalized profiles have smeared out the bulge contributions severely in the very central parts where the spheroid surface brightness increases very sharply.

The generalized histogram of μ_0 is presented in Fig.3.13. The distribution has a mean and standard deviation of 21.05 ± 0.75 V $mag\ arcsec^{-2}$. Sub–sample

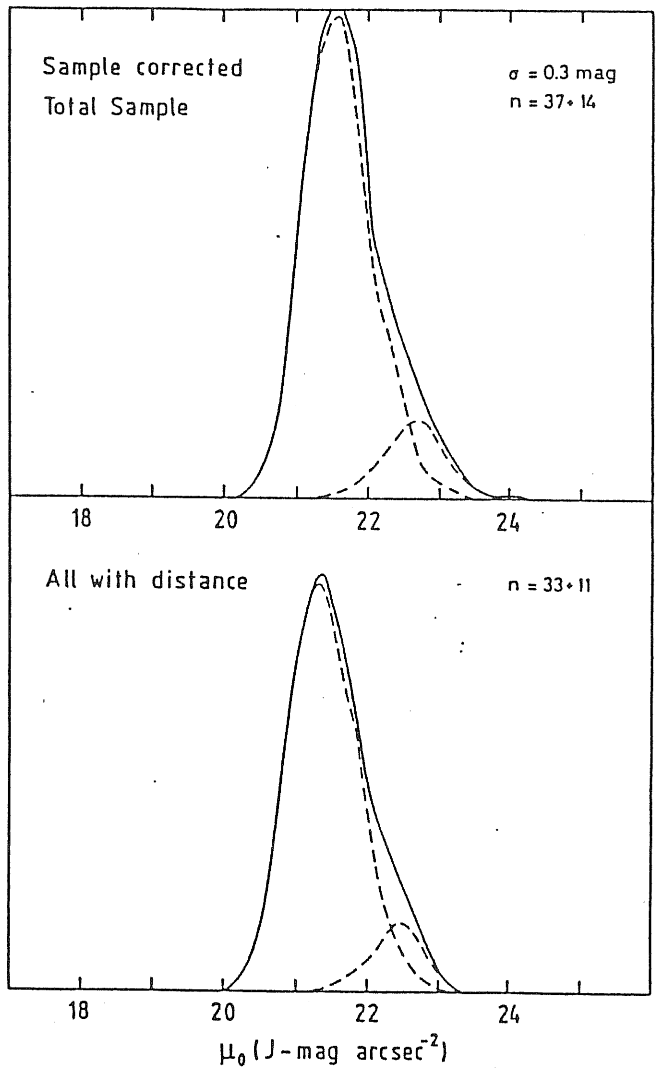

Figure 3.12: Generalized histogram after correction for the volume sampled (from van der Kruit, 1987).

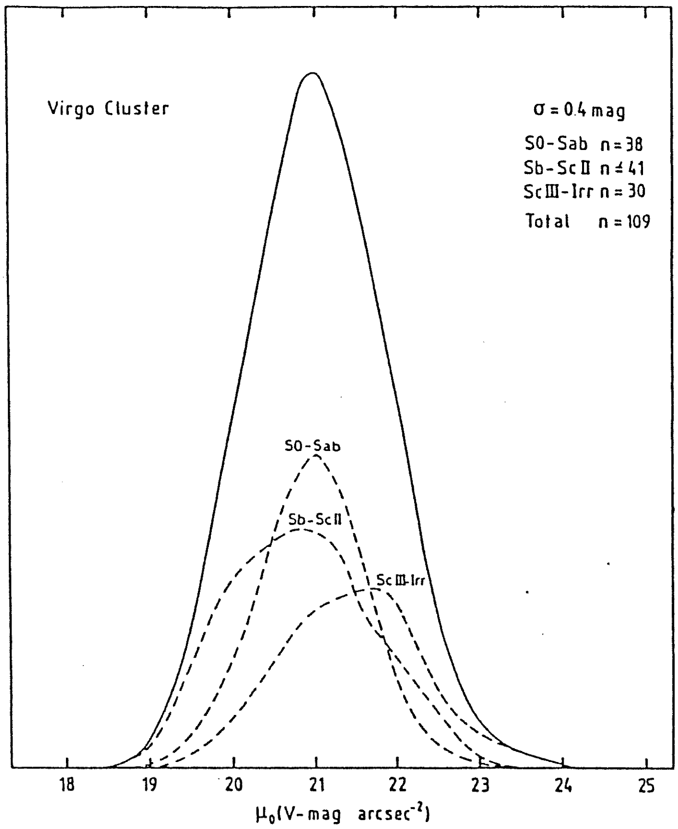

Figure 3.13: Generalized histogram of the distribution of μ_0 in the Virgo cluster (from van der Kruit, 1987).

have been formed using the morphological types of Binggeli *et al.* (1985). The distribution of ScIII to Irr systems is equivalent to that of "dwarfs" above. The total of these S0 to ScII have $\mu_0 = 20.89 \pm 0.69$ with no significant dependence upon morphological type. This is in quite reasonable agreement with the value for field galaxies, considering the larger error in μ_0 for the Virgo sample and the conversion from the V–band to the J–band.

A point that is not yet understood, is the possible influence of internal extinction on the derived surface brightness of a disk. It seems probable, from studies of our Galaxy (de Vaucouleurs *et al.* 1976; Burstein and Heiles, 1982) and M31 (Walterbos, 1986; Capaccioli *et al.* 1989), that effects of the order of a few tenth of a magnitude are possible. In this case the color of the galaxies do not carry informations to determine the reddening, because the dust layers are inside the stellar disk.

Disney and Phillipps (1985) found for a large sample of galaxies that the overall color index does not correlate with the intrinsic surface brightness, which for exponential disks relates with the central surface brightness. However the question of expected correlations between colors and central surface brightness needs more additional data.

In conclusion, van der Kruit (1987) believe that the small spread in μ_0 in the universe is probably the result of the existence of a constant ratio of visible to dark matter in all galaxies. This could be real, if galaxies collapse with detailed conservation of angular momentum from uniformly rotating, uniform spheres, that derive their angular momentum from tidal torques in a universe with hierarchical clustering. This model also explains the approximate exponential nature of the light distribution in the disks, and the cutoffs in the stellar disks at about 4–5 scalelengths.

References

Allen, R.J., and Shu, F.M.: 1979, *Astrophys. J.*, **227**, 67.

Balkowski, C.: 1973, *Astron. Astrophys.*, **29**, 43.

Binggeli, B., Sandage, A., and Tamman, G.A.: 1985, *Astron. J.*, **90**, 1681.

Boroson, T.: 1981, *Astrophys. J. Supp.*, **46**, 177.

Boroson, T., Strom, K.E., and Strom, S.E.: 1983, *Astrophys. J.*, **274**, 39.

Bothun, G.C.: 1982, *Astrophys. J. Supp.*, **50**, 39.

Brosche, P.: 1973, *Astron. Astrophys.*, **23**, 259.

Burstein, D.: 1979a, *Astrophys. J. Supp.*, **41**, 435.

Burstein, D.: 1979b, *Astrophys. J.*, **234**, 435.

Burstein, D.: 1979c, *Astrophys. J.*, **234**, 829.

Burstein, D., and Heiles, C.: 1982, *Astron. J.*, **87**, 1165.

Capaccioli, M., Della Valle, M., D'Onofrio, M., and Rosino, L.: 1989, *Astron. J.*, **97**, 1622.

de Vaucouleurs, G.: 1959, *Hand. der Physik*, **53**, 311.

de Vaucouleurs, G., de Vaucouleurs, A., and Corwin, H.G.,Jr.: 1976, *Second Reference Catalog of Bright Galaxies* (Austin: University of Texas Press) (RC2).

Disney, M.J.: 1976, *Nature*, **263**, 573.

Disney, M.J., and Phillipps, S.: 1983, *Mont. Not. R. astr. Soc.*, **205**, 1253.

Disney, M.J., and Phillipps, S.: 1985, *Mont. Not. R. astr. Soc.*, **216**, 53.

Faber, S.M.: 1973, *Astrophys. J.*, **179**, 731.

Faber, S.M.: 1982, In *Astrophysical Cosmology: Proceedings of the Study Week on Cosmology and Fundamental Physics*, eds. H.A.Brück, G.V.Coyne and M.S.Longair (Vatican City: Pontifical Academy of Sciences), p.220.

Fish, R.A.: 1964, *Astrophys. J.*, **139**, 284.

Freeman, K.C.: 1970, *Astrophys. J.*, **160**, 811.

Gunn, J.E.: 1982, In *Astrophysical Cosmology: Proceedings of the Study Week on Cosmology and Fundamental Physics*, eds. H.A.Brück, G.V.Coyne and M.S.Longair (Vatican City: Pontifical Academy of Sciences), p.230.
Hamabe, M.: 1982, *Pub. Astr. Soc. Japan*, **34**, 423.
Houten, C.J. van: 1961, *Bull. Astr. Inst. Netherlands*, **16**, 1.
Kent, S.M.: 1984, *Astrophys. J. Supp.*, **56**, 105
Kent, S.M.: 1985, *Astrophys. J. Supp.*, **59**, 115
Kent, S.M.: 1986, *Astron. J.*, **91**, 1301.
King, I.R.: 1978, *Astrophys. J.*, **222**, 1.
Kodaira, K., Watanabe, M., and Okamura, S.: 1986, *Astrophys. J. Supp.*, **62**, 703.
Kormendy, J.: 1977a, *Astrophys. J.*, **214**, 359.
Kormendy, J.: 1977b, *Astrophys. J.*, **217**, 406.
Kormendy, J.: 1977c, *Astrophys. J.*, **218**, 333.
Kormendy, J.: 1985, *Astrophys. J.*, **295**, 73.
Kruit, P.C. van der: 1987, *Astron. Astrophys.*, **173**, 59.
Lauer, T.R.: 1985, *Astrophys. J. Supp.*, **57**, 473.
Okamura, S., Kodaira, K., and Watanabe, M.: 1984, *Astrophys. J.*, **280**, 7.
Ostriker, J.P.: 1982, in *Astrophysical Cosmology/*, eds. H.A. Br*ddotu*ck, G.V. Coyne, and M.S. Longair (Vatican City: Pontificial Academy of Sciences).
Roberts, M.S.: 1978, *Astron. J.*, **83**, 1026.
Phillipps, S., and Disney, M.J.: 1983, *Mont. Not. R. astr. Soc.*, **203**, 55.
Rubin, V.C., Ford, W.K., and Thonnard, N.: 1980, *Astrophys. J.*, **238**, 471.
Rubin, V.C., Ford, W.K., and Thonnard, N.: 1982, *Astrophys. J.*, **261**, 439.
Shostak, G.S.: 1978, *Astron. Astrophys.*, **68**, 321.
Simien, F., and de Vaucouleurs, G.: 1983, In *Internal Kinematics and Dynamics of Galaxies*, IAU Symp. No. 100, ed. E.Athanassoula (Dordrecht: Reidel), p.375.
Simien, F., and de Vaucouleurs, G.: 1986, *Astrophys. J.*, **302**, 564.
Thomsen, B., and Frandsen, S.: 1983, *Astron. J.*, **88**, 789.
Toomre, A.: 1977, In *The Evolution of Galaxies and Stellar Populations*, edited by B.M.Tinsley and R.B.Larson (Yale University Observatory, New Haven), p.418.
Toomre, A., Toomre, J.: 1972, *Astrophys. J.*, **178**, 623.
Tremaine, S.: 1981, In *The Structure and Evolution of Normal Galaxies*, eds. S.M. Fall and D. Lynden–Bell (Cambridge: Cambridge University), p.69.
Tsikoudi, V.: 1980, *Astrophys. J. Supp.*, **43**, 365.
Tully, R.B., Mould, J.R., and Aaronson, M.: 1982, *Astrophys. J.*, **257**, 527.
Walterbos, R.A.: 1986, *Ph.D. Dissertation*, University of Leiden.
Watanabe, M.: 1983, *Ann. Tokyo. Astr. Obs.*, **19**, 121.
White, S.M.D.: 1982, In *Morphology and Dynamics of Galaxies*, eds. L. Martinet and M. Mayor (Geneva: Geneva Observatory), p.291.
Whitmore, B.C.: 1984, *Astrophys. J.*, **278**, 61.

Chapter 4

Mass–to–Light ratio and Dark matter

More than fifty years ago, Zwicky (1933) and Smith (1936) showed that if the Virgo cluster of galaxies is bound, the total mass must considerably exceed the sum of the masses of the individual member galaxies, *i.e.*, there appeared to be "missing mass" in the cluster. This discrepancy, between masses determined from optical rotation curves and the mass needed to bind groups and clusters, persisted as more data became available (*e.g.*, Neyman *et al.* 1961), even if decreasing, after the suggestion by Ostriker and Peebles (1973), that spiral galaxies must be embedded in optically undetected, stabilising massive halos. Ostriker, Peebles and Yahil (1974) and Einasto, Kaasik and Saar (1974) collected further observational evidences in support of the existence of such halos, although Burbidge (1975) reached the opposite conclusion from similar data. However, in the same years, high–resolution 21 cm observations were showing that HI often extends well beyond the optical boundaries of galaxies, giving a substantial support to the presence of mass outside the optically visible dimensions of the galaxies.

Up to present days, there has been growing evidence that $\sim 90\%$ of the mass in the Universe is dark matter of unknown nature (Kormendy, 1989). Its presence is detected only through its gravitational influence. Rotation curves have suggested that mass type does not correlate with galaxy morphology (Burstein and Rubin, 1985). Galaxy with almost identical rotation curves can be found over a wide range of Hubble types, and in particular, over a range in bulge to disk ratios of as much as a factor of 40. This means that the visible mass distribution does not control the shape of the rotation curve.

In this context, we are led to the following question: How much dark matter is present in the old stellar disks? The Oort–Bahcall analysis (Bahcall, 1987) implies a local galactic disk mass to light ratio of $M/L_V \sim 3$. This is consistent with values obtained by van der Kruit and Freeman (1984, 1986) for old disks in external galaxies, by statistically comparing scale heights in edge–on galaxies with vertical velocity dispersions in face–on galaxies. However, there are still significant uncertainties (Faber, 1987; Gunn, 1987; Trimble, 1987).

New evidences suggest that the mass to light ratio is nearly constant with radius ($M/L_B \sim 6 \pm 2\ M_\odot/L_\odot$ for the old disk population in a few Sb and Sc galaxies), but that variations of a factor of two in M/L can be expected for disks over the range Sa to Irr, due to different contributions of the young population (van der Kruit, 1987).

Faber and Gallagher (1979) pointed out that the M/L_B ratio seems to show a weak dependence on Hubble type, but that the trend in M/L with morphological type seen with B luminosities disappears when K magnitudes are used. In any case, the observed trend is generally what one would expect from variations in stellar content along the Hubble sequence. For example, Larson and Tinsley (1978) have found that M/L_B is well correlated with $(B-V)$ for model stellar population over a wide range of ages.

Concluding this introduction, we can say that the knowledge of the M/L ratio is important for many astrophysical questions, and in particular it is of fundamental importance for understanding the formation and the evolution of galactic disks.

Therefore, for solving these problems, considerable efforts have been done till now to provide surface photometry and rotation curves of spiral galaxies. In the following I firstly shall review many of the basic properties, and results obtained from photometric studies.

4.1 Surface photometry

Edge–on spiral galaxies enable a detailed study of light profiles, color gradients and flattenings of the spheroidal component of these galaxies, and with reliable photometry we should be able to decide whether spirals have thick and truncated disks. Owing to the line–of–sight integration, we can also study the disks to much larger radii than is possible for face–on disks. We can infer also the spatial distribution of the old population in disks of spiral galaxies, that is a fundamental piece of information for studying the structure, the formation and the evolution of disk galaxies. This population is very well seen through photometric analyses of edge–on systems.

A successful example of a model that describe the three–dimensional distribution of light in spiral galaxies has been derived by van der Kruit and Searle (1981) from photometric studies of edge–on systems. The adopted model represents a locally isothermal, self gravitating, truncated exponential disk:

$$L(R,z) = \begin{cases} L_0 e^{-R/h} sech^2(z/z_0) & \text{if } R < R_{max}, \\ 0 & \text{if } R > R_{max}. \end{cases}$$

The light distribution consist of a canonical exponential distribution in the radial direction and an isothermal sheet approximation in the vertical coordinate. These two aspects of the distribution arise by different mechanisms. The exponential nature could results from the angular momentum distribution in the protogalaxy (Freeman, 1970; Gunn, 1982; van der Kruit, 1987), if this approximates that of an uniformly rotating, uniform density sphere. On the other hand the vertical distribution of stars is the result of secular evolution, whereby the stellar component is continuously heated by various agents, such as giant interstellar molecular clouds, spiral structure, etc. (Spitzer and Schwarzschild, 1951; Lacey, 1984; Carlberg and Sellwood, 1985) and it carries therefore no information on the structure of the protogalaxy.

The main results found through the surface photometry of edge–on spirals can be summarized as follows:
a) the value of z_0, the scale parameter in the z–direction, is independent of R,
b) there is a sharp cut–off in the light distribution at R_{max}, which occur at about 4–5 h.

In contrast to this is the case of the disk of the S0 galaxy NGC 3115. Capaccioli, Held and Nieto (1987) and Capaccioli, Vietri and Held (1988) found that: **1)** the disk's scale height z_0 increases steadily with galactocentric distance inside $R \sim 40''.0$ and outside $R \sim 80''.0$, while it flattens up in the intermediate range; **2)** the major axis light profile is only roughly exponential from $R \sim 20''.0$ over the observed range to the last observed point ($R \sim 135''.0$).

The constancy of z_0 implies that the velocity dispersion of the old disk stars, $\langle V_z^2 \rangle^{1/2}$, decreases with radius until it reaches values of about 10 km sec^{-1}or less at R_{max}. It is interesting to see that the stars near the edge of the disk have the same kinematics as the gas from which they were born. The result also implies that dark matter, inferred from the flat rotation curve and the corresponding increase of M/L with radius (Bosma and van der Kruit, 1979), resides in the halos of spiral galaxies.

It is also instructive to estimate the numerical value of z_0 that is appropriate to the solar neighbourhood. Fitting Oort's (1960, 1965) curve of K_z (where K_z denote the gravitational force in the z–direction as a function of z) with z, van der Kruit and Searle (1981) obtained for their model, $z_0 \sim 0.6 \div 0.7$ Kpc and $\rho_0 \sim 0.08 M_{\odot} pc^{-3}$.

Near R_{max} the edge–on disk quickly drop below detectable levels suggesting that they have rather well defined outer edges. Note that the mass at large radii indicated by the flat rotation curves does not require the disks to continue beyond R_{max} since the measurements of the HI z–velocity dispersion suggest that this mass is probably distributed in a more spherical volume. Although this can help to explain the persistence of the HI warps (Tubbs and Sanders, 1979) the origin of the fairly sharp–off is puzzling. One possibility might be that in the primordial gaseous disk, at this point R_{max}, the gas density dropped below some value critical for the occurrence of star formation. Alternatively in a scenario with slow disk formation (Larson, 1976) R_{max} might be the radius where the disk formation time equals the present age of the galaxy. Fall and Efstathiou (1980) have suggested that spiral galaxies have edges corresponding to those radii at which the shear due to differential rotation becomes large enough to overcome self–gravity in the primordial disk, so that star formation is inhibited.

The existence of the sharp cut–off places an upper limit on the velocity dispersion at the edge of the disk. For a flat rotation curve at 200–250 km $sec^{-1}$the stars at a mean radius of 20–25 Kpc will go through epycycles with half–axes in the R–direction of 1 Kpc, if their random velocities are 10–15 km sec^{-1}.

Fig.4.1 show the comparison of the model and observed z and R profiles for NGC 4244 (van der Kruit and Searle, 1981). The fit is extremely good except for small z and for R near R_{max}. The good agreement for the small z distances indicates that the presence of younger populations is roughly compensated for by the extinction due to the dust.

What is most surprising is the absence of any significant dependence of z_0 upon R. Such dependence would be seen very directly in the slopes of the z profiles. Sometimes the outer profiles do seem to indicate smaller slopes, and therefore is possible that the disk thickens just before the cut–off. However, z_0 independent of R is a good approximation and the minor deviations might be associated with warps in the HI–layers.

The isothermal sheet approximation was originally introduced for two reason. Firstly because at large values of z it approximates an exponential, as indicated by existing observations in actual galaxies. Further, it is known from kinematical studies of stars in the solar neighborhood (Wielen, 1977) that stars that have ages above a few Gyrs all have roughly the same velocity dispersion. In view of the strong dependence of velocity dispersion on age for younger generation of stars, this approximation must be expected to break down near the plane.

Two recent studies (Fuchs and Wielen, 1987; Villumsen, 1983) of the vertical density distribution suggest two contrasting results. Fuchs and Wielen conclude that the exponential function approximate better the actual vertical density distribution than the $sech^2$ function of the isothermal sheet, while Villumsen finds excellent fits with isothermals and very poor fits with exponentials. The former calculated the resulting z–distribution of stars and their kinematics in dynamical evolution models of the galactic disk that reproduce the observed local velocity dispersion–age relation, the further is a numerical study that do not allow significant contributions from young age groups, which are precisely the ones that produce strong enhancements at low z over the isothermal distribution.

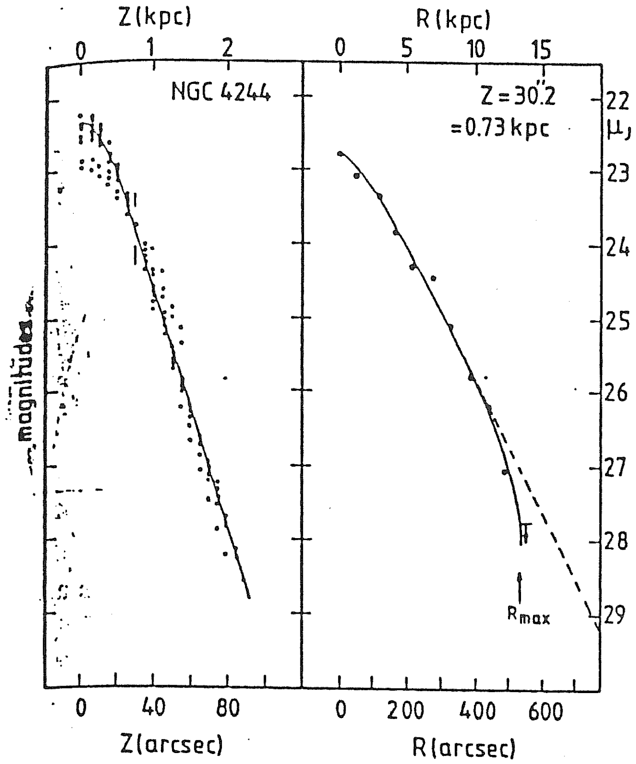

Figure 4.1: Comparison of the model and observed composite z and R profile for NGC 4244. The dashed line in the parallel profile at the right indicates the infinite disk (from van der Kruit and Searle, 1981).

Wainscoat (1986) performed surface photometry of the edge-on spiral IC 2531 both at optical and near infrared wavelengths. His z-profiles at low z just above the dust lane in the R band and in the IR J,H, and K bands indicate that "a better fit in the unobscured parts may well be produced by a pure exponential".

There is also related evidence from star counts studies in the disk of our Galaxy. Gilmore and Reid (1983) find that the space density of main sequence stars near the turn-off in the old disk population ($4 \lesssim M_V \lesssim 6$) follows an exponential above 100 pc or so from the plane.

Similarly, the starcount analysis of Pritchet (1983) and the Pioneer background starlight distribution studied by van der Kruit (1986) both indicate better fits with exponentials in the z-direction than with the $sech^2$ function.

As far as the problem of thick disk is concerned, we remember that Burstein (1979) performed decompositions of S0 systems that are highly inclined to the plane of the sky. He found that there is an excess of light not accounted for by the model, at relatively large distance from the plane, which can be identified as a new component of galactic structure, the so-called "thick disk". Burstein claimed that most spirals do not exhibit this component. His result largely agree with those from the limited sample of Tsikoudi (1977). Freeman (1978) noted that this is an expected result of the two-component model of galactic structure, providing that the bulge and disk are each approximately isothermal. Subsequently, Freeman (1980) has suggested that the thick disks are nothing other than the response of the spheroidal component to the gravitational field of the flattened disk.

The luminosity component in S0's termed a "thick disk" has the following physical properties which differentiate it from a bulge or thin disk: **1)** The thick disk has an intrinsic ratio of total z-thickness to diameter, z/a, of between 1/4 to 1/5 at $\mu_B \sim 25$, while an E4 elliptical has $z/a = 0.6$ and a thin disk $z/a \lesssim 0.1$; **2)** The luminosity of the thick disk parallel to the major axes decreases very slowly with increasing galactocentric radius, in marked contrast to the radial luminosity gradients of bulges and thin disks; **3)** The thick disk also does not appear to be as sharply peaked as bulge or a thin disk perpendicular to the major axes.

Thick disks contribute a substantial amount of the blue luminosity in the five S0 studied by Burstein (see Fig.4.2), perhaps 10–40 percent of the total disk light. Furthermore, the lack of a strong luminosity gradient parallel to the major axes gives the disk a very distinctive "boxy" appearance.

Van der Kruit and Searle (1981) measured the vertical z surface brightness profiles for several edge-on galaxies. In those spirals with negligible bulges, the profiles showed only the thin disk component. However, for spiral like the Galaxy, with small bulges, the profiles also showed a second, more extented flat component. Gilmore and Reid (1983) derived the vertical density profile for the Galaxy from stellar photometry at the SGP. They interpreted their profiles as the sum of two components: the thin disk with scale height $h_z \sim 300$ pc and a thick disk

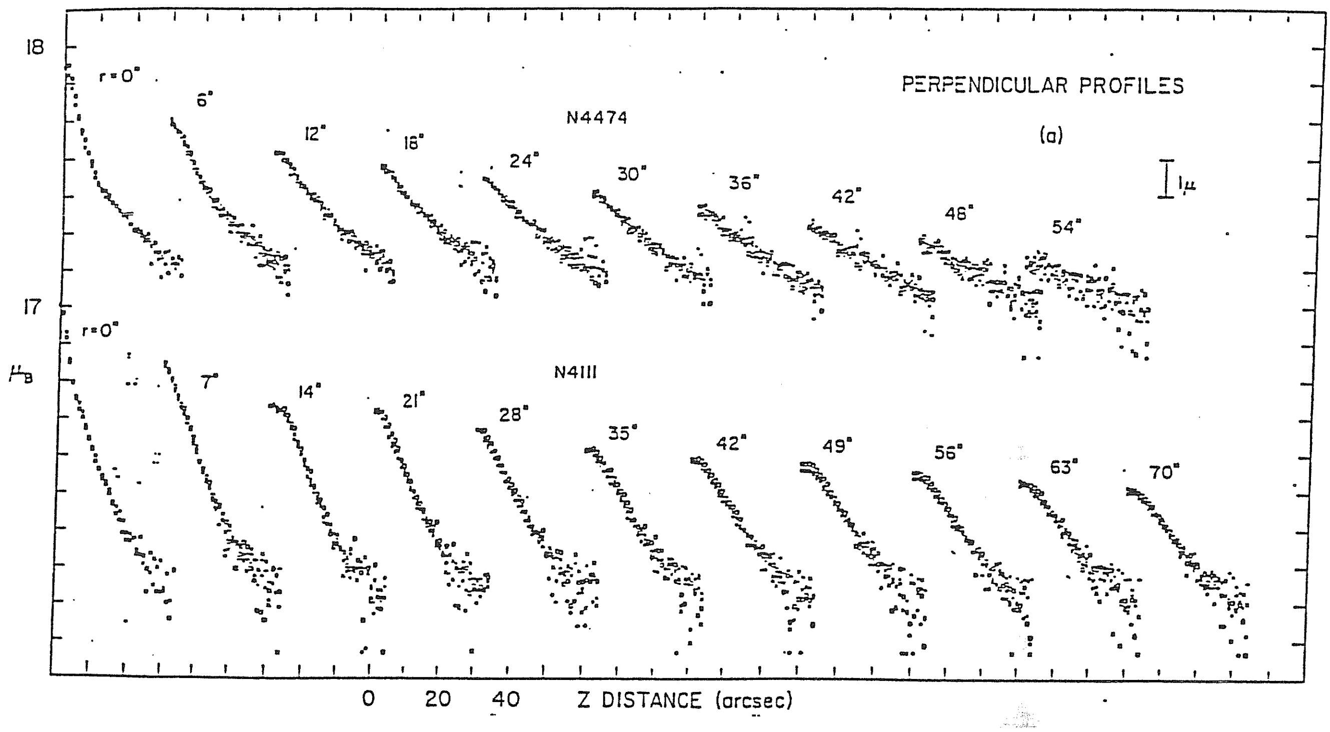

Figure 4.2: Perpendicular profiles of the S0 galaxies NGC 4474 and NGC 4111, plotted as μ_B versus z for radii along the major axis as noted (in arcsec). Plus and square are on the same side of the nucleus, plus and cross are in the same direction from the major axis (from Burstein, 1979).

with scale height ~ 1500 pc. In an important paper, Hartkopf and Yoss (1982) observed the kinematics and abundances of G and K giants at the galactic poles, at distance of up to about 5 Kpc. Within a few hundred parsecs of the Galactic plane, almost all their stars have abundances in the range $0 > [Fe/H] > -0.5$, and their velocity dispersion σ_z is 22 km sec^{-1}. These stars belong to the old thin disk, whose scale height is about 300 pc. At greater heights there are many metal–weak stars ($[Fe/H] < -1$), which belong to the Galactic halo. However, there are also about 30 relatively metal–rich giants ($[Fe/H] > -1$) far from the Galactic plane ($2 < z < 5$ Kpc), and these stars could not belong to a thin exponential disk population. They are instead tentatively identified with the thick disk.

In its vertical structure and kinematics, the thick disk is intermediate between the rapidly rotating thin disk ($\sigma_z \sim 20$ km sec^{-1}) and the slowly rotating metal–weak halo ($\sigma_z \sim 75$ km sec^{-1}). Ratnatunga and Freeman (unpublished data) measured abundances and kinematics of K giants in a field well situated for estimating the mean rotation of the different populations. They found a thick disk population of metal rich stars, in the region $2 < z < 5$, with a mean velocity of 36 ± 14 km sec^{-1}and a line–of–sight velocity dispersion of 50 ± 10 km sec^{-1}.

However, the relationship between the thin and thick disks is not yet clear. Are they discrete components, or is the thick disk just the higher energy, slightly metal–weaker tail of the thin disk population, as argued by Norris (1987)?

Thick disk and bulges appear to go together: Disk galaxies with negligible bulges do not appear to have the second. The absence Surface photometry of external edge–on galaxies, in particular of the very similar Sb spiral NGC 891, cannot provide independent evidence for or against the occurrence of intermediate components.

There are at least three possibilities for the origin of the thick disk components in S0's. It could be **1**) a truly separate dynamical component of the galaxy; **2**) a severe modification of the bulge light distribution due to the presence of the disk; **3**) an enhanced high–velocity tail of the velocity distribution of the thin disk.

The third possibility appear today the most reliable. For example, looking at the apparent similarity of the anisotropy ratio σ_R/σ_z for the thin and the thick disk, similar heating mechanisms are probable. It would be particularly useful to know whether the thick disk stars lie on the same Age–Velocity relation and Age–Metallicity relation as the thin disk stars.

4.2 Rotation curves and dark matter

The study of rotation curves has become our most powerful tool for determining mass distributions inside galaxies. For many decades, optical spectroscopists dominated the field by measuring velocities of HII regions. Lately, it has been discovered that neutral hydrogen extends outwards past the optically bright regions of most spiral galaxies.

The fundamental theory of inferring mass distributions from rotation curves has been discussed by Burbidge and Burbidge (1975), de Vaucouleurs and Freeman (1973), Freeman (1975), and Schmidt (1965).

A convenient measure of the optical extent of a galaxy is the Holmberg radius (Holmberg, 1958), which is the major axis radius at which the surface brightness is 26.5 photographic $magarcsec^{-2}$. Roberts (1975a) found that the median extent of optical rotation curves was only 0.3 Holmberg radii. Radio 21–cm observations, which in many galaxies now extent well beyond the Holmberg radius, show that rotation curves remain flat to the limit of observation, indicating much larger total masses (Bosma, 1978, 1981a,b).

The reality of flat rotation curves has been questioned on several grounds. Doubts have been raised, for example, as to whether the HI is truly in circular motion. There are indeed good reasons to fear that within the inner regions of galaxies, ionized gas is not always in circular orbit. Even at large radii, the interpretation of observations has been criticized in several ways.

A flat rotation curve in itself does not imply the presence of dark matter. To establish the existence of dark halos it is necessary to measure the circular velocity well beyond the turnover radius of the disk (*i.e.*, the radius where the predicted rotation curve of luminous matter in the disk starts to decline; for an exponential disk this occur around 2.2 disk scalengths). In this meaning 21 cm radio observations are indispensable.

With surface photometry it is possible to estimate the contribution to the rotation curves from the stellar component alone. Any excess in the observed rotation curve provides a measurement of the contribution of a dark component. The number of galaxies with a complete set of data (that is, with rotation curve and surface photometry) is slowly growing, and a joint analysis has been made by Bosma and van der Kruit (1979), Kalnajs (1983), Casertano (1983), Carignan and Freeman (1985), and van Albada *et al.* (1985). This last work suggests that the mass in dark matter is roughly the same as that in stars within a Holmberg radius, but whether this ratio is universal or depends on luminosity or morphological type is still not well known. Kalnajs shows that the rotation curves which are flat or rising can be explained entirely in terms of constant M/L ratio, suggesting that dark halos may not be as ubiquitous as is usually assumed. However, Van Albada *et al.* (1985) and Carignan and Freeman (1985) both point out that optical rotation curves seldom extend much past the expected peak in the rotation curve from the stellar disk and that 21–cm rotation curves leave little doubts to the existence of dark halos.

Kent (1986) presented luminosity profiles of 37 Sb and Sc galaxies with existing optical rotation curves measured by Rubin *et al.* (1980, 1982). The rotation curves are used to determine the mass–to–light ratio of the bulge and disk components and two parameters that modeled the halo mass distribution. He claims that if it is assumed the M/L constant in the bulge and disk components, it is possible to compute the mass distribution and hence the rotation curve due to each component. By combining this information with the observed rotation curve, it should be possible to derive the distribution and mass of the dark halo. His major result is that optical rotation curves usually do not place strong constraints on the amount of dark matter in these galaxies.

Rubin *et al.* (1985) presented a comparison of the dynamics of different Hubble types spiral galaxies (Sa,Sb,Sc), through rotation curves of a set of these galaxies, obtained by homogeneous observations. They showed that Sa rotation curves have the similar behaviour of Sb and Sc rotation curves, from low central gradient, low rotational velocity for Sa's of low luminosity, to high central gradient, high rotational velocity for Sa's of high luminosity. There is a large similarity of forms, but not of amplitude, among rotation curves of galaxies with morphologies as different as large–bulged Sa's and small–bulged Sc's. This suggest that the form of the gravitational potential is not strongly correlated with the form of the optical luminosity distribution.

Fig.4.3 shows the rotation curves for an Sa, an Sb, and an Sc galaxy, plotted on a (log V, log R) scale to emphasize the similarity of form of the rotation curves, even for galaxies of very different morphology. For example, in this case, the three galaxies have bulge–to–disk ratio which ranges from 4.0 to 0.1, yet the shapes of the rotation curves do not reflect these differences.

For Sa's, velocities range from 367 km s^{-1}($M_B = -22.8$) to 163 ($M_B = -19.3$), compared with 330–144 km s^{-1}for the Sb and 304–99 for the Sc. The median value of the rotational velocity decreases from 299 to 222 to 175 km s^{-1}from types Sa through Sc. There is, however a wide overlap among the Hubble types: the velocity $V_{rot} = 250$ km s^{-1}can identify an Sc of high luminosity, an Sb of intermediate luminosity, and an Sa of low luminosity.

In principle, matching the rotation curve models to the observed profiles is straightforward. For any galaxy, a model rotation curve is computed from the observed bulge and disk profiles and the assumed halo profile: $v_c^2(r) = v_B^2 + v_D^2 + v_H^2$. Four free parameters, the bulge and disk M/L ratios and the scale parameters σ and a of the halo density profile, are adjusted by a least–squares fit to the observed rotation curve profile. In practice, it is found that if a fit is made solving for all four parameters simultaneously, the solution is nearly singular. The problem is that the observed rotation curves do not extend far enough to decouple the interdependence of the disk M/L ratio and halo parameters. Consequently people constrain the disk or halo parameters in some way:

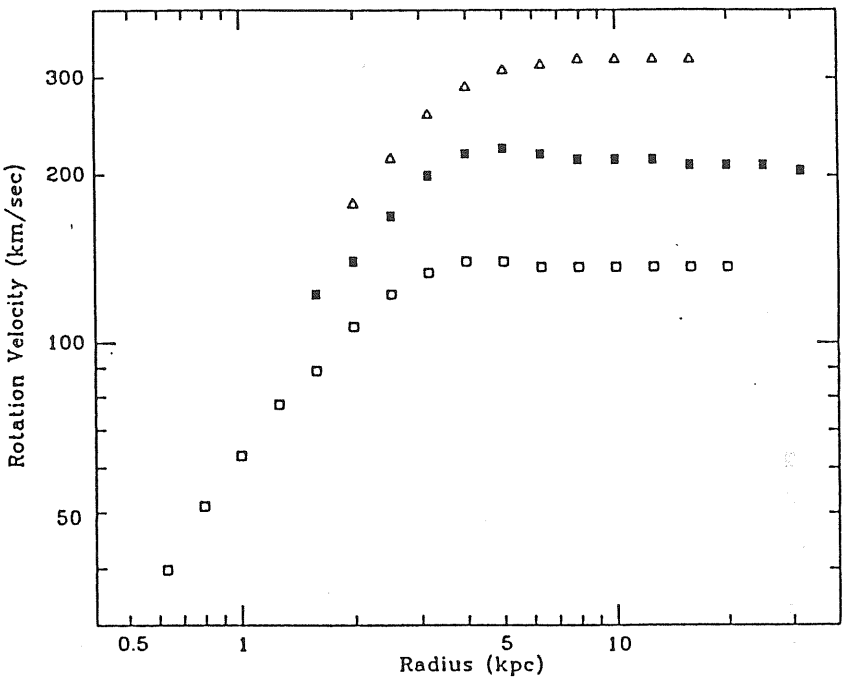

Figure 4.3: Rotation curves of typical Sa, Sb, and Sc galaxies (from Rubin *et al.* 1985).

Maximum disk method. It is assumed that the stellar component dominates the mass distribution in the inner part of a galaxy. The M/L ratio for the disk and bulge are set to the maximum value consistent with matching the inner part of the rotation curve. Any excess in rotation velocity at large radii is then attributed to a dark halo component.

Fixed-σ method. This approach is motivated by the fact that 21 cm rotation curves usually remain flat well beyond the optical edge of a galaxy. If the asymptotic velocity v_c is known, then the halo parameter σ can be set to a value $v_c(\infty)/\sqrt{2}$. For most galaxies, this velocity can be determined reasonably well by inspection of the rotation curve. With v_c and σ so determined, the remaining three parameters are found by a least-squares fit.

Is the maximum disk case closer to the truth? There are three suggestive reason that support this possibility: (i) Measurements of mass and luminosity density in the solar neighborhood yields $M/L_V = 3.1 \pm 0.6\ M_\odot/L_\odot$ (Bahcall, 1984). This value of M/L includes the dark material that must reside in the disk. For NGC 3198 Van Albada *et al.* (1985) find $M/L_V \lesssim 4.4\ M_\odot/L_\odot$. (ii) The shape of the rising part of the rotation curve agrees with that expected for a disk with scale length as given by the distribution of light. If the rotation curve were determined by the dark halo, such agreement would be a coincidence. (iii) The close relationship between luminosity of spiral galaxies and maximum rotational velocity, implied by the small scatter in the Tully–Fisher relation (1977), indicates that it is the amount of visible matter that determines the maximum rotation velocity in a galaxy.

Burstein and Rubin (1985) have argued that if the amount of dark matter is comparable to the amount of luminous matter at each radius, the study of the mass distribution rather than the light distribution might be a more fundamental method of studying galaxies. They introduced the concept of *mass curve*, the integral mass distribution as a function of radius. Three basic "mass types" are defined that fit a majority of the observations.

Fig.4.4 shows the three different mass type distributions. The rotation curves of two fictitious galaxies are fitted to different regions of the mass type III curve. The figure shows that a rotation curve which is rising rapidly at all radii, and/or a rotation curve that turns over and is falling, can result in a mass type III distribution.

They found no correlation between mass types and other observational properties of spirals, leading them to suggest that the environment may play a dominant role in determining the mass distribution. Rotation curves of galaxies in the central region of clusters are generally falling, while the outer galaxies in a cluster and field galaxies tend to have flat or rising rotation curves (Whitmore *et al.* 1988).

This speculation was verified by Burstein *et al.* (1986), who reported a difference in the distribution of mass types for cluster galaxies compared with field galaxies (Fig.4.5), with 33% of field galaxies being mass type I, while none of the

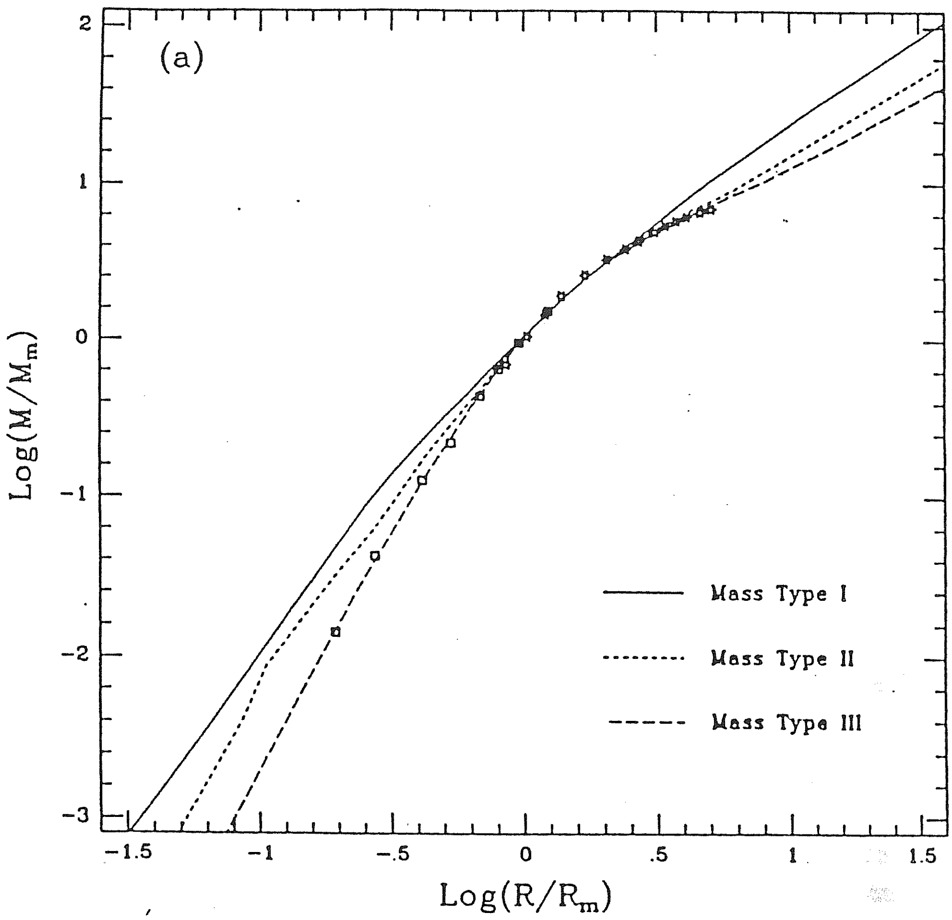

Figure 4.4: Templates for the three mass type, as defined by Burstein and Rubin, (1985), with two different fits to mass type III (from Forbes and Whitmore, 1989).

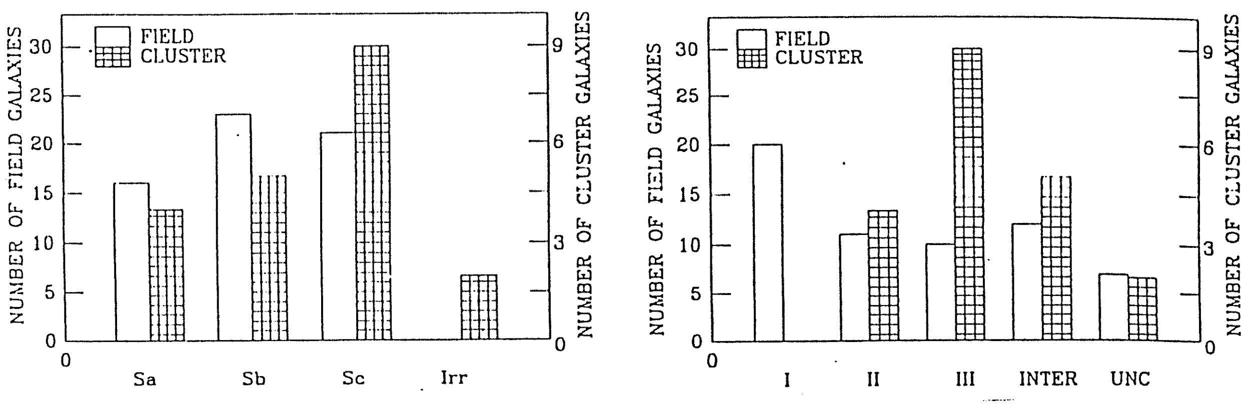

Figure 4.5: Different distributions of mass types in the cluster and in the field (from Burstein *et al.* 1986).

20 cluster galaxies were of type I.

This result is confirmed also by Forbes and Whitmore (1989), who find, contrary to the previous works, that mass types are a function of both the Hubble type and luminosity.

If mass types are not directly a function of luminosity, of mass, of mass density, of Hubble type, or of the bulge–to–disk ratio, this would mean that the dark matter dominate at all radii, and this appear to contradict the results of Kent (1986), who claims that the rotation curves can be predicted fairly well from the luminous distribution, at least over most of their optical extent.

Rotation curves that fit mass type I tend to have fairly similar velocity gradients at all radii, while rotation curves that fit mass type III tend to have steep inner gradients and flat outer gradients. However, it is important to note that because both the mass and the radius are allowed to shift when fitting the curves, it is not possible to characterize the three mass type as simply rising, flat, and falling rotation curves.

From the general study of the rotation curves of spiral galaxies result that a fair number of them are characterized by slowly rising velocities. When the mass distribution derived from these curves is compared with that of light (Fillmore, Boroson and Dressler, 1986; Kent 1988) it results an apparent decrease towards the center of the mass–to–light ratio. Several explanations have been put forward for this phenomenon in spirals. For NGC 4594, it has been suggested that we observe a ring of gas on edge (van Albada and Sancisi, 1986) or that the gas is shed by slowly rotating stars or cooled by an X–ray halo (Kormendy and Westpfahl, 1989). In this case, the presence of a triaxial potential offer a straightforward explanation, as it has been done for the case of NGC 5077 (Bertola *et al.* 1989). Slowly rising curves are in fact predicted when the intermediate axis of the bulge lies near the line of nodes, while fast rising occurs when the major axis lies close to it (Gerhard and Vietri, 1986).

References

Bahcall, J.N.: 1984, *Astrophys. J.*, **287**, 52.

Bahcall, J.N.: 1987, in *IAU Symposium 117, Dark Matter in the Universe*, ed. J. Kormendy and G.R. Knapp (Dordrecht: Reidel), p.17.

Bertola, F., Bettoni, D., Danziger, I.J., Sadler, E.M., Sparke, L.S., and de Zeeuw, P.T.: 1989, in preparation.

Bosma, A.: 1978, *Ph.D. Dissertation*, University of Groningen.

Bosma, A.: 1981a, *Astron. J.*, **86**, 1791.

Bosma, A.: 1981b, *Astron. J.*, **86**, 1825.

Bosma, A., and van der Kruit, P.C.: 1979,*Astron. Astrophys.*, **79**, 281.

Burbidge, G.R.: 1975, *Astrophys. J. Letters*, **196**, L7.

Burbidge, E.M., and Burbidge, G.R.: 1975, in *Galaxies and the Universe*, ed. A. Sandage, M. Sandage, and J. Kristian, (Chigago: Chigago University Press), p.81.

Burstein, D.: 1979, *Astrophys. J.*, **234**, 829.

Burstein, D., and Rubin, V.C.: 1985, *Astrophys. J.*, **297**, 423.

Burstein, D., Rubin, V.C., Ford, W.K., and Whitmore, B.C.: 1986, *Astrophys. J. Letters*, **305**, L11.

Calberg, R.G., and Sellwood, J.A.: 1985, *Astrophys. J.*, **292**, 79.

Capaccioli, M., Held, E., and Nieto, J.–L.: 1987, *Astron. J.*, **94**, 1519.

Capaccioli, M., Vietri, M., and Held, E.: 1988, *Mont. Not. R. astr. Soc.*, **234**, 335.

Carignan, C., and Freeman, K.C.: 1985, *Astrophys. J.*, **294**, 494.

Casertano, S.: 1983, *Mont. Not. R. astr. Soc.*, **203**, 735.

de Vaucouleurs, G., and Freeman, K.C.: 1973, *Vistas Astron.*, **14**, 163.

Einasto, J., Kaasik, A., and Saar, E.: 1974, *Nature*, **250**, 309.

Faber, S.M.: 1987, in *IAU Symposium 117, Dark Matter in the Universe*, ed. J. Kormendy and G.R. Knapp (Dordrecht: Reidel), p.17.

Faber, S.M., and Gallagher, J.S.: 1979, *Ann. Rev. Astr. Ap.*, **17**, 135.
Fall, S.M., and Efstathiou, G.: 1980, *Mont. Not. R. astr. Soc.*, **193**, 189.
Fillmore, J.A., Boroson, T., and Dressler, A.: 1986, *Astrophys. J.*, **302**, 208.
Forbes, D.A., and Whitmore, B.C.: 1989, *Astrophys. J.*, **339**, 657.
Freeman, K.C.: 1970, Ap.J., **160**, 811.
Freeman, K.C.: 1975, in *Galaxies and the Universe*,ed. A. Sandage, M. Sandage, and J. Kristian, (Chigago: Chigago University Press), p.409.
Freeman, K.C.: 1978, IAU Symp.**77**, *Structure and Properties of Nearby Galaxies*, eds. E.M. Berkhuijsen and R. Wielebinski, Reidel, Dordrecht, p.3.
Freeman, K.C.: 1980, in *Photometry, Kinematics, and Dynamics of Galaxies*, ed. D.S. Evans, Univ. of Texas Press, p.85.
Fuchs, B., and Wielen, R.: 1987, in *The Galaxy*, eds. G. Gilmore, R. Carswell, Reidel, Dordrecht, p.375.
Gerhard, O.E., and Vietri, M.: 1986, *Mont. Not. R. astr. Soc.*, **223**, 377.
Gilmore, G., and Reid, N.: 1983, *Mont. Not. R. astr. Soc.*, **202**, 1022.
Gunn, J.E.: 1982, in *Astrophysical Cosmology*, eds. H.A. Bruck, G.V. Coyne, M.S. Longair: Pont. Acad. Sci., Vatican, p.233.
Gunn, J.E.: 1987, in *IAU Symposium 117, Dark Matter in the Universe*, ed. J. Kormendy and G.R. Knapp (Dordrecht: Reidel), p.17.
Hartkopf, W.I., and Yoss, K.M.: 1982, *Astron. J.*, **87**, 1679.
Kalnajs, A.: 1983, in *Internal Kinematics and Dynamics of Disk Galaxies*, IAU Symp.No.100, ed. E. Athanassoula (Reidel, Dordrecht), p.87.
Kent, S.: 1986, *Astron. J.*, **91**, 1301.
Kent, S.: 1988, *Astron. J.*, **96**, 514.
Kormendy, J., and Westpfahl, D.J.: 1989, *Astrophys. J.*, in press.
Kruit, P.C. van der: 1986, *Astron. Astrophys.*, **157**, 230.
Kruit, P.C. van der: 1987, *Astron. Astrophys.*, **173**, 59.
Kruit, P.C. van der: 1988, *Astron. Astrophys.*, **192**, 117.
Kruit, P.C., and Freeman, K.C.: 1984, *Astrophys. J.*, **278**, 81.
Kruit, P.C., and Freeman, K.C.: 1986, *Astrophys. J.*, **303**, 556.
Kruit, P.C. van der, and Searle, L.: 1981, *Astron. Astrophys.*, **173**, 59.
Lacey, C.G.: 1984, *Mont. Not. R. astr. Soc.*, **208**, 687.
Larson, R.B.: 1976, *Mont. Not. R. astr. Soc.*, **176**, 31.
Larson, R.B., and Tinsley, B.M.: 1978, *Astrophys. J.*, **219**, 46.
Neyman, J., Page, T.L., and Scott, E.: 1961, *Astron. J.*, **66**, 633.
Norris, J.E.: 1987, *Astrophys. J.*, **314**, L39.
Oort, J.H.: 1960, *Bull. Astron. Inst. Neth.*, **15**, 45.
Oort, J.H.: 1965, in *Star abd Stellar System V: Galactic Structure*, eds. A. Blaauw and M. Schmidt, Univ. of Chigago Press, p.445.
Ostriker, J.P., and Peebles, P.J.E.: 1973, *Astrophys. J.*, **186**, 467.
Ostriker, J.P., Peebles, P.J.E., and Yahil, A.: 1974, *Astrophys. J. Letters*, **193**, L1.
Pritchet, C.: 1983, *Astron. J.*, **88**, 1476.

Rubin, V.C., Ford, W.K., and Thonnard, N.: 1980, *Astrophys. J.*, **238**, 471.
Rubin, V.C., Ford, W.K., and Thonnard, N.: 1982, *Astrophys. J.*, **261**, 439.
Rubin, V.C., Burstein, D., Ford, W.K., and Thonnard, N.: 1985, *Astrophys. J.*, **289**, 81.
Schmidt, M.: 1965, in *Galactic Structure*, ed. A. Blaauw, and M. Schmidt, (Chigago: Chigago University Press), p.513.
Smith, S.: 1936, *Astrophys. J.*, **83**, 23.
Spitzer, L., and Schwarzschild, M.: 1951, *Astrophys. J.*, **114**, 385.
Tsikoudi, V.: 1977, *Univ. Texas. Publ. Astron.* No. 10.
Trimble, V.: 1987, *Ann. Rev. Astr. Ap.*, **25**, 425.
Tubbs, A.D., and Sanders, R.H.: 1979, *Astrophys. J.*, **230**, 736.
van Albada, T.S., Bahcall, J.N., Begeman, K., and Sancisi, R.: 1985, *Astrophys. J.*, **295**, 305.
van Albada, T.S., and Sancisi, R.: 1986, *Phil. Trans. R. Soc. Lond.*, **A 320**, 447.
Villumsen, J.V.: 1983, *Astrophys. J.*, **274**, 632.
Wainscoat, R.J.: 1986, *Ph.D. Thesis*, Australian Nat. Univ.
Whitmore, B.C., Forbes, D.A., and Rubin, V.C.: 1988, *Astrophys. J.*, **333**, 542.
Wielen, R.: 1977, *Astron. Astrophys.*, **60**, 263.
Zwicky, F.: 1933, *Helv. Phys. Acta*, **6**, 110.

Chapter 5

The Virgo cluster

This chapter presents a review of some of the basic characteristics of the Virgo cluster as a whole and in particular of its spiral member galaxies.

The Virgo cluster would has been discovered by Charles Messier in 1781, if he had only plotted the objects in his catalog of nebulae on a map of the sky. This was practically done by Zwicky (1959) almost two hundred years later. Anyway, already the catalogs of the two Herschels revealed the excess of nebulae in the Virgo region.

Probably the first paper devoted entirely to the Virgo's nebulae was that of Schwassmann (1902), who analysed the positions of 301 objects.

An all sky map of the distribution of the spirals (known at that time), which delineates well the Virgo cluster was provided by Hinks (1911, 1914).

More than a decades later Shapley and Ames (1926) analysed the magnitudes, color and diameters of 103 NGC galaxies in the Virgo region and estimated a distance of 10 million light years.

Ames (1930) compiled a catalog of 2278 galaxies brighter than ~ 18, and Hubble and Humason (1931) attributed several hundred member galaxies to what they called the "Virgo cluster".

Beginning in the mid–1950s de Vaucouleurs (1956, 1961) studied in great detail the galaxy distribution as a function of galaxian type; he found that the "halo" galaxies of the Virgo cluster are concentrated toward a "supergalactic plane".

A new phase of the Virgo cluster research was initiated by Reaves (1956), who isolated new faint cluster members on the basis of their low surface brightness.

At last, Binggeli *et al.* (1985) catalogued 2096 galaxies within an area of ~ 140 deg^2 centered on the Virgo cluster. This catalog was realized with appropiate plates material, with the task of identify all the cluster members down to the limiting magnitude of $B_T = 20$.

In recent years the Virgo cluster has been the subject of an enormous quantity of papers, testimoning the increasing interest of the astronomical community versus this irregular cluster, that for its proximity offers the possibility of studying many astrophysical problems. This advantage stimulated the observations of the Virgo galaxies in all the bands of the electromagnetic spectrum, from the radio, to the infrared, optical and X.

A great number of studies concerns the HI and CO content of the Virgo spiral galaxies. Observations pointed out the existence of an HI deficiency with respect to the field spiral counterparts, while there are not significantly differences for the CO content (see Chapter 6 for more).

The IRAS survey detected 88 galaxies listed in the Virgo Cluster Catalog of Binggeli *et al.* (1985), and among these only two ellipticals, M84 and M87. It resulted that the infrared properties of Virgo and field galaxies are overall very similar, with the exception of early type spirals. In the cluster early type spirals experience more than two times less star formation than in the field, making them very similar in their infrared properties to lenticulars (de Jong, 1984), and it has been speculated that this anomalous behaviour may be related to the cluster environment, which lead to periods of enhanced star formation during galaxy encounters.

A good correlation is established between the 60 μm/100 μm color of galaxies and the mean HI surface density in their disks; galaxies severely depleted in HI fall clearly below that correlation, and are therefore deficient in infrared emission for their infrared color and their blue luminosity. This is not surprising, since HI depletion will lead to lower dust content.

X–ray surveys of the Virgo cluster demonstrated that the differences in the X properties for the member and the field galaxies are rather small, and this is likely due to the low density of the Virgo cluster compared to the richest clusters like Coma. The cluster, in X–ray, is dominated by the emission from M87. The emission is produced by hot gas which is centered on M87 and extends up to 100 arc minutes from the galaxy (Fabricant *et al.* 1980; Fabricant and Gorenstein, 1983). The thermal nature of the emission from the centers of rich clusters has been verified by a number of arguments. First, the spectrum of the emission shows the characteristic emission lines expected from an optically thin hot gas. Second, the actual temperature of $\sim$ 2.5 KeV (3×10^7 $^\circ K$) differs from that of other types of sources (*e.g.*, stars, compact objects, supernova remnants) which might contribute to the emission. Third, the distribution of the X–ray emission (its slow decline with radius compared to the optical light) suggest that the emission is not produced by stellar systems, and fourth, the total X–ray luminosity is more than can be explained by the integrated contributions of known types of sources.

All early type galaxies are found to be surrounded by hot gaseous coronae, which can be used to probe the masses of these galaxies. In addition the masses of these coronae can be explained as the accumulated gas lost by stellar systems during their evolution.

In the following three sections I present a brief review of the studies on the luminosity function of the Virgo galaxies, on the kinematics of the member objects, and on the distance of the entire cluster.

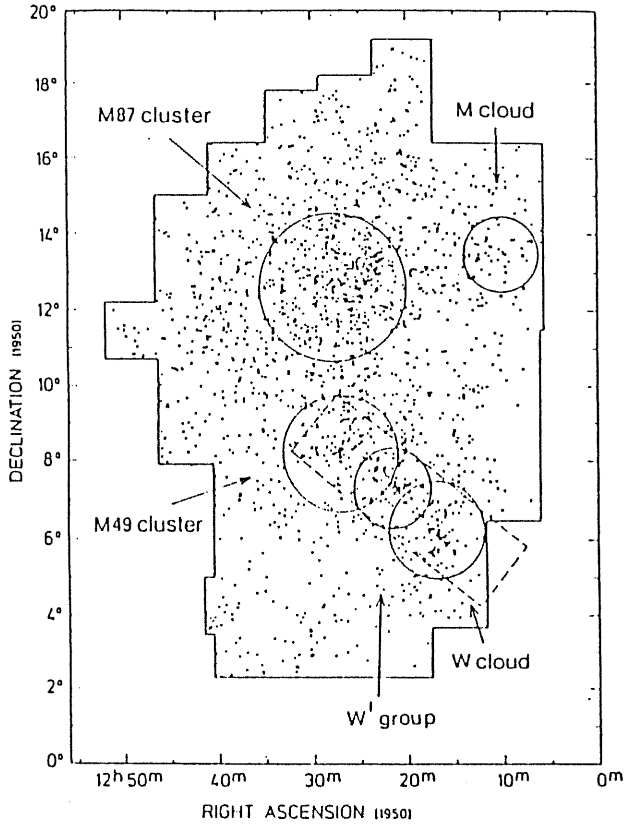

Figure 5.1: Distribution of galaxies in the Virgo cluster (from Binggeli *et al.* 1987).

5.1 Luminosity functions of Virgo galaxies

The determination of the general luminosity function $\phi(M)$ for galaxies of different types is necessary for many problems in astrophysics. As examples, the function is needed to calculate the expected redshift distribution of galaxies of each type in various apparent magnitude intervals, the E–to–Spiral ratio as a function of apparent magnitude (with and without evolution), the expected redshift distribution of any sample whose selection criteria are known and the synthetic galaxy count–magnitude $N(M)$ function at large redshifts. It is also important because the luminosity distribution of spiral galaxies of different types and luminosity classes provides clues for the understanding of spiral structure as a function of total mass.

The determination of $\phi(M)$ has generally presented serious problems due to the effects of observational selection in magnitude–limited samples, or because of insufficient redshift data, or because the apparent magnitude grasp in particular volume–limited samples was not deep enough.

In the common definition, the differential luminosity function $\phi(M)dM$ is the number of galaxies in a complete volume–limited sample in the absolute magnitude interval dM centered on M, summed over all galaxy types T. It is

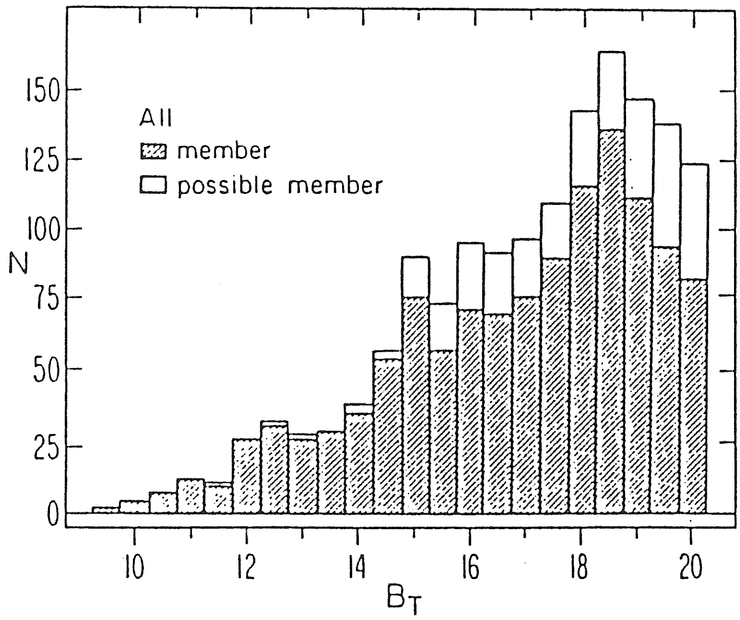

Figure 5.2: Histogram of the differential luminosity function for members and possible members and for galaxies of all types of the sampled area (from Sandage *et al.* 1985).

known that this narrow definition presents certain operational problems that lead to quite different observed forms for the LF, depending on what types of galaxies are counted.

Hubble and Humason (1931) found that the shape of the LF is similar to a Gaussian with a dispersion of $\sim$ 1 mag for galaxies in clusters and in the general field, but the ratio of ellipticals to spirals depends on the number density of galaxies in the particular environment. E galaxies predominate in clusters; spirals dominate the general field.

This morphology–density relation has often been rediscovered (Abell 1958, Morgan 1961, Oemler 1974), and was put on a quantitative basis by Dressler (1980). Adding the number density ρ as a new parameter gives the more general function $\phi(M, T, \rho)$, but even this specificity proves inadequate to understand an early debate over two different claims concerning the existence or absence of a maximum in $\phi(M)$ at some M.

Hubble (1936a,b) extending his early work with Humason found again a near Gaussian distribution for the LF, but his galaxies were almost all of high surface brightness.

Some years later Zwicky (1942) believed that $\phi(M)$ could not have a maximum

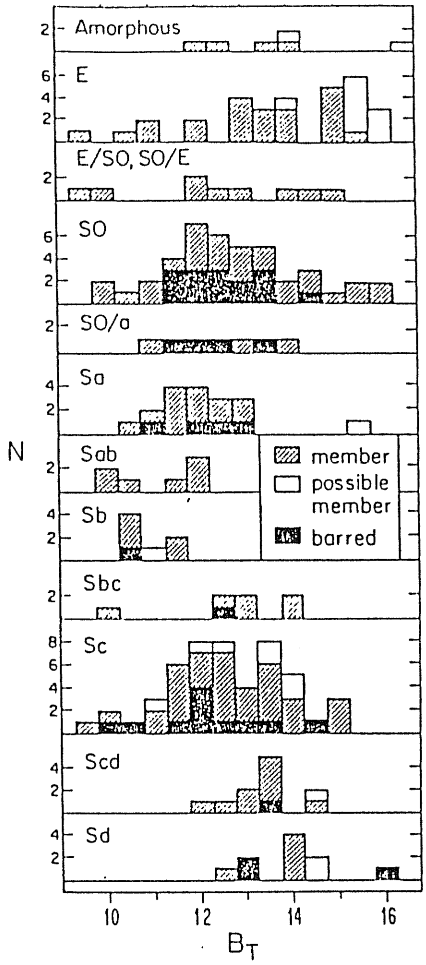

Figure 5.3: Magnitude distributions for Hubble types in the standard sample. No correction for incompleteness are made because the end of the distributions are above the limiting magnitude of the survey ($B_T = 18$) (from Sandage *et al.* 1985).

but must be exponential toward faint magnitudes. In support to his idea, he cited the large number of dwarf Magellanic Cloud-like galaxies, whether in the Local Group (*e.g.*WLM, IC 1613) or slightly beyond (Sextans A and B, Pegasus dwarf, Leo A, etc.).

It is now clear that both Hubble and Zwicky were correct and that the surface brightness (SB) must be added as a fourth parameter for a complete specification of the LF. High SB galaxies have indeed a LF that is approximately Gaussian, while in general galaxies of lower SB, like Sm and Im types or the dE family of Baade (1944) (NGC 147, NGC 185), follow an exponential distribution.

Following Zwicky, a number of studies of groups and clusters began (Holmberg 1969, 1975; Krupp, 1974; Abell 1975). Reaves (1956) discovered the existence of many dwarf ellipticals in the Virgo cluster. In parallel, calculations of $\phi(M,T)$ for galaxies in the general field were repeatedly made as the redshift coverage of the Shapley–Ames (Sandage and Tammann, 1981) catalog of galaxies became progressively more complete. Felten (1977) reviewed the studies of the LF up to 1976, and suggested an exponential form at the faint end of the field galaxies samples as well as for the clusters. Of the same epoch is the analytical represen-

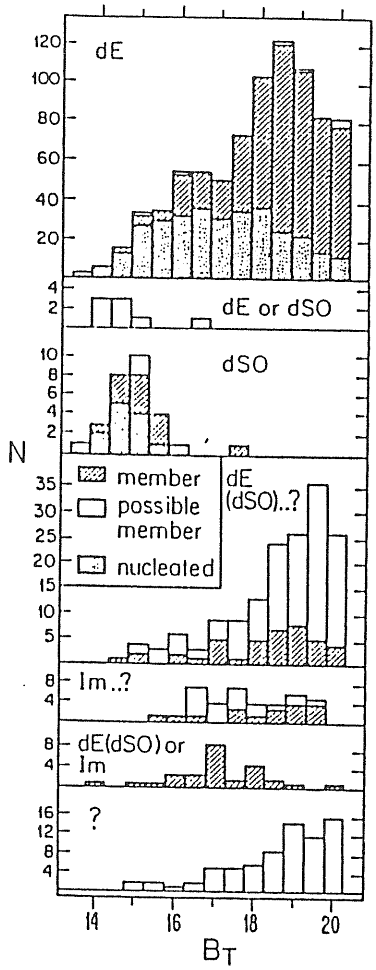

Figure 5.4: Magnitude distributions for dE through Im types. No correction for incompleteness has been applied (from Sandage *et al.* 1985).

tation of the LF by Schechter (1976), which has only two free parameters (plus a normalization factor). The form is exponential at the faint end and a power law at the bright end.

Measurements of redshifts permitted calculation of the LF in more detail for spiral field galaxies of various van der Bergh luminosity classes, and for the E and S0 types separately. Correction for the selection effects of the magnitude-limited sample, whose incompleteness is known, was the principal feature of the calculation (Sandage *et al.* 1979; Tammann *et al.* 1979). The results gave broad $\phi(M,T)$ functions whose maxima were hardly reached (except for Sc I and II spirals) over the range $-23 \lesssim M^{0,i}_{B_T} \lesssim -18$ ($H_0 = 50$). Calculations by Tammann and Kraan (1978) using a local volume limited sample of radius 10 Mpc from the catalog of Kraan–Korteweg and Tammann (1979) were suggestive of maxima to $\phi(M)$ for field spirals near $M_{B_T} \sim -16$. A turnover in $\phi(M)$ for spirals in the Virgo cluster was also suggested by Kraan–Korteweg (1981) in a study of the bright end part of the LF for 176 members.

With the completion of the Virgo cluster catalog (Bingelli, Sandage and Tammann, 1985) Sandage *et al.* (1985) had the opportunity to determine $\phi(M)$ to faint enough magnitude ($B_T \sim 20$) for well defined sample of galaxies all nearly at the same distance. These luminosity functions, for galaxies of various Hubble

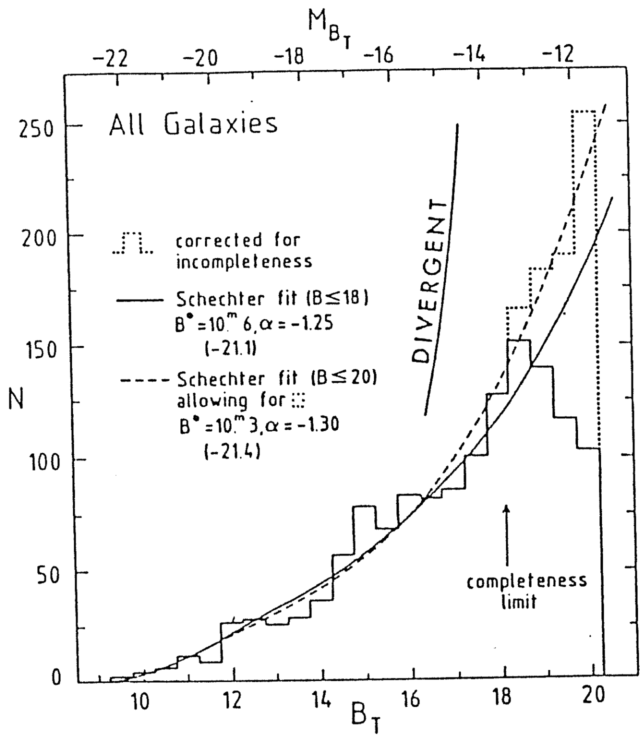

Figure 5.5: The Luminosity Function for galaxies of all types in the standard region (from Sandage *et al.* 1985).

types in the central 6° radius core, show fundamentally different forms for the high and low surface brightness systems.

The classical E, S0, and all of the spiral types have luminosity functions that are closely Gaussian, bounded at both the bright and faint limits, as originally proposed by Hubble (1936a,b), while dwarf ellipticals have an ever increasing differential luminosity function which is similar to the exponential LF proposed by Zwicky (1942).

Three membership criteria are used: **1)** the degree of resolution into the stellar content for the late type galaxies, **2)** the low surface brightness of the dE family, and **3)** velocities, if the two first criteria fail. As Fig.5.1 shows, the LF has been evaluated only in the inner region of the cluster, excluding the M and W Cloud and the Souther Extention, since there are no reliable ways, either from morphology or from velocities, to determine enough accurate distances to assign any given galaxy of these regions to the cluster.

Fig.5.2 shows the magnitude distribution of all morphological types set out together. The LF is closely exponential even taken into accunt the corrections for incompleteness from $B_T = 18$ to 20.

Fig.5.3 shows the data in a more detailed form, separating different morphological types. The order of the presentation is that of the Hubble sequence. This

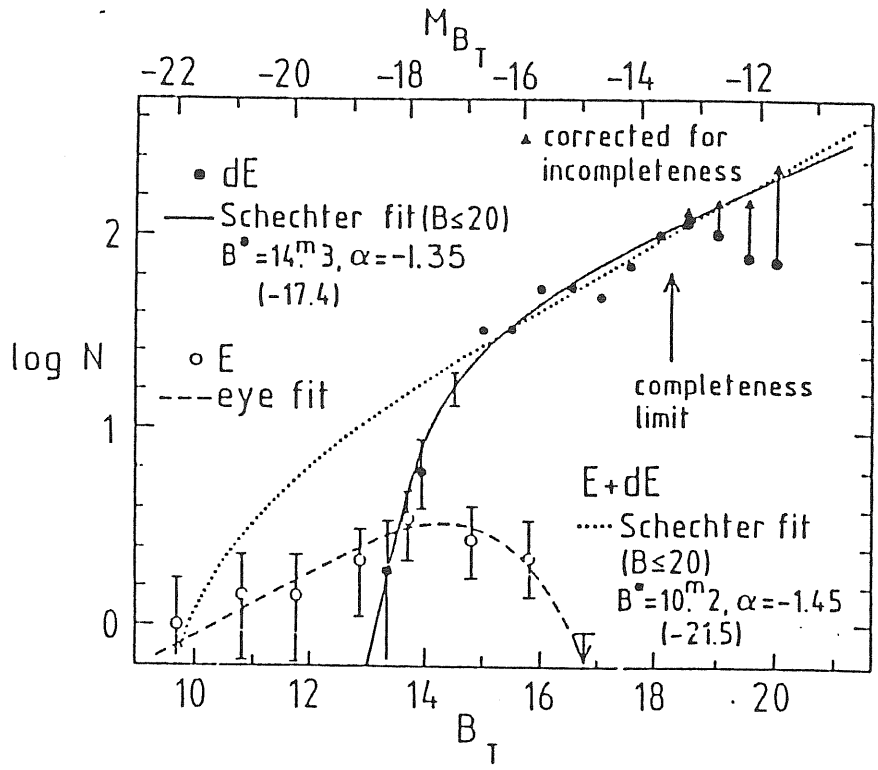

Figure 5.6: Fits to the E and dE separately and in logarithmic form (from Sandage *et al.* 1985).

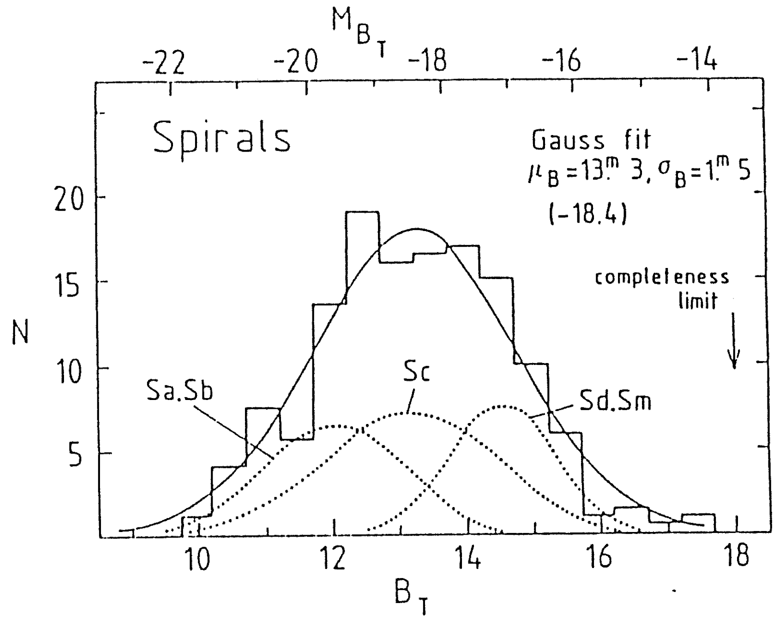

Figure 5.7: LF of all the spirals (from Sandage *et al.* 1985).

figure is the main conclusion of their work. The LF's for the giant E's, the S0's, and all spirals are limited on both the bright and faint ends of the distributions. The diagram also shows that the mean absolute magnitude varies among the types. Here the Sa galaxies are fainter than the Sab and Sb types by $\Delta\langle B\rangle \sim 0.4$ mag. The same was found among the field galaxies (de Vaucouleurs, 1977; Kraan–Korteweg, Sandage, and Tammann, 1984) and it appears as an unexpected result that the brightest spirals are not the Sa's as might be expected from their large maximum rotational velocities (Rubin, Ford, and Thonnard, 1980).

There is almost no uncertainty concerning membership of the dE types in the Virgo cluster within the standard sample because of the existence of the surface brightness–M_B relation. This explains the absence of possible members in the first frame of Fig.5.4. The strong increase in the number of dE's and dE(dS0) types with magnitude is the principal feature of this diagram, in direct contrast with the near Gaussian behavior of the LF for the spirals.

The data fitting has been performed with the Gauss function for symmetrical distributions and with the Schechter (1976) function for exponential and skewed distributions. These have the forms:

$$\phi(M) \sim e^{\frac{(M-\mu)^2}{2\sigma^2}} \tag{5.1}$$

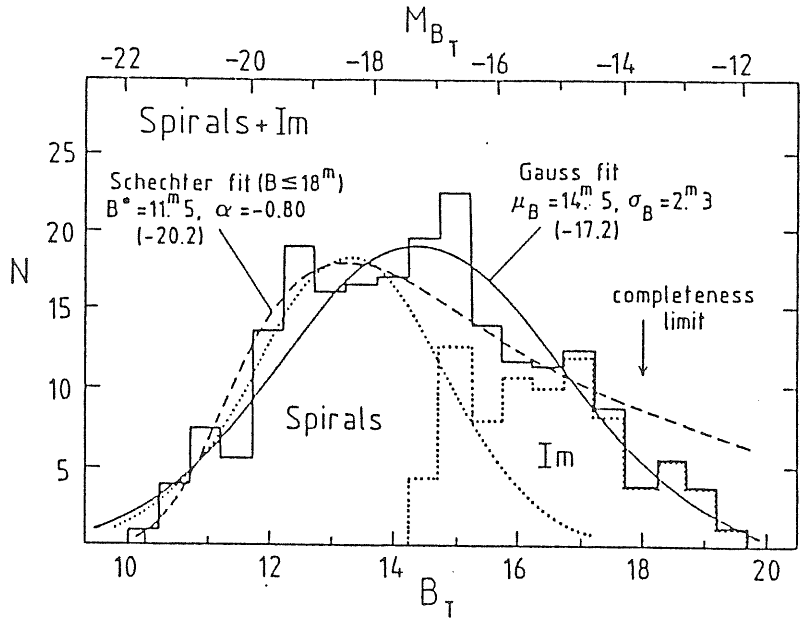

Figure 5.8: Composite LF for all spirals and irregular galaxies (from Sandage *et al.* 1985).

and

$$\phi(L) \sim (L/L^*)^\alpha e^{-(L/L^*)} \tag{5.2}$$

where μ is the mean magnitude, σ is the dispersion, and L^* is a fitting parameter.

Fig.5.5 shows the result of the fitting for galaxies of all types in the standard region. The parameters of the Schechter fit are indicated, as is the special "divergent" case $\alpha = -2$. We can also see in Fig.5.6 the fit obtained considering only E and dE types. The figure suggests that dE's do not form a continuum with the giant E's, but rather the two form separate families, as argued for example by Wirth and Gallagher (1984). A similar conclusion has been reached by Kormendy (1985): he found, in his study of the centers of E and dE systems with high spatial resolution, no continuity of nuclear properties (core radius and surface brightness) between the types, despite the apparent continuity that was found by Binggeli *et al.* (1984) in the effective surface brightness and the central density parameters.

Fig.5.7 shows the LF for the spirals alone, not separated in the histogram by Hubble types. The luminosity functions of the separate types are shown as individual dotted Gaussian, where the progressive dimming of $\langle M_B \rangle$ in the progression Sa+Sb, Sc, Sd+Sm is evident, although there is much overlap in the distributions. Some observations are necessary: **1**) there are no low–luminosity spirals; **2**) there are very few Sm and Im irregular galaxies brighter than $M_B \sim -18$; **3**) most disk galaxies brighter than this value develop arms; **4**) the composite LF for all current star–producing galaxies in the Virgo cluster show a maximum (see Fig.5.8).

5.2 Morphology and Dynamics of the Virgo cluster

Recently, the structure of the Virgo cluster has been analyzed by Binggeli, Tammann, and Sandage (1987) on the basis of the positions, Hubble types, and radial velocities of the 1277 galaxies listed in the catalog of Virgo galaxies of Binggeli, Sandage, and Tammann (1985).

The principal results are as follows:

1) The Virgo cluster shows pronounced double structure. The main concentration, cluster A, containing M87, is made up predominantly of early type galaxies and has a large velocity dispersion of $\sigma_v \sim 750$ km s^{-1}. A second, smaller and looser concentration, cluster B, near M49, contains mainly late types and has the much smaller velocity dispersion of $\sigma_v \sim 400$ km s^{-1}. The mean radial velocity of B is lower than that of A by $\Delta v \sim 100$ km s^{-1}, and there are several arguments that suggest that cluster B is falling towards cluster A from behind.

2) There is a strong spatial segregation of Hubble types. Early–types (E, S0, dE, dS0) galaxies are more concentrated towards the cluster center than late types (spirals and irregulars). The morphology–density relation is in good agreement with Dressler's (1980) mean relation derived from 55 clusters. Late–types also show a larger velocity dispersion than early–types ($\sigma_v = 890$ versus 570 km s^{-1}, but with similar velocity means), giving support to the hypothesis that Virgo late–type galaxies are still in a stage of infall, or have fallen into the cluster only recently (Tully and Shaya, 1984).

3) Ring counts about cluster A are well fitted by either an exponential or a King profile, giving an e–folding scale length of $2^\circ.1$, or a King core radius of $1^\circ.7$ (0.65 Mpc). The central luminosity density is 5×10^{11} solar luminosities B per Mpc^3.

4) There is a significant substructure in the cluster core. M87 is not the center of cluster A, neither in space nor in velocity. This is taken as evidence that the core of the Virgo cluster is not yet dynamically relaxed.

5) The mean heliocentric cluster velocity is $\langle v \rangle = 1094 \pm 42$ km s^{-1}. Correcting to the frame of the Local Group gives $\langle v_0 \rangle = 976 \pm 45$ km s^{-1}. Correcting for the 220 km s^{-1}infall of the Local Group towards Virgo gives a true Hubble expansion rate for the Virgo cluster of $\langle v_{220} \rangle = 1196 \pm 67$ km s^{-1}, which would be the observed velocity from the Local Group centroid in the absence of the local Virgocentric flow.

It is worth to note that the structure of the Virgo cluster is complex. Infact, it is generally classified as an irregular cluster. Regular cluster have been presumed to be more evolved and relaxed, whereas, at a closer looks, the cluster shows several clouds of distinct structural and kinematical properties (de Vaucouleurs, 1961; de Vaucouleurs and de Vaucouleurs, 1973). Further, because of its large angular extent, the Virgo cluster is very hard to map photographically at a high angular resolution.

As we have summarized above, the cluster consists of two main concentration, A (near M87) and B (around M49). Cluster A is the dominant feature of the Virgo cluster. It contains about five times as many galaxies as cluster B. Cluster A is dominated by early type galaxies, whereas cluster B consists mainly of late type members. Cluster B is measured to be marginally more distant by 0.46 ± 0.31 mag than cluster A. Both are embedded in a large, elongated halo. The isophotes also reveal a third concentration C, which surrounds M59, and is connected by a bar–like isophote with cluster A.

In the following we address the question of the different morphological types of galaxies distributed in the cluster, and of their kinematical properties.

E and S0 galaxies form the inner core of the Virgo cluster. These galaxies are strongly concentrated around M87, and they are the bright galaxies in cluster A. Separating S0 and E types we can see that the latter are preferentially distributed along the EW axis. This apparent chain of E galaxies was first identified by Arp (1968), who showed that it is aligned with the jet of M87. Fig.5.9 shows the distribution of early type galaxies in the Virgo cluster.

dE galaxies greatly outnumber every other galaxy type in the Virgo cluster. Their distribution is similar to that of the early–type (E+S0) giants, showing also a strong concentration towards cluster A, which is in sharp contrast to the distribution of late–type (S+Irr) galaxies.

An interesting difference emerges by distinguishing between bright and faint, and between nucleated (dE,N) and non–nucleated (dE) dwarf ellipticals. Faint dwarfs are more dispersed than bright ones, and non–nucleated dwarfs are more dispersed than nucleated ones (Fig.5.10).

Spiral and irregular (Im) galaxies are scattered over the whole face of the cluster, making it difficult to see any clear boundary in their distribution. These galaxies occupy a wider area and presumably larger volume than the early type galaxies. Moreover, the wider velocity distribution shows that they are in a different stage of dynamical evolution than the early type galaxies. Some authors suggest that many Virgo spirals and Im's are presently falling towards the cluster core for the first time (de Vaucouleurs, 1982; Tully and Shaya, 1984; Shaya, 1986). Fig.5.11 shows the distribution of late–type galaxies in the Virgo cluster.

The heliocentric velocity distributions for all Virgo members, divided into the main morphological classes and into the members of cluster A and B, are shown in Fig.5.12. It can be seen that early type galaxies (E+S0+dE+dS0) have a narrow velocity distribution with a dispersion of $\sigma_v = 573$ km s^{-1}, while late type galaxies (spiral+irr) show a broad distribution with $\sigma_v = 888$ km s^{-1}. This means that late type are not only more dispersed in space, but also in velocity. This higher velocity dispersion for late type galaxies has suggested the idea of the existence of infalling and/or expanding shell or streams of these galaxies surrounding the cluster core (Moss and Dickens, 1977; Sulentic, 1977; de Vaucouleurs, 1982; Tully and Shaya, 1984; Huchra, 1985). There is growing support for this view, for example, by Rivolo and Yahil (1983). The formation of a cluster embedded in the wider surroundings of the supercluster is a process that is still going on today. Shell after shell decouple from the universal Hubble flow and fall towards the cluster and move through it until the shell galaxies are virialized. Consequently, "the bulk of the mass of the central cluster is made up of galaxies which are not in hydrostatic equilibrium, but are streaming radially inward or outward, either in their initial collapse, or in their first orbit following rebound".

The mean velocity of the system of dwarf ellipticals is higher ~ 200 km s^{-1}than the mean velocity of the E+S0 system. The mean velocity of the dE+dS0's is the same within the errors as that of M87. However, only the innermost dwarf ellipticals within a $2°$ circle around M87 have a high mean velocity of $\langle v \rangle = 1436 \pm 108$ km s^{-1}, exceeding, in fact M87 by $\Delta v = 178 \pm 108$ km s^{-1}, whereas the dwarf ellipticals outside of this circle have $\langle v \rangle = 1133 \pm 129$ km s^{-1}, in close agreement with the value of $\langle v \rangle = 1079 \pm 48$ km s^{-1}for all the remaining cluster members. Hence, the conclusion is that the inner dE's are dynamically connected with M87.

The peculiar velocity field of the Virgo cluster can be described as a sum of two terms: the overall velocity of the entire Virgo Supercluster with respect to the Robertson–Walker frame, *i.e.*, the microwave backgroud radiation, and the internal velocities within the Virgo Supercluster. Fortunatly, these flow patterns are well decoupled, because the tidal force due to distant density perturbations is small compared with the force induced by the Virgo Supercluster itself. The internal motions within the Virgo Supercluster have been approximated by a spherical Virgocentric inflow pattern, and this can be justified a posteriori because of the smallness of the peculiar velocities, and the strong central concentration of the

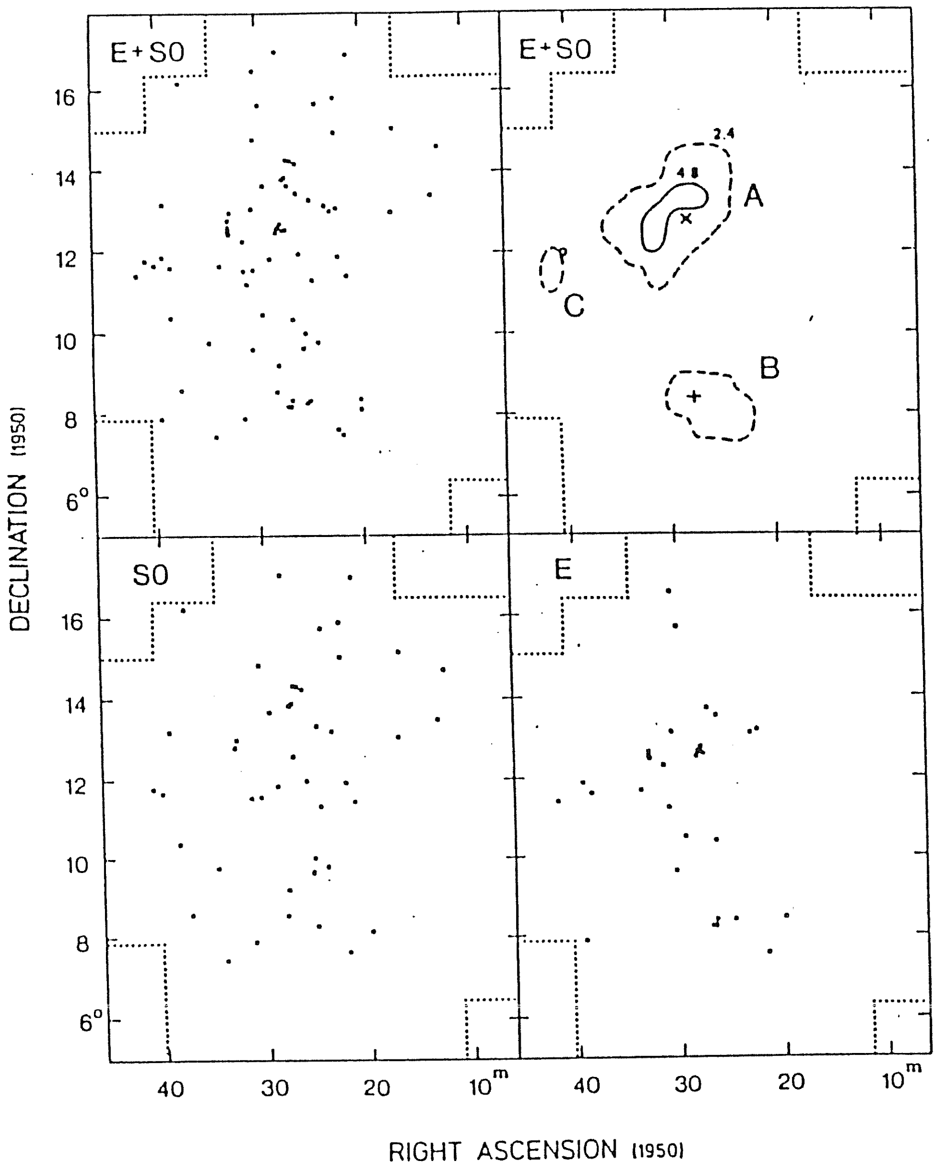

Figure 5.9: Distribution of E and S0 members of the Virgo cluster (from Binggeli *et al.* 1987).

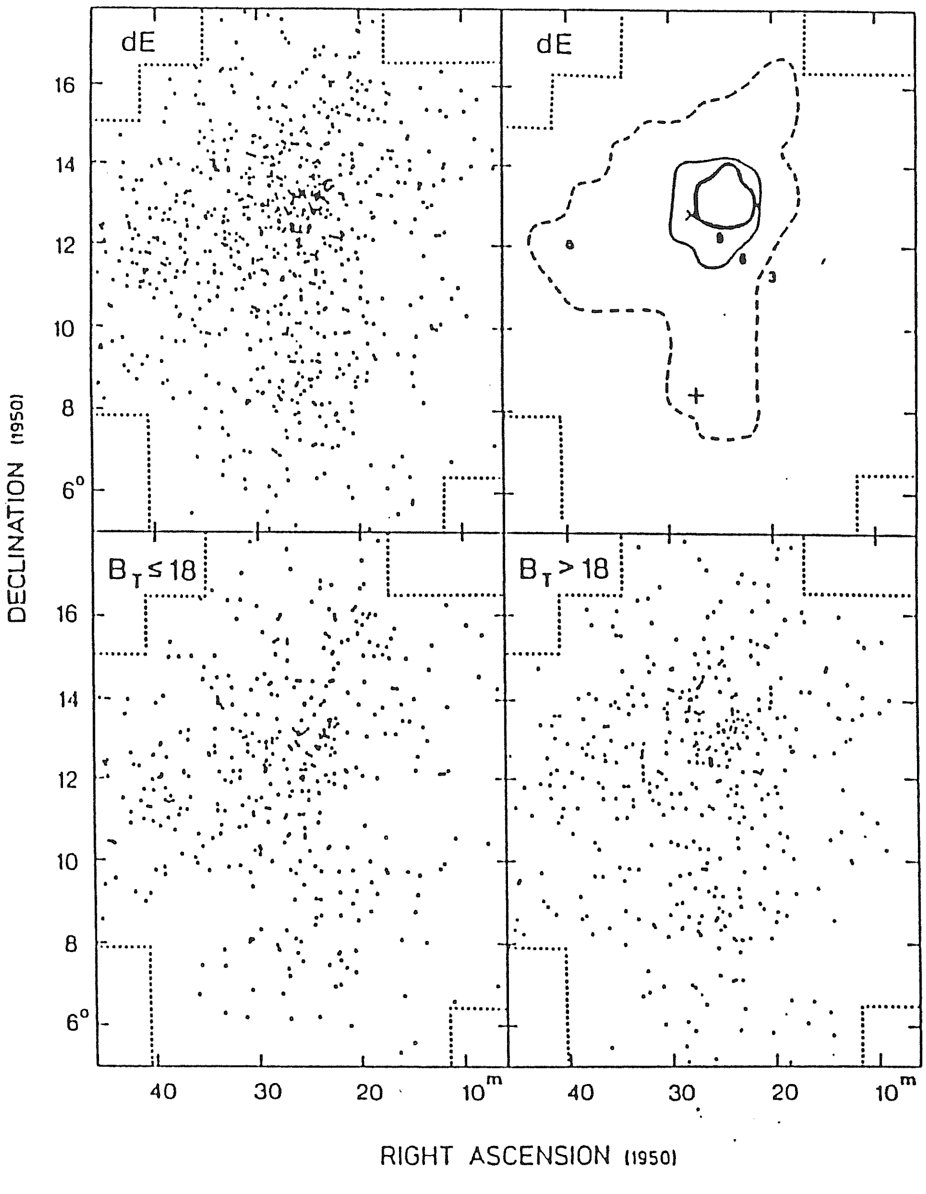

Figure 5.10: Distribution of dwarf elliptical galaxies in the Virgo cluster. (a) All dE members. (b) Corresponding isopleths. (c) dE members with $B_T = 18$ or brighter. (d) dE members fainter than $B_T = 18$ (from Binggeli *et al.* 1987).

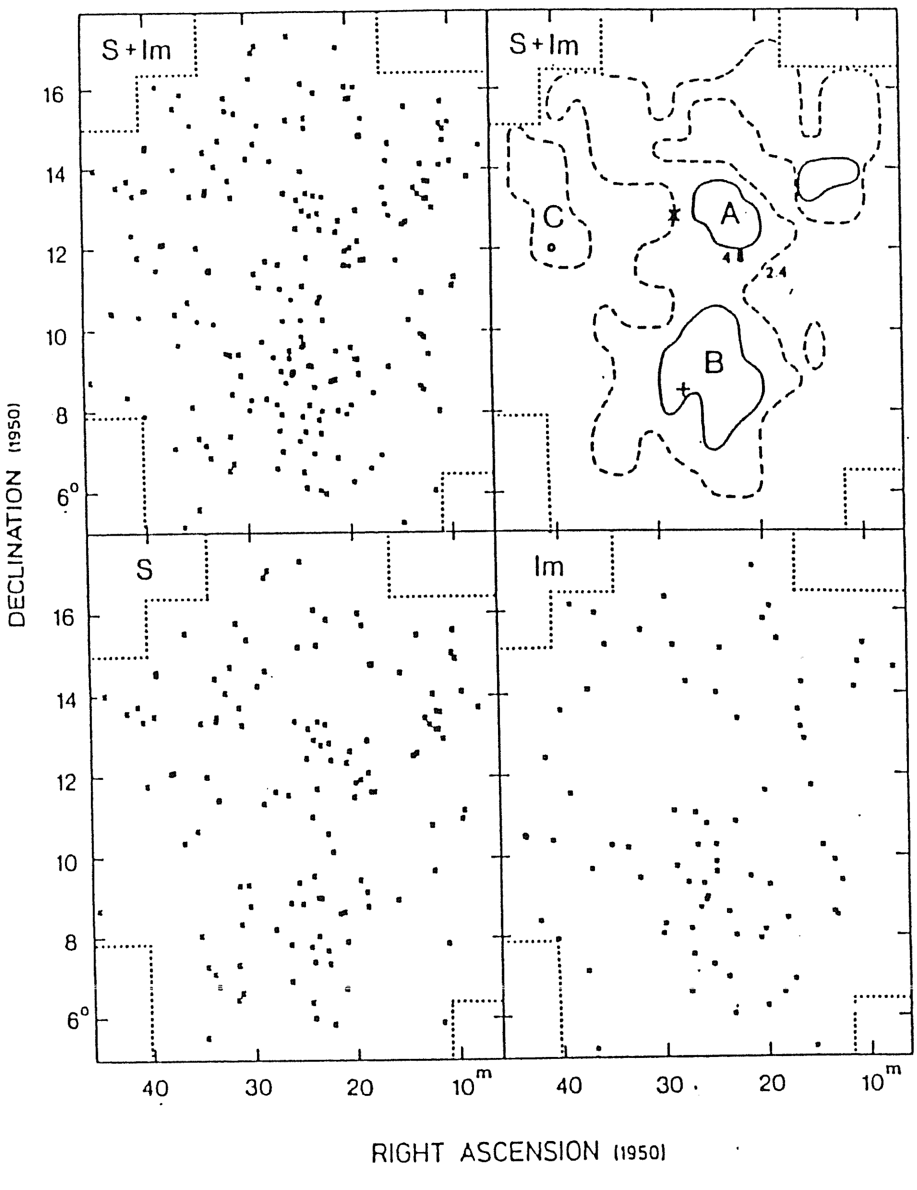

Figure 5.11: Distribution of late type galaxies in the Virgo cluster. (a) All spiral and Im galaxies (no blue compact dwarf). (b) Corresponding isopleths. (c) Spirals alone. (d) Im galaxies alone (from Binggeli *et al.* 1987).

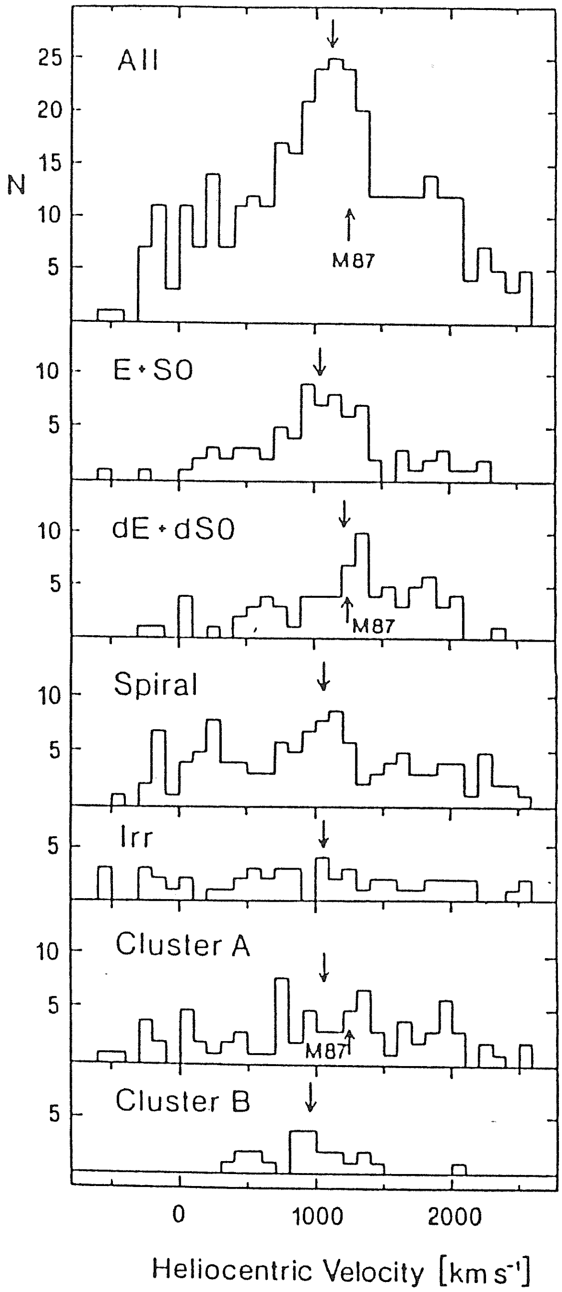

Figure 5.12: Velocity distribution for the entire Virgo cluster sample broken up into four different morphological groups, and into galaxies of all types in the areas of cluster A (around M87), and cluster B (around M49). The arrows pointing downwards mark the corresponding velocity means (from Binggeli *et al.* 1987).

density perturbations (Yahil, 1984). A quantitative understanding of the Virgocentric infall field is of great importance for the calculation of the local mass density ρ_L within the Virgo complex and of the large-scale mean mass density ρ_0, as well as for an understanding of the locally complex correlation between distance and recession velocity.

5.3 The distance of the Virgo cluster

The Virgo cluster provides one of the most important stepping stones in the determination of the extragalactic distance scale. Its distance modulus has been used to determine the Hubble constant ever since the 1920's.

Recently Tammann (1986) argued that the Virgo cluster is roughly three times more distant than the M101 group (Sandage and Tammann, 1976), *i.e.*, at a distance of $\sim$ 20 Mpc. His arguments involve, besides 21 cm line widths, the brightest stars, the HII region sizes, the luminosity class of galaxies, the diameters and the redshifts. In principle, a bias free distance of Virgo can be derived from IR magnitudes and 21 cm line witdths, since B magnitudes may suffer of intrinsic absorption; using the data of Aaronson *et al.* (1982), Tammann (1986) estimated a distance modulus of 31.57 ± 0.25.

On the other hand, de Vaucouleurs (1984) using seven different calibrators, give a value of 30.40 ± 0.10 for the E cloud, and 30.70 ± 0.10 for the S cloud, which he distinguished as the two main components of the Virgo cluster (de Vaucouleurs, 1961).

Today, the question of the true distance modulus of the Virgo cluster is still open. Many different distance indicators have been used, leading to slightly different values for the distance modulus. I want to mention only a few of these recent determinations.

Globular cluster have resisted for a long time to yield a meaningful Virgo distance. However, the recent discovery of the turnover of the magnitude distribution of the globulars of M87 at $B = 25.0 \pm 0.3$ leads to a modulus of 31.43 ± 0.3.

The Faber–Jackson relation applied to the bulges of early type spirals, enabled Dressler (1986) to evaluate a distance modulus of 31.64 ± 0.3.

Capaccioli *et al.* (1989) determined the distance of the Virgo cluster using novae, which has been discovered by Pritchet and van den Bergh (1987b). Prouving the reliability of novae as primary distance indicators by means of the Maximum Magnitude vs. Rate of Decline (MMRD) relationship applied to M31, they found an absorption corrected distance modulus for the Virgo cluster of 31.30 ± 0.40. This value is in agreement with the determination of 31.45 ± 0.44, obtained by

Pritchet and van den Bergh (1987b), calibrating the M31 MMRD through the RR Lyrae.

The mean corrected magnitudes of four well–observed Type I supernovae in the Virgo cluster ($\langle m_{pg} \rangle = 11.58 \pm 0.22$) imply a mean corrected distance modulus of 30.55 ± 0.41, corresponding to a distance of 12.9 ± 2.5 Mpc (de Vaucouleurs, 1985).

As I said before, an important question related to this topic, is the determination of the Hubble constant. The value of H_0 is rigidly tied to the use of the distance indicators. In particular there are problems with the evaluations of: **a)** the galactic absorption, **b)** the k–term, **c)** the luminosity and diameter of the galaxies, **d)** the malmquist bias, **f)** the deviations from the Hubble flow, etc.

The classical values are $H_0 = 55 \pm 7$ (Tammann, 1986), and $H_0 = 100 \pm 10$ (de Vaucouleurs, 1984); they derive from the different assumptions used for the primary and secondary distance indicators. In this context, it is worth to note the recent determination of H_0 by Capaccioli *et al.* (1989); they used an approach to evaluate H_0, which is not strongly dependent upon assumptions on the solar motion, on the Virgo infall and on the mean heliocentric velocities, but uses the redshift of the Coma cluster and the ratio between the distances to Virgo and Coma (evaluated through the critically revised maximum magnitude of Type I supernovae). The value of 70 ± 0.15 is in good agreement with other recent determinations obtained through different distance indicators.

References

Aaronson, M., Huchra, J., Mould, J.R., Tully, R.B., Fisher, J.R., van Woerden, H., Goss, W.M., Chamaraux, P., Mebold, U., Siegman, B., Berriman, G., and Persson, S.E.: 1982, *Astrophys. J. Supp.*, **50**, 241.

Abell, G.O.: 1958, *Astrophys. J. Supp.*, **3**, 211.

Abell, G.O.: 1975, in *Star and Stellar System IX: Galaxies and the Universe*, eds. A. Sandage, M. Sandage, and J. Kristian (Chicago: University of Chicago Press), p.601.

Ames, A: 1930, Harvard Ann., **88**, 1.

Baade, W.: 1944, *Astrophys. J.*, **100**, 147.

Binggeli, B., Sandage, A., and Tammann, G.A.: 1985, *Astron. J.*, **90**, 1681.

Binggeli, B., Sandage, A., and Tarenghi, M.: 1984, *Astron. J.*, **89**, 64.

Binggeli, B., Tammann, G.A., and Sandage, A.: 1987, *Astron. J.*, **94**, 251.

Capaccioli, M., Cappellaro, E., Della Valle, M., D'Onofrio, M., Rosino, L., and Turatto, M.: 1989, *Astrophys. J.*, in press.

de Vaucouleurs, G.: 1956, *Vistas in Astronomy*, **2**, 1984.
de Vaucouleurs, G.: 1961, *Astrophys. J. Supp.*, **6**, 213.
de Vaucouleurs, G.: 1977, in *The Evolution of Galaxies and Stellar Populations*, eds. B. Tinsley and R.B. Larson (Yale University, New Haven), p.43.
de Vaucouleurs, G.: 1982, *Astrophys. J.*, **253**, 520.
de Vaucouleurs, G.: 1984, *Eso Workshop on the Virgo Cluster*, eds. O.G. Richter and B. Binggeli, p.413.
de Vaucouleurs, G.: 1985, *Astrophys. J.*,
Dressler, A.: 1980, *Astrophys. J.*, **236**, 351.
Dressler, A.: 1986, *Astrophys. J.*,
Fabricant, D., Lecar, M., and Gorenstein, P.: 1980, *Astrophys. J.*, **241**, 552.
Fabricant, D., and Gorenstein, P.: 1983, *Astrophys. J.*, **267**, 535.
Felten, J.E.: 1977, *Astron. J.*, **82**, 861.
Hinks, A.: 1911, *Mont. Not. R. astr. Soc.*, **71**, 588.
Hinks, A.: 1914, *Mont. Not. R. astr. Soc.*, **74**, 707.
Holmberg, E.: 1969, *Ark. Astron.*, **5**, 305.
Holmberg, E.: 1975, in *Star and Stellar System IX: Galaxies and the Universe*, eds. A. Sandage, M. Sandage, and J. Kristian (Chigago: University of Chigago Press), p.123.
Hubble, E.:1936a, *Astrophys. J.*, **84**, 158.
Hubble, E.:1936b, *Astrophys. J.*, **84**, 270.
Hubble, E., and Humason, M.L.: 1931, *Astrophys. J.*, **74**,43.
Jong, T. de: 1984, *Eso Workshop on the Virgo Cluster*, ed. O.G. Richter and B. Binggeli, p.111.
Kormendy, J.: 1985, *Astrophys. J.*, **295**, 73.
Kraan–Korteweg, R.C., and Tammann, G.A.: 1979, *Astron. Nachr.*, **300**, 181.
Kraan–Korteweg, R.: 1981, *Astron. Astrophys.*, **104**, 280.
Kraan–Korteweg, R.C., Sandage, A., and Tammann, G.A.: 1984, *Astrophys. J.*, **283**, 24.
Krupp, E.C.: 1974, *Publ. Astron. Soc. of Pacific*, **86**, 385.
Morgan, W.W.: 1961, *Proc. Natl. Acad. Sci.*, **47**, 905.
Moss, C. and Dickens, R.J.: 1977, *Mont. Not. R. astr. Soc.*, **178**, 701.
Oemler, A.: 1974, *Astrophys. J.*, **194**, 1.
Pritchet, C.J., and van den Bergh, S.: 1987b, *Astrophys. J.*, **318**, 507.
Reaves, G.: 1956, *Astron. J.*, **61**, 69.
Rivolo, A.R. and Yahil, A.: 1983, *Astrophys. J.*, **274**, 474.
Rubin, V.C., Ford, W.K., and Thonnard, N.: 1980, *Astrophys. J.*, **238**, 471.
Sandage, A., and Tammann, G.A.: 1976, *Astrophys. J.*, **210**, 7.
Sandage, A., and Tammann, G.A.: 1981, *A revised Shapley–Ames Catalog of Bright Galaxies*, (Washington: Carnegie Institute of Washington), Publication No. 635.
Sandage, A., Tammann, G.A., and Yahil, A.: 1979, *Astrophys. J.*, bf 232, 352.
Sandage, A., Binggeli, B., and Tammann, G.A.: 1985, *Astron. J.*, bf 90, 1759.

Schechter, P.: 1976, *Astrophys. J.*, **203**, 297.
Schwassamann, A.: 1902, *Publ. Astr. Obs.*, Königstuhl Heidelbergh, **1**, 17.
Shapley, H., and Ames, A.: 1926, Harvard Circ. 294.
Shaya, E.: 1986, in *Galaxy Distances and Deviations from Universal Expansion*, eds. B.F. Madore and R.B. Tully (Reidel, Dordrecht), p.229.
Tammann, G.A.: 1986, in *Observational Cosmology*, IAU Symp. No. 124, (Beijing: China).
Tammann, G.A., and Kraan, R.C.: 1978, in *The Large Scale Structure of the Universe*, IAU Symp. No. 79, eds. M.S. Longair and J. Einasto (Reidel, Dordrecht), p.71.
Tammann, G.A., Yahil, A., and Sandage, A.: 1979, *Astrophys. J.*, **234**, 775.
Tully, R.B., and Shaya, E.: 1984, *Astrophys. J.*, **281**, 31.
Wirth, A., and Gallagher, G.A.: 1980, *Astrophys. J.*, **282**, 85.
Yahil, A.: 1984, *Eso Workshop on the Virgo Cluster*, eds. O.G. Richter and B. Binggeli, p.359.
Zwicky, F.: 1942, *Phys. Rev.*, **61**, 489.
Zwicky, F.: 1959, *Hand. der Physik*, **53**, 390.

Chapter 6

HI and CO observations of Virgo spiral galaxies

6.1 HI surveys and role of the IGM

It is becoming apparent that the evolution and present properties of galaxies are determined, not only by their genetic inheritance, but also in a non negligible way by the environmental conditions they experience in the course of their lifetime. Evidence for such a view is provided by the various dissimilarities between cluster and field galaxies.

Van den Bergh (1976) has suggested that all the peculiarities of cluster galaxies can be accounted for by the continuous stripping of their interstellar gas resulting from galactic collisions and from their interaction with the intracluster medium, the most striking proof of this being the existence of a class of "anemic" spirals in the Virgo cluster. Infact, if the intergalactic medium plays an important role in the evolution of spiral galaxies, then the Virgo cluster offer the nearest example of such process at work.

Subsequent 21–cm surveys of the cluster have been used in an attempt to test his conjecture (Huchtmeier, Tamman, and Wendker 1976; Chamaraux, Balkowsky, and Gerard 1980; Giovanardi, Helou, Salpeter, and Krumm 1983; Hoffman *et al.* 1989). Three important 21 cm line works have been devoted to this subject: first those by Davis and Lewis (1973) and Huchtmeier *et al.* (1976), which conclude that the cluster members have an HI deficiency of about a factor of 1.7. Another study has been carried out by Krumm and Salpeter (1979a,b); it concerns S0 and early type spirals, and clearly shows that they are also HI deficient.

Chamaraux, Balkowsky and Gerard (1980) determined, in their work based on 21 cm data for 56 of the Virgo spiral galaxies, that **1)** spirals of type Sb and later within 6° of the center of Virgo are HI deficient by a factor of 2.2 relative to the field sample of Balkowski (1973) and that the Virgo members external to that radius have normal gas content (the gas deficiencies do not appear to depend on galaxy luminosity or morphological type); 2) the Virgo spirals, on average, are red for their type (as shown by Holmberg 1958), but blue relative to field galaxies of the same type and HI content.

The comparison between the HI masses of Virgo spirals and that of the "normal" field sample, is made possible because the HI mass $(M_H)_N$ of a normal galaxy is not arbitrary; it is infact well determined by two parameters only, the morphological type T and the photometric linear diameter A_0 of the galaxy, as shown in previous studies (Gouguenheim, 1969; Roberts, 1969; Balkowski, 1973).

In general, while all investigators have observed a significant difference between the HI properties of Virgo cluster and field galaxies, their interpretations have differed, attributing the differences to everything from simple observational selection effects to ram–pressure sweeping of the disk in the cluster.

In order to test the contention that the cluster spirals possess anomalously evolved disks, Kennicutt (1983) combined $H\alpha$ integrated emission lines with published HI and $B-V$ color data, and compare them with analogous data of a large sample of field spirals (Kennicutt and Kent 1983). The combined data point to a real difference between the two sample of galaxies and make it possible to place constraints on the possible causes of the differences. A similar analysis has been reported also by Stauffer (1983), but limited exclusively to nuclear emission.

Two relevant quantities are extracted from the photometry, an absolute $H\alpha$ + [NII] emission line flux, which is related to the total number of OB stars in the galaxy, and a line to continuum ratio, expressed as an emission line equivalent width, which to first order represents a ratio of young to old starlight, and hence serves as a luminosity–independent index of the relative star formation rate.

A comparison of the $H\alpha$ + [NII] distributions in the cluster and the field reveals that both samples possess a broad range in emission line properties, but the Virgo core members exhibit significantly weaker emission on average. The distribution of line emission in Sc galaxies is shown in Fig. 6.1, subdivided into cluster and field members.

Histograms of $\log(M_H/L_B)$ for the Virgo and field galaxies are shown in Fig.6.2 for individual Hubble types. Again we see a broad dispersion in HI content, and differences between field and cluster members. However, a "deficiency" in M_H/L_B does not necessarily imply low M_H.

Finally, the color distributions are shown in Fig.6.3. The Virgo Sb and Sc galaxies are 0.1 redder on average, confirming previous results of Holmberg (1958), Chester and Roberts (1969), and Davies and Lewis (1973).

While simple selection effects are clearly not the cause of the cluster–field differences (Kennicutt, 1983), it does not necessarily follow that the Virgo spirals are "anemic", as suggested by van den Bergh. The distribution of Hubble types among the spirals is different in Virgo, and hence it is possible that a small part of the cluster–field difference is due to classification effects.

However, systematic biases could exist if the Virgo spirals span a consider-

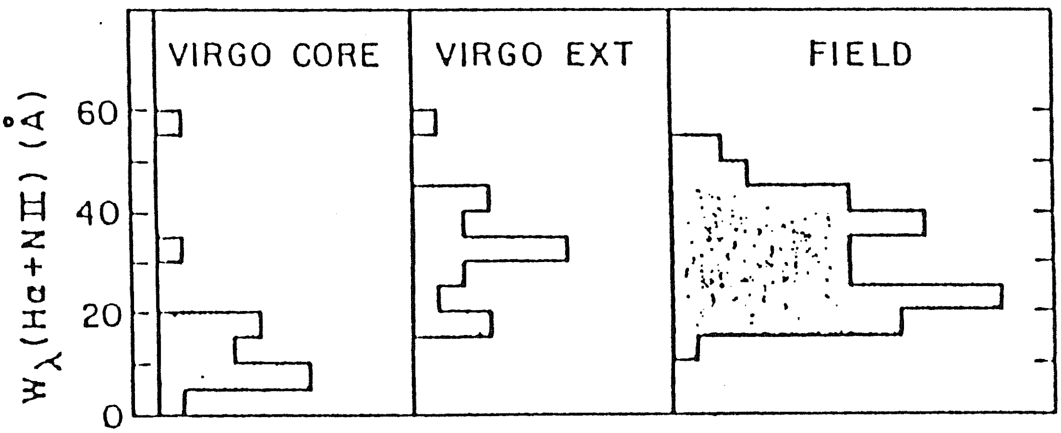

Figure 6.1: Distribution of emission equivalent width among Sc galaxies, for the Virgo core and the field. The "Virgo Ext" sample is composed of field spirals near the Virgo cluster (from Kennicutt, 1983).

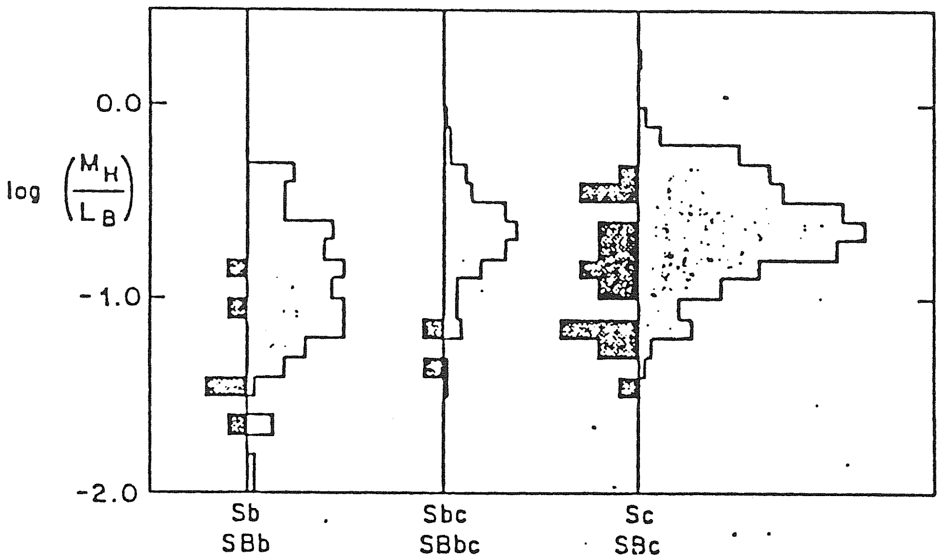

Figure 6.2: A comparison of the distance independent H mass to blue luminosity ratio distributions in the Virgo cluster and in the field (from Kennicutt, 1983).

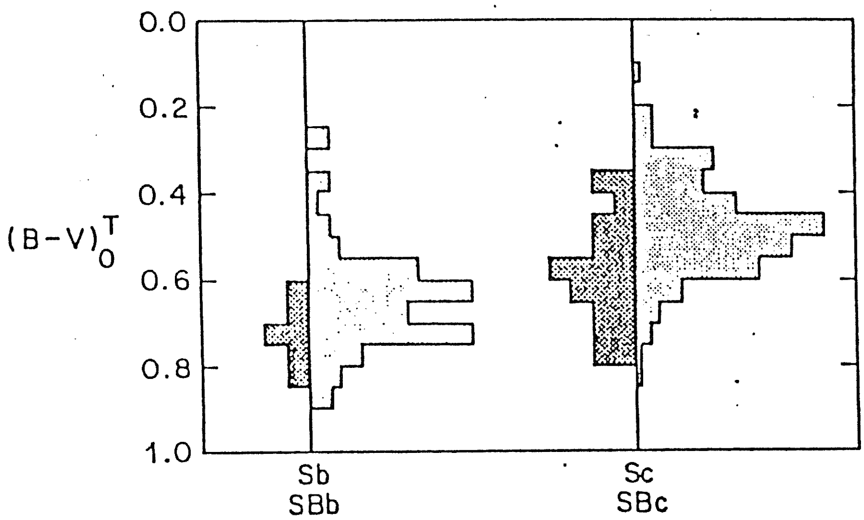

Figure 6.3: Comparison of the $(B - V)$ color distributions in the Virgo cluster core and in the field (from Kennicutt, 1983).

ably different range in absolute luminosity, since it is known that the hydrogen contents and color are at least weakly luminosity dependent.

The HI–color correlation diagram for field and Virgo galaxies is shown in Fig.6.4 (Stauffer, 1983). Simple visual comparison of the two figures leads to the following conclusion: **1**) There is a significant population of quite HI deficient galaxies in Virgo that fall in a portion of the diagram that is nearly unoccupied from the field sample. Most of those Virgo galaxies fall along the major axis of the ellipse, indicating that they are also quite red for their morphological type. Approximately 50% have not yet interacted appreciably with the IGM and so fall within the ellipse. **2**) The other significant difference between the Virgo and the field distributions is the absence in Virgo of blue, HI rich galaxies, which are present in abundance in the field sample.

One can use the following parameters to define the overall state of a galaxy in a cluster, namely the morphological type and the diameter, which give its intrinsic properties, and its position and velocity, which define its relation to the cluster. A priori, the HI deficiency displayed by the Virgo spirals may be related to these four quantities. For example, a very striking feature is that the HI deficiency is closely related to the membership. Among the 50 galaxies of the sample of Chamaraux *et al.* (1980), 31 are defined members of the Virgo cluster,

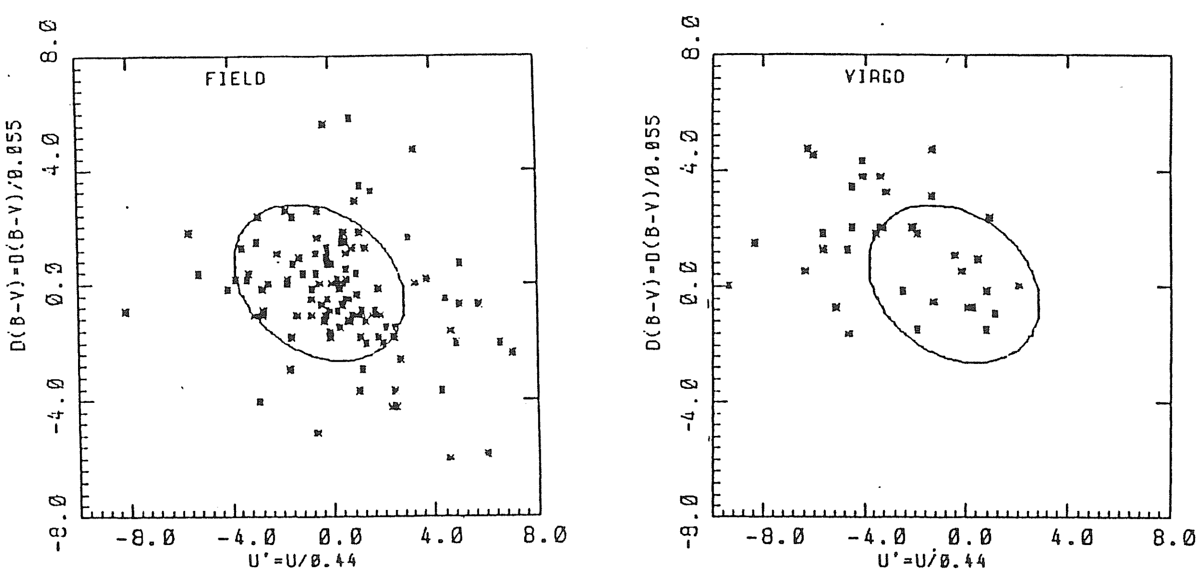

Figure 6.4: HI–color diagram for field and Virgo galaxies. The two axes measures deviations of a galaxy's integral color and HI content from the mean value for that morphological type. Positive $\delta(B-V)$ corresponds to being redder than normal, and positive u' corresponds to being HI rich (from Stauffer, 1983).

9 pertain to the X cloud, and 10 are uncertain. For these uncertain members the HI content is perfectly normal, for the 31 members the measured HI deficiency is of a factor of 2.2, and for the 9 members of the cloud there is only a possible marginal deficiency. Observations also show that possibly exist an East–West effect: galaxies in the East half of the cluster are generally more deficient than those located in the West half.

A deficiency of HI content becomes obvious when the mass of neutral hydrogen M_{HI} is correlated with other global parameters such as absolute magnitude $M_{B_T}^{0,i}$, total mass M_T, or the corrected HI line width $\Delta v_{0,i}$. In the innermost 3° the galaxies are HI deficient by a factor of 2 to 5, and occasionally, up to 10. Brighter galaxies seem to be more deficient than fainter galaxies. Similarly, early type galaxies are far more deficient than late type galaxies (Huchtmeier and Richter, 1989).

The relation of the HI line width and linear diameter versus morphological type is shown in Fig.6.5. Note that the Virgo Sa galaxies do have systematically smaller HI line widths than corresponding field galaxies, and similarly have systematically smaller linear diameters. Since $\Delta v_{0,i}$ is the most important parameter

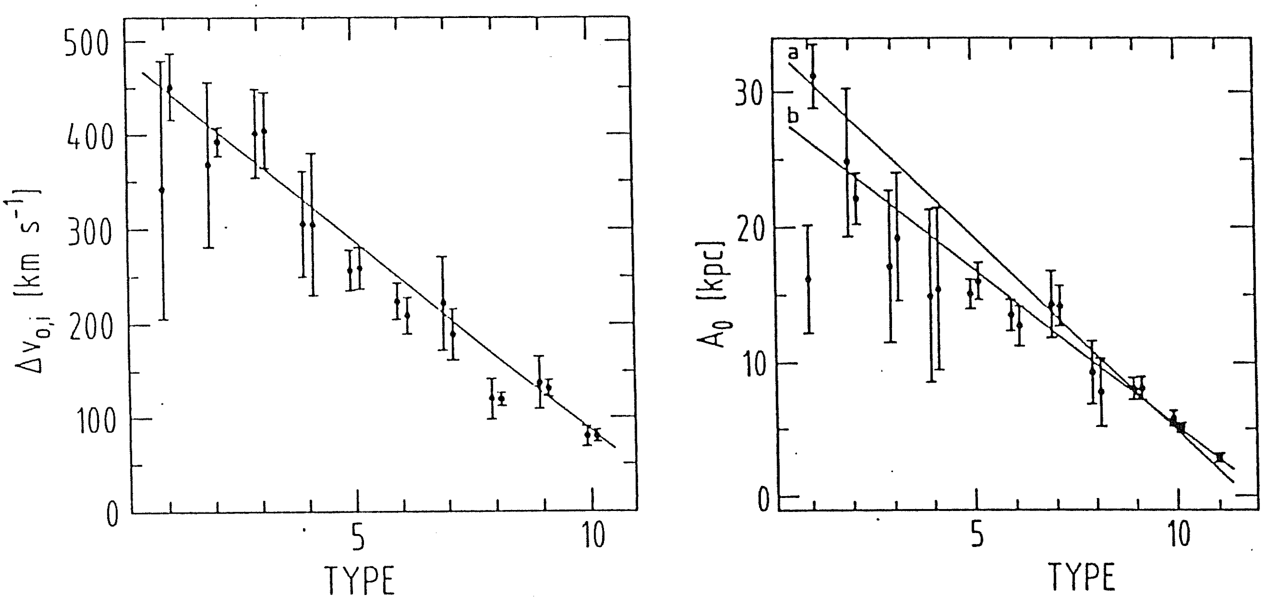

Figure 6.5: (a) The corrected HI line width as a function of T for Virgo (left symbols) and the field sample (right symbols). (b) The type dependence of the linear diameter (from Huchtmeier and Richter, 1989).

for deriving the total mass M_T, the diagram is another way to demonstrate that M_T is a strong function of the morphological type T.

A number of theoretical mechanisms exist which are known to be sufficiently efficient to separate disk galaxies from their interstellar gas in rich clusters. Ram–pressure ablation models (Gunn and Gott, 1972; Lea and de Young, 1976; Gisler, 1978) posit that the impulsive pressure of the IGM against the ambient gas in galaxies as they pass near the cluster core should sweep gas out of their gravitational potential well. Thermal–evaporation models (Cowie and Songalia, 1977; Balbus and McKee, 1982) argue that just the immersion of the cool disk gas in the hot cluster medium should eventually result in transfer of the disk gas to the IGM. As an alternative not based on the cluster IGM, Larson *et al.* (1980) have proposed that the gas deficiency in cluster disk galaxies results from the truncation of gas inflow due to tidal stripping of the gas–rich dwarf companions (Magellanic Cloud analogs) of those galaxies during cluster collapse. It is also possible that the observed present–day HI deficiency in cluster spirals is the result of a birth defect and that cluster galaxies are simply endowed with less post–formation residual gas than field galaxies.

The Virgo cluster offers two advantages that make it an attractive testing ground to attempt a discrimination among these models. The most self-evident advantage is proximity, while the other advantage is the fact that the mechanism for producing gas deficiency has not yet come to complete fruition in Virgo. In a further evolved cluster, such as the Coma cluster, it is likely that all the disk galaxies near the cluster center have been stripped of nearly all of their gas (Sullivan *et al.* 1981).

The question of the color of a spiral galaxy is of particular importance: if a disk galaxy has gas removed from it over a relatively short time scale (*e.g.*, by ram-pressure ablation), the stellar component of the disk will readjust to the lower residual HI content but with a longer time constant. That is, the star formation rate in the disk after the HI stripping event should be lower and the disk color should gradually turn redder. From models developed by Larson *et al.* (1980), the time for the stellar disk to adjust to the new HI content should be of the order of 10^9 years. Therefore, if most of the stripping events in Virgo took place more than 10^9 years in the past, the stripped spirals should have had time to adjust their colors to their HI content and they should appear red as well as HI deficient.

6.2 Molecular clouds in spiral galaxies

Studies of molecular clouds in external galaxies are important for understanding star formation and the evolution of galactic disks since new generations of stars form in the dense component of the ISM.

For several late type spirals the CO distribution has been found to follow the roughly exponential blue luminosity profile in the disk out to $\sim$ 10 Kpc (Young and Scoville, 1982a; Scoville and Young, 1983; Solomon *et al.* 1983). Furthermore, the CO luminosities in the central 5 Kpc diameter in a sample of Sc galaxies have been found to exhibit a one-to-one proportionality with the optical luminosities in the same regions (Young and Scoville, 1982b).

The Virgo cluster provides the ideal setting for a survey of the molecular content of galaxies as a function of morphological type and luminosity. Because the determination of molecular masses depends on the square of the distance to a given galaxy, the fact that the members in the cluster are all at roughly the same distance enables the mass of one galaxy relative to another to be determined with little ambiguity. CO studies of these galaxies also provide information on the effect of environment on the dense component of the ISM, and indicate whether the molecular medium has suffered a similar fate to the less dense clouds of atomic gas.

CO observations of 25 spiral galaxies in the cluster have been made by Young, Scoville and Brady (1985). For Sc galaxies, they confirmed the relationship between the optical and the CO luminosity in the central 5 Kpc, while for the early type spirals this relation is slightly displaced, in the sense that for a given CO content the early type galaxies are more luminous. This trend may be due to the presence of old stars in the nuclear bulge, which contribute significantly to the blue light in these galaxies.

In general, the shapes of the CO distributions with radius in the Virgo cluster and the total CO luminosities agree well with those found in field galaxies, suggesting that the molecular contents of these galaxies are not significantly different from field galaxies of the same type and luminosity. The maximum CO content observed is similar for the early and late type galaxies, however, the fraction of the galaxy mass in molecular form is a factor of ~ 4 smaller in luminous Sa's than Sc's since the early type galaxies have higher dynamical masses for a given luminosity. Figure 6.6 shows representative CO spectra (solid line) for the central $50''.0$ in four of the Sc galaxies sample. The upper two panels are spectra from high luminosity galaxies, while the lower two are from low luminosity galaxies; it is immediately apparent that high luminosity galaxies have more CO in their centers than do low luminosity galaxies.

To derive masses of H_2 Young (1984) adopted a CO to H_2 conversion of 4×10^{20} H_2 cm^{-2} (K km s^{-1})$^{-1}$. This conversion was determined from observations of dark clouds and giant molecular clouds in our galaxy (*e.g.*, Frerking *et al.* 1982), and does not account for either the effects of cloud temperature variations or of metallicity variations from galaxy to galaxy. The validity of this conversion factor can be investigated by comparing the CO emission with other indicators of total gas mass, such as far–infrared emission.

Observations of 47 spiral galaxies were also made by Stark *et al.* (1986). The total CO emission is found to be correlated with radio continuum emission and 60μm + 100μm band far infrared, reflecting direct relationships among molecular gas content, CO emission, and massive star formation in these galaxies. However, the total CO flux is only poorly correlated with visual blue luminosity.

Observed correlations among these quantities have been discussed by Telesco and Harper (1980), Rickard and Harvey (1984) and Dickey and Salpeter (1984). The strength of the CO emission may be proportional to the total amount of dense gas, even though the CO emission from individual molecular clouds is highly optically thick. Since the clouds are not expected to shadow each other much, a measurement of the total CO emission is a measurement of the total projected surface area of molecular cloud times their temperature.

The ratio of CO flux to HI flux is greater for galaxies near the center of the Virgo cluster. This increase is probably due to sweeping and removal of the lower density HI gas by the IGM, whereas the denser molecular gas is apparently unaffected.

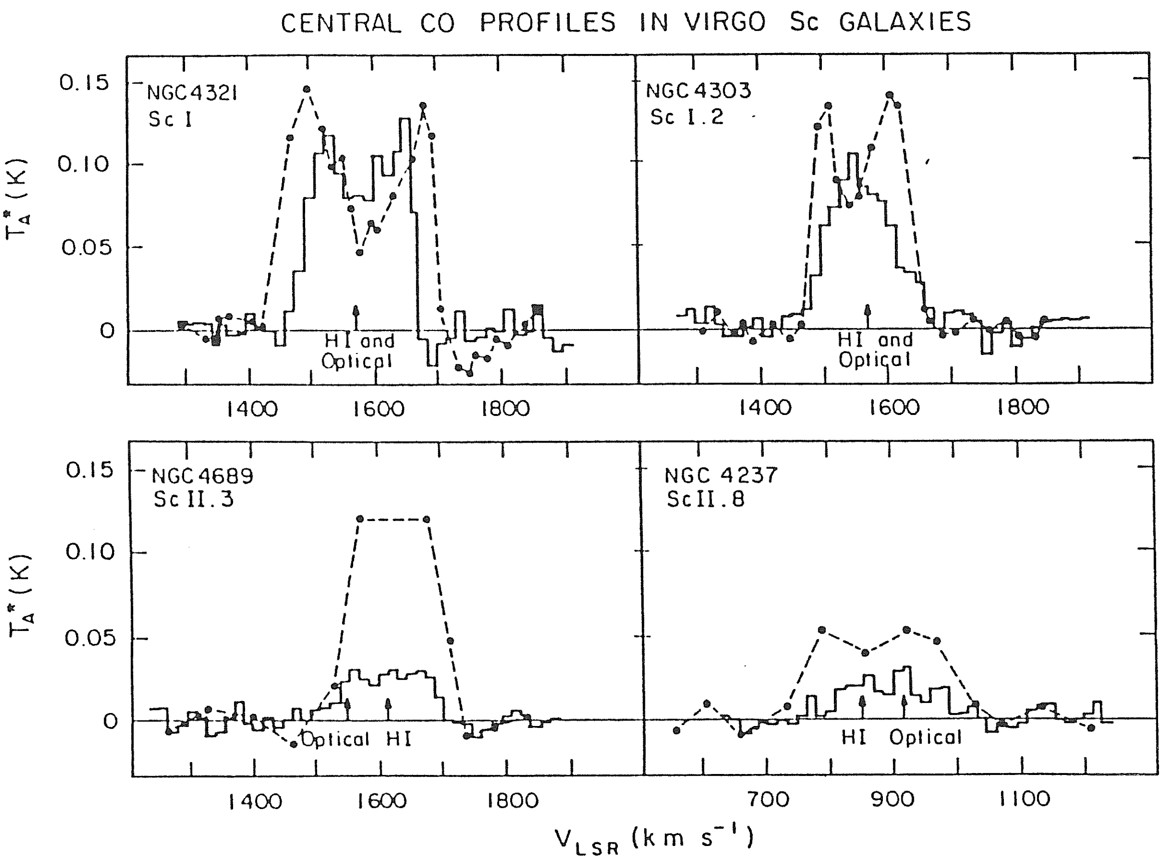

Figure 6.6: CO spectra in central 50."0 of 4 Sc galaxies in Virgo (solid histograms). Also shown are the HI profiles of each galaxy (dashed histograms) (from Young, 1984).

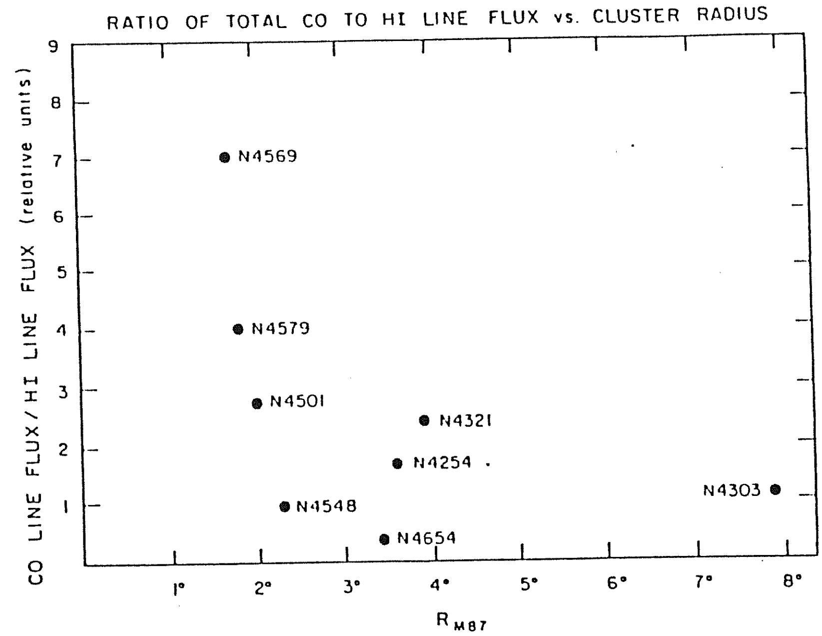

Figure 6.7: Ratio of CO to HI line flux vs. angular separation from M87 (from Kenney and Young, 1984).

Figure 6.2 shows the ratio of total CO intensity to HI flux, plotted against projected angular distance from M87, taken as the center of the cluster. The data show a strongly declining value of this ratio with distance from M87. The galaxies plotted in Fig. have been subdivided by morphological type. The points are well mingled, showing that morphological type is much less important than are environmental effects.

The atomic to molecular gas comparison is an independent test of the HI deficiency. The existence of roughly normal molecular gas content in HI–deficient galaxies argues strongly that some mechanism has removed the low density atomic gas, while leaving the high density molecular gas unscathed.

References

Balbus, S. and McKee, C.: 1982, *Astrophys. J.*, **252**, 529.

Balkowski, C.: 1973, *Astron. Astrophys.*, **29**, 43.
Bergh, S., van den: 1976, *Astrophys. J.*, **206**, 883.
Chamaraux, P., Balkowsky, C., and Gerard, E.: 1980, *Astron. Astrophys. Suppl. - Ser*, **47**, 171.
Chester, C., and Roberts, M.S.: 1964, *Astron. J.*, **69**, 635.
Cowie, L., and Songalia, A.: 1977, *Nature*, **266**, 501.
Davies, R.D., and Lewis, B.M.: 1973, *Mont. Not. R. astr. Soc.*, **165**, 231.
Dickey,.., and Salpeter, E.E.: 1984, *Astrophys. J.*, **284**, 461.
Frerking,.., Langer, W.D., and Wilson, R.W.: 1982, *Astrophys. J.*, **262**, 590.
Giovanardi, C., Helou, G., Salpeter, E.E., and Krumm, N.: 1983, *Astrophys. J.*,
Gisler, G.: 1978, *Mont. Not. R. astr. Soc.*, **183**, 633.
Gouguenheim,....: 1969
Gunn, J., and Gott, J.: 1972, *Astrophys. J.*, **176**, 1.
Hoffman, G.L., Lewis, B.M., Helou, G., Salpeter, E.E., and Williams, H.L.: 1989, *Astrophys. J. Supp.*, **69**, 65.
Holmberg, D.: 1958, *Medd. Lunds. Astr. Obs. Ser.*, **2**, No.136.
Huchtmeier, W.K., and Richter, O.G.: 1989, *Astron. Astrophys.*, **210**, 1.
Huchtmeier, W.K., Tamman, G.A., and Wendker, H.J.: 1976, *Astron. Astrophys.*, **46**, 381.
Kennicutt, R.C.: 1983, *Astron. J.*, **88**(4), 483.
Kennicutt, R.C, and Kent, S.M.: 1983,
Krumm, N, and Salpeter, E.E.:1979a, *Astrophys. J.*, **227**, 776.
Krumm, N, and Salpeter, E.E.:1979b, *Astrophys. J.*, **228**, 64.
Larson, R., Tinsley, B., and Caldwell, N.: 1980, *Astrophys. J.*, **237**, 692.
Lea, S., and de Young, D.: 1976, *Astrophys. J.*, **210**, 62.
Rickard, L.J., and Harvey, P.: 1984, *Astron. J.*, **89**, 1520.
Roberts, M.S.: 1969, *Astron. J.*, **74**, 859.
Scoville, N.Z., and Young, J.: 1983, *Astrophys. J.*, **265**, 148.
Solomon, P.M., Barrett, J., Sanders, D.B., and de Zafra, R.: 1983, *Astrophys. J. Letters*, **266**, L103.
Stark, A.A., Knapp, G.R., Bally, J., Wilson, R.W., Penzias, A.A., and Rowe, H.E.: 1986, *Astrophys. J.*, **310**, 660.
Stauffer, J.R.: 1983, *Astrophys. J.*, **264**, 14.
Sullivan, W., Bothun, G., Bates, B., and Schommer, R.: 1981, *Astron. J.*, **86**, 919.
Telesco, C.M., and Harper, D.A.: 1980, *Astrophys. J.*, **235**, 392.
Young, J.: 1984, in *Proc. ESO Workshop on the Virgo Cluster of Galaxies*, (Munich)(Garching:ESO), p.151.
Young, J., and Scoville, N.Z.: 1982a, *Astrophys. J.*, **258**, 467.
Young, J., and Scoville, N.Z.: 1982b, *Astrophys. J. Letters*, **260**, L11.
Young, J., Scoville, N.Z., and Brady, E.: 1985, *Astrophys. J.*, **288**, 487.

Chapter 7

Surface photometry of galaxies

7.1 Technical aspects

In this conclusive chapter I want to review some of the basic technical aspects of the surface photometry of galaxies, and to point out which are the most important information we can extract from the photometric data in different astrophysical problems. In the final section I will also introduce the characteristics of a new photometric technique, that coupled photographic plate material with CCD frames. Such new technique will be applied to the study of spiral Virgo galaxies that I will do for my Ph.D. thesis.

We can say that surface photometry is born well before that the nature of galaxies as extragalactic objects was clearly established, infact only in 1913 Reynolds measured the light profile of the bulge of M31 and proposed the fitting formula that now we as the Hubble formula (after his work in 1930):

$$J(\xi) = 4(1+\xi)^{-2} \tag{7.1}$$

where $\xi = r/r_0$, and $J = I(r)/I(r_0)$.

Since that epoch, surface photometry has given an enormous contribution to our understanding of galaxies. Several luminosity laws other than Hubble–Reynolds' and de Vaucouleurs' have been proposed to represent the manifold of the light profiles, in particular for the early type galaxies. Some of these alternative formulae are listed in Table 7.1.

Baum's (1955) formula coincides with Hubble–Reynolds' for $r \gg r_0$, and is steeper at small galactocentric distances, diverging at $r = 0$. In addition, its area integral (total luminosity) diverges with r. Oemler's (1976) formula is instead almost coincident with Hubble–Reynolds' in the core region, and is progressively steeper at increasing distances. King's (1962) formula was developed to model the projected density distribution of star cluster, and it was lately applied to describe the luminosity profiles of elliptical galaxies (King, 1966). It is semi–empirical in the sense that is related to quasi–isothermal isotropic dynamical models. This

Baum: 1955	$I(r)/I_o = 2\,r_o^2[r\,(r+r_o)]^{-1}$
Oemler: 1976	$I(r)/I_o = 4\,r_o^2(r+r_o)^{-2}\exp[-(r^2-r_o^2)/\beta^2]$
King: 1966	$(I(r)/k) = \left\{[1+(r/r_c)^2]^{-1/2} - [1+(r_t/r_c)^2]^{-1/2}\right\}^2$
Sersic: 1968	$I(r)/I(0) = \mathrm{dex}\{A\,r^{2/n}\}$

Table 7.1: Photometric laws.

formula has two characteristic lengths, one of which is a free parameter: the *core radius*, r_c, is where the surface brightness is 2.5 $log2 = 0.753$ mag fainter than the peak brightness $I(0)$, and the *tidal radius*, r_t, is where $I = 0$. Finally, the Sersic's (1968) formula is the generalization of the $r^{1/4}$ law ($n = 8$); it contemplates also the case of exponential light–profiles ($n = 2$) holding for face–on disks.

The data bank of surface photometric data is mainly contained in some of the classical catalogs like 'RC1' and 'RC2' (de Vaucouleurs and de Vaucouleurs, 1964; de Vaucouleurs *et al.* 1976), 'UGC' (Nilson, 1973), 'RSA' (Sandage and Tammann, 1981), 'SGC' (Corwin *et al.* 1985), and is pubblished in a lot of papers (see Davoust and Pence, 1982 for a compilation of references up to 1980), the most recent of which are contained in Table 7.2. Review papers are quite common in the astronomical literature (*e.g.*, Kormendy 1980, 1982, 1987; de Vaucouleurs 1976, 1979, 1983; de Vaucouleurs and Capaccioli 1979; Capaccioli and de Vaucouleurs 1983; Capaccioli 1984, 1985, 1987; Okamura, 1988).

King, 1978	photographic	16 E+S0s
Watanabe, 1983	photographic	261 gal. in Virgo
Binggeli et al., 1984	photographic	109 gal. in Virgo
Kent, 1984	CCD	105 E+S0s
Michard, 1985	photographic	36 E+S0s
Lauer, 1985	CCD	42 E+S0s
Djorgovski, 1986	CCD	262 E+S0s
Schombert, 1986	photographic	261 gal. in clusters
Lauberts, 1988	photographic	~17,000 galaxies

Table 7.2: The most recent reviews on photometry of galaxies.

7.2 Photographic plates

Until the recent advent of CCD detectors, the photographic emulsion has been pratically the only detector available for galaxy photometry. The principal characteristic that make this detector not replaceable by CCDs, up to date, is the large size of the plates (up to 50 cm), which coupled with large field telescopes give the possibilities of studying extended objects. A digitization process through a microphotometer is necessary for having a quantitative photometry, even if this process adds noise to the data and sets the final resolution, both *spatial*, because of the convolution of the microdensitometer aperture with the instrumental point spread function, and *photometric*, because of the non–linearity of the signal integrated within the aperture.

The quantum efficiency of the emulsion is always rather poor ($\leq$ a few percent), and the sensivity depends on many factors, such as pre and post processing (hypersensitization and development). The key feature of all photographic emulsions is the non–linear and rather complex (*e.g.*, non–reciprocity and adjacency effects, solarization, *etc.*) response. The dynamical range is low compared with the excursion of the galaxy light profiles, and further it is necessary an accurate calibration.

Indirect calibrations of plates lacking of photometric spots has been tempted by Kormendy (1973) and Piotto (1986), through stellar light profiles. A popular linear interpolation formula for the sensitometric readings has been introduced by de Vaucouleurs (1968):

$$I = A\omega^n, \tag{7.2}$$

where $\omega = dex(D - D_{fog}) - 1$ is the opacitance, D is the density of the photometric spot of relative density I, D_{fog} is the average density in a non exposed part of the plate and n an opportune exponential factor. The final output is the relative intensity in units of the mean sky background:

$$I_R(x,y) = \frac{I_{gal}(x,y)}{\langle I_{sky}(x,y)\rangle} = \frac{dex\{P[log(\omega)]\} - dex\{P[log(\omega_{sky})]\}}{dex\{P[log(\omega_{sky})]\}} \tag{7.3}$$

where $P[log(\omega)]$ is the polinomium used for the calibration. The galaxy signal I_g is obtained as the difference $I_g = I_{g+s} - I_s$ between the measured (specific) intensity (I_{g+s}, galaxy + sky) and the intensity of the local night–sky light I_s (airglow+zodiacal light+ atmospheric, instrumental and interstellar scattering) interpolated across the area of the galaxy between adjacent "blank sky" fields. In the faint outer parts of a galaxy, where $I_g << I_s$, the possibility of having an error in the light profile increases, because $\delta\mu_g$ diverges. This effect can be seen in Fig.7.1 (from Capaccioli and de Vaucouleurs, 1983); in particular it can introduced "tidal radii" or "tidal extension" depending on whether the sky background is placed slightly too high or too low.

The zero point of the photographic photometry is usually fixed by photoelectric photometry, either by direct photoelectric scans calibrated versus standard stars, or by comparing the integral photographic luminosity to the photoelectric flux measured through circular aperture centered on the nucleus of the galaxy. The magnitude scale is affected by errors in the magnitudes of the standard stars, in the atmospheric extinction corrections, and in the color trasformation equations.

7.3 CCD detectors

CCDs are small ($\sim$ 2 cm) and are constitute by pixels ($15 \div 30$ μm in size) of high sensivity (quantum efficiency up to $\sim$ 80%). This digital detector is practically linear (to 10^{-3}) over a range of 3-4 dex. A number of steps are required before using CCD frames: **1)** The subtraction of dark–current and bias. The first is

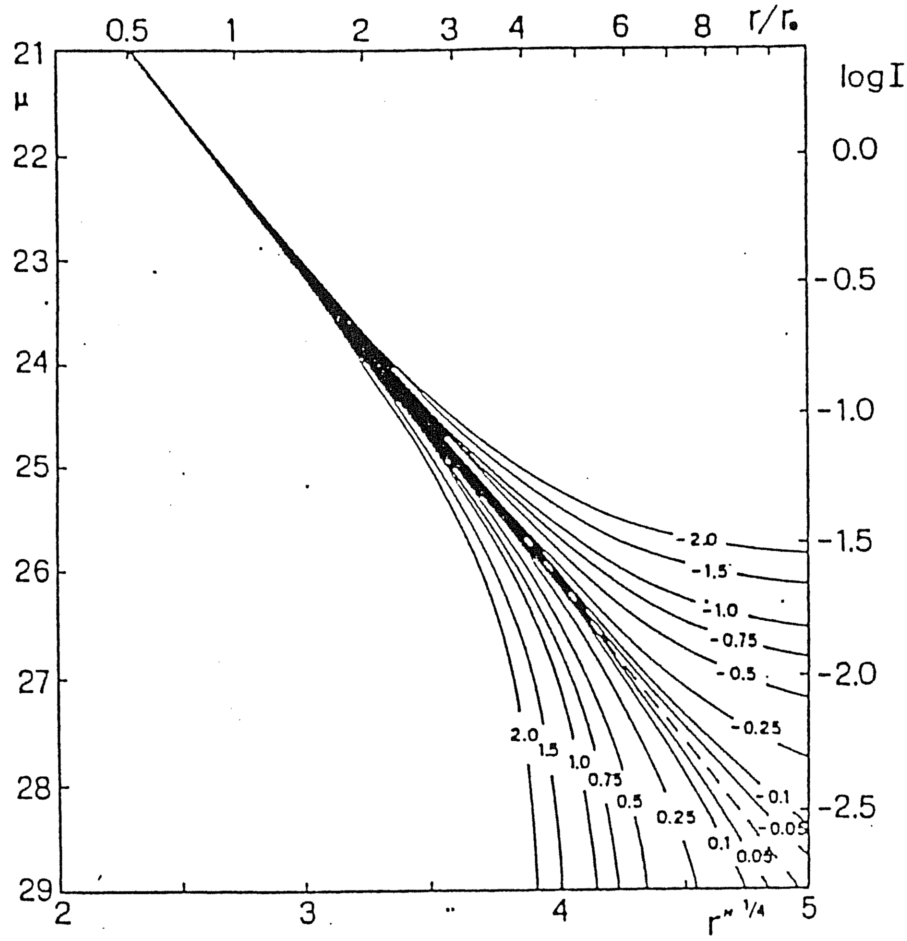

Figure 7.1: Effect of incorrect sky level on the apparent luminosity profile of the E0 galaxy NGC 3379 (from Capaccioli and de Vaucouleurs, 1983).

a signal caused by thermal electrons, and the second is an artificial threshold provided by the electronics in order to increase the charge–transfer efficiency; **2**) A division by a "flat–field", that is an exposure of the chip to a uniform light source, which is necessary to map variations of sensivity across it; **3**) The remotion of "bad" columns and "hot" spots by linear interpolation procedures.

The small field of CCD detectors poses additional problems to the determination of the background level. Infact, if the galaxy fills the CCD frame, the blank–sky level must be recovered in another frame, while a correct procedure would require simultaneous exposure of both the object and the sky, because of rapid time–variability of the airglow. For this reason it is useful to separate two frames of the galaxy with an exposure close to the object, in a region as blank as possible (Capaccioli *et al.* 1987). Another observing strategy is the so–called "drift scanning": the image of the galaxy is let drift across the detector field (Boroson and Thompson, 1987). Each time the shift is applied, the last line is read and stored, so that the final output is a rectangular frame, with one side as long as wanted and with pixels elongated in the direction of the drift proportionally to the timing interval. In some cases the background has been evaluated in the regions of the exposure where the galaxy is already faint (Lauer, 1985; Djorgovski, 1986), but this method leads inevitably to overstimate I_{sky}.

It is worth to note that the observed luminosity distribution $I(x, y)$ recorded by the detector in the focal plane of the telescope, is the convolution of the true source function $S(x, y)$ with the point spread function (PSF) $G(x, y)$, that is with the apparent luminosity profile of a star in that particular atmospheric and instrumental conditions. The typical PSF is shown in Fig.7.2. We can see that two distinct regimes are in evidence: (i) a steep decline, which is extended up to $30''.0$, and is dominated by atmospheric turbolence and telescopic diffraction; (ii) a shallower decline extending out to the limit of measurements, which is called the "aureole", and depends on distant atmospheric and telescopic scattering. The innermost part is often called the "seeing disk" and is dominated by atmospheric turbolence. In general, the core of the image is well approximated by a Gauss function (de Vaucouleurs, 1948b; King, 1971; Brown, 1978), and it includes up to 80%–90% of the energy of the star image. The first component (i) dominates the nuclear regions of galaxies through convolution effects, whereas in the faint outer parts light from the central region can be scattered in the second component (ii) and produce fictitious "coronae". Although it is in principle possible to restore the source function $S(x, y)$ by a variety of methods, for example by Fourier transform (*e.g.*, Brault and White, 1972), this is neither convenient nor desirable in practice because the process amplifies the noise in the data and in the PSF. Thus, in general, it is far easier to compare the observed distribution $I(x, y)$ with the convolution of the PSF with an opportune model of $S(x, y)$.

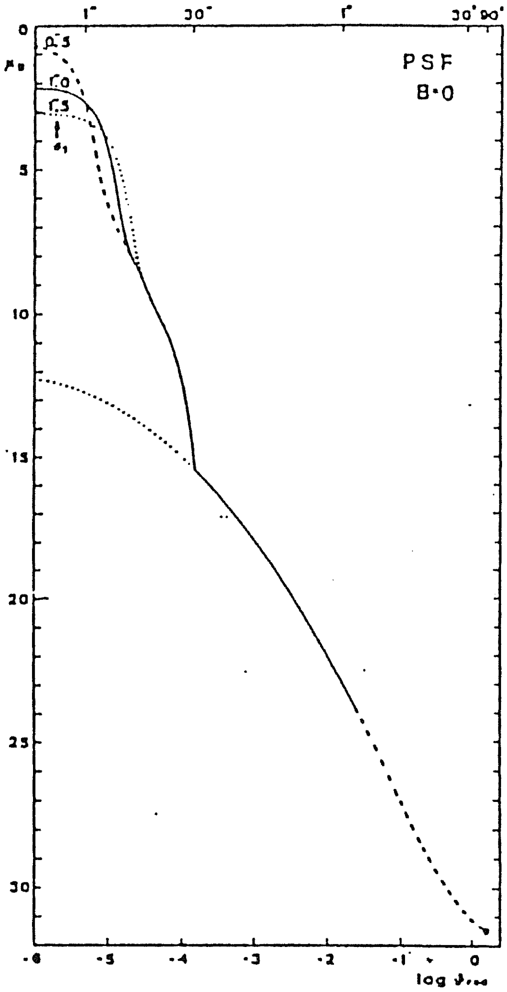

Figure 7.2: The typical PSF. Solid line represents the observed part, dashed line the extrapolated Rayleigh–scattering part, and the dotted line the molecular scattering (from Capaccioli and de Vaucouleurs, 1983).

7.4 A new photometric technique

The advantages and disadvantages of the two detectors, plates and CCDs, can be overcome by combining their properties and using them complementary: the plates map the outer and fainter regions, while CCDs the inner and brighter regions.

The key feature of this photometric technique is the determination of the background sky level of the CCD images. The procedure, successfully applied by Capaccioli *et al.* (1987), Capaccioli *et al.* (1988), Caon (1989), is based on the comparison of CCD light profiles of the galaxy with similar data from deep photographic plates (Fig.7.3), using only the region where the two profiles can be matched. The idea is that of exploring a set of values for the background level of the CCD image, $I_{sky}(CCD)$ and to choose the one leaving no trend in the residual $\Delta m(r) = \mu_{pg}(r) - \mu_{CCD}(r)$. The error on the sky background level, estimated as the standard deviation of this quantity from the light profiles along different axes of early type galaxies, is likely $\lesssim 2\%$ (Caon, 1989). This result is less then the common accepted value of 5%, obtained with the usual technique. Of course the photometric bands of the two detectors must match as well as possible, and whereas this is not a serious problem for early type galaxies, it could be important in the study of spiral galaxies.

The zero point of CCD images ($\mu_{sky}(CCD)$) can be established either through photometric standard stars (even if there could be some uncertainties related to the presence of color terms and to the very short exposure time) or, in a more straightforward way, by comparing a set of photoelectric aperture magnitudes with an analogous set of integrated CCD fluxes within circular apertures. As well, the zero point of the photographic images is determined as the sum of $\mu_{sky}(CCD)$ plus Δm, the difference between the two sky values (plate and CCD), which is the by-product of the procedure used to determine $I_{sky}(CCD)$. We can check the reliability of our results looking at the residuals among the photographic zero point of different galaxies on the same plate.

The application of this technique allows us to perform the photometric and geometrical analysis on the whole galaxy, from the very center (possibly with appropriate deconvolution) up to the intrinsic limit of the surface photometry at $28.5 \div 29.0$ mag arcsec^{-2}(Capaccioli and de Vaucouleurs, 1983). Previous experiences with the same technique have shown that the mean error on the final (CCD+Schmidt) profile is less than ± 0.1 mag in the interval $18.5 \leq \mu_B \leq 26.0$.

A very important consequence is that the photometrical parameters (μ_e, r_e) of the bulge and the disk, and the ratio B/D can be calculated from the entire light profiles of the galaxy and not from a limited portion of them. Moreover, the total apparent magnitude can be obtained by direct integration of the images, with a much better precision than the values extrapolated from standard growth curves.

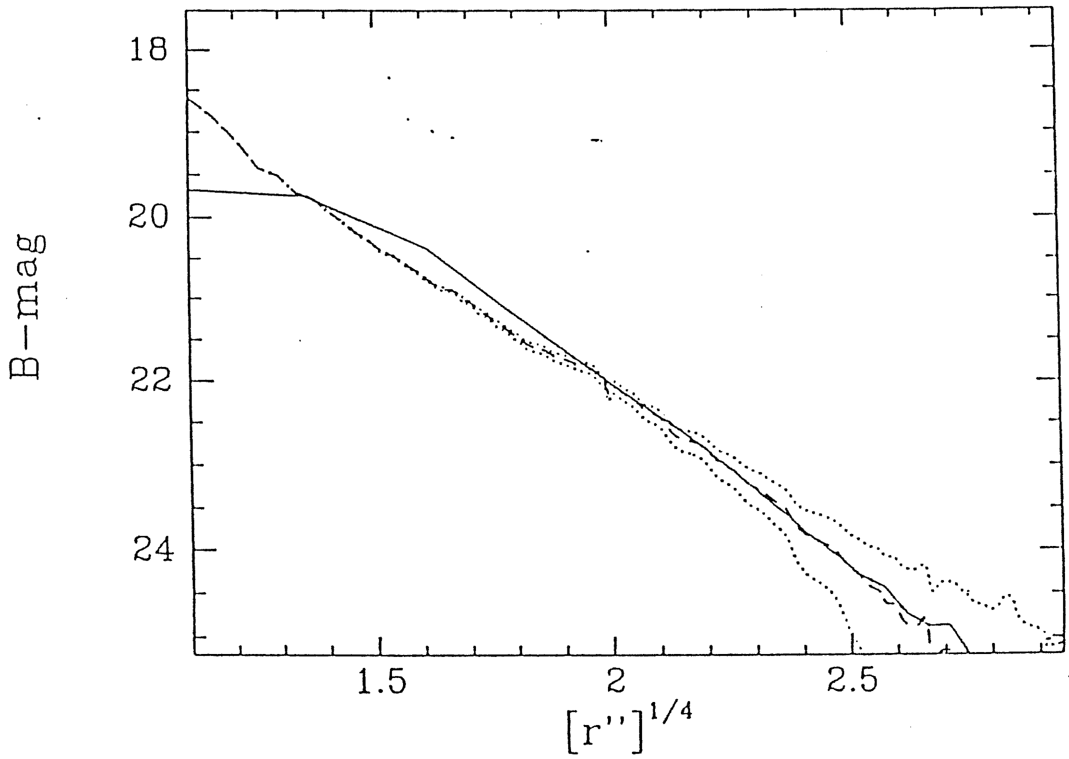

Figure 7.3: Solid line represent the Schmidt profile and the dashed line the CCD profile after their matching. The dotted lines are the CCD profiles that would be obtained with an error of 5% in the determination of the sky background (from Caon, 1989).

In this context the collection of good photometric data for a great number of spiral galaxies is of fundamental importance for attempting answers to many astrophysical problems concerning this class of objects.

We plan to study the dependence of the B/D ratio on the morphological type and on the position in the cluster, which could provide constraints to the theories of galaxy formation and evolution. At the same time we wish to tackle some aspects of the disk component that need further analyses; in particular the question of the constancy of the central surface brightness and the existence of thick and/or truncated disks. Furthermore, the photometric and geometric properties of spheroids can be analyzed to verify whether they follow the same statistical relationships of elliptical galaxies (Faber and Jackson, μ_e–r_e, etc.).

However, there are many other advantages in the new technique. Infact, CCDs and Schmidt plates together, allow studies of galaxy cores and nuclei, can discover details like dust and shells, give better values for the parameters of the fitting laws, and provide accurate measurements of departures from elliptical isophotes and color gradients.

Our present aim for the next future is to applied this technique to a great number of spiral galaxies (up to 50) in the Virgo cluster. This project is part of a most vast program of photometric analysis of the Virgo galaxies, and has been successfully applied to 33 early type galaxies by Caon (1989) up to now, and will be used again for another set of these galaxies (Trevisani, 1990).

The choosing of the Virgo cluster come from the following reasons. First, all the galaxies are approximately at the same distance, and this allows a more accurate determination of the relative absolute magnitude. Second, it is likely that all of them are born nearly at the same epoch, and this can give information on the SFR and the IMF. Third, the cluster is not too rich, and we can have an idea of the environmental influences that the galaxies experience in their lifetime. The last advantage is that all the galaxies are on the same plate and this fact greatly reduces the accidental errors that we encounter in the statistical relationships.

As we have seen in the previous chapters there are many astrophysical problems concerning the spiral galaxies that need more good quality photometric data, and in this context the Virgo galaxies provide us with the best sample.

References

Baum, W.A.: 1955, *Publ. Astron. Soc. of Pacific*, **83**, 199.

Boroson, T.A., and Thompson, I.B.: 1987, *Astron. J.*, **93**, 33.
Brault, J.W., and White, O.R.: 1972, *Astron. Astrophys.*, **13**, 169.
Brown, G.S.: 1978, *Pub. Astr. Univ. Texas*, No.11.
Caon, N.: 1989, *Dissertation*, University of Padova (Italy)
Capaccioli, M.: 1984, in *Data Analysis in Astronomy*, (Erice: Italy), eds. V.DI Ges.Scarsi, P.Crane, J.H.Friedman and S.Levialdi, Plenum Press, p.363.
Capaccioli, M.: 1985, in *New Aspects of Galaxy Photometry*, (Toulouse), ed. J.-L. Nieto, Springer Verlag: Lectures on Phys. Ser. No. 231, p.53.
Capaccioli, M.: 1987, in IAU Symp. No. 127, *Structure and Dynamics of Elliptical Galaxies*, (Princeton), ed. T.P. de Zeew, Reidel: Dordrecht, p.47.
Capaccioli, M., and de Vaucouleurs, G.: 1983, *Astrophys. J. Supp.*, **52**, 465.
Capaccioli, M., Held, E., and Nieto, J.-L.: 1987, *Astron. J.*, **94**, 1519.
Capaccioli, M., Piotto, G., and Rampazzo, R.: 1988a, *Astron. J.*, **96**, 497.
Davoust, E., and Pence, W.D.: 1982, *Astron. Astrophys. Suppl. Ser*, **49**, 631.
de Vaucouleurs, G.: 1948b, *Ann. Ap.*, **11**, 247.
de Vaucouleurs, G.: 1968, *Applied Optics*, **7**, 1513.
de Vaucouleurs, G.: 1976, in *Le Monde de Galaxies*, Lectures given at the college de France, Nov.1976, Besançon Observatory.
de Vaucouleurs, G.: 1979, in *Photometry, Kinematics and Dynamics of Galaxies*, (Austin), ed. D.S. Evans, The Univ. of Texas Press, p.1.
de Vaucouleurs, G.: 1983, in IAU Colloquium No.78, *Astronomy with Schmidt type Telescopes*, (Asiago), ed. M. Capaccioli, Reidel: Dordrecht, p.367.
de Vaucouleurs, G., and de Vaucouleurs, A.: 1964, *Reference Catalogue of Bright Galaxies*, Univ. of Texas Press, Austin (RC1).
de Vaucouleurs, G., de Vaucouleurs, A., and Corwin H.G.: 1976, *Second Reference Catalogue of Bright Galaxies*, Univ. of Texas Press, Austin (RC2).
de Vaucouleurs, G., and Capaccioli, M.: 1979, *Astrophys. J. Supp.*, **40**, 699.
Djorgovski, S.: 1986, *Ph.D. Thesis*, University of California (Berkeley).
Hubble, E.: 1930, *Astrophys. J.*, **71**, 231.
King, I.R.: 1966, *Astron. J.*, **71**, 276.
King, I.R.: 1971, *Publ. Astron. Soc. of Pacific*, **83**, 199.
Kormendy, J.: 1973, *Astron. J.*, **137**, 733.
Kormendy, J.: 1980, in *Proc. ESO Workshop on Two-Dimensional Photometry*, eds. P. Crane and K. Kjaär, (Leiden: Sterrewacht), p.191.
Kormendy, J.: 1982, in *Morphology and Dynamics of Galaxies*, XII Advanced Course of Swiss Soc. Astron. Astrophys., eds. L. Martinet and M. Mayor, (Sauverny: Geneva Obs.), p.115.
Kormendy, J.: 1987, in IAU Symp. No. 127, *Structure and Dynamics of Elliptical Galaxies*, (Princeton), ed. T.P. de Zeew, Reidel: Dordrecht, p.17.
Lauer, T.R.: 1985, *Astrophys. J. Supp.*, **57**, 473.
Nilson, P.: 1973, *Uppsala General Catalogue of Galaxies*, Acta Univ. Uppsala, Ser. V:A, Vol. 1 (UGC).
Oemler, A.: 1976, *Astrophys. J.*, **209**, 693.

Okamura, S.: 1988, preprint.
Piotto, G.: 1986, *Ph.D. Thesis*, University of Padova.
Sandage, A., and Tammann, G.: 1981, *A Revised Shapley-Ames Catalogue*, Carnegie Inst. of Washington, Publ. No. 635 (RSA).
Sersic, J.-L.: 1968, *Atlas de Galaxias Australes*, Observatorio Astronomico: Cordoba.
Trevisan, S.: 1990, *Dissertation*, Univ. of Padova (Italy),in preparation.